

ACTA PHARMACEUTICA SCIENCIA

International Journal in Pharmaceutical Sciences, Published Quarterly

ISSN: 2636-8552
e-ISSN: 1307-2080,
Volume: 57, No: 3, 2019
Formerly: Eczacılık Bülteni
Acta Pharmaceutica Turcica

Aims and Scope of Acta Pharmaceutica Scientia

Seref Demirayak

Instructions for Authors

Original articles

Isolation of two homologous Triterpenes with Antimalarial Activities from the Leaf Extract of Combretum Zenkeri

Wande Oluyemi, Babatunde Samuel, Kahlig Hans-Peter, Taramelli Donatella, Krenn Liselotte

Flax Seed Mucilage-chitosan Polyelectrolyte Complex Nanoparticles: Optimization, Characterization and Evaluation

Meenakshi Bhatia, Sunidhi Lohan

Synthesis and Characterization of Novel Tetrazole Derivatives and Evaluation of their Anti-candidal Activity

Hiba Maher Tawfeeq, Rasim Farraj Muslim, Obaid Hasan Abid, Mustafa Nadhim Owaid

Comparative Study of Chemical Characteristics, Phytochemical Contents and Antioxidant Activity of Polar and Non-polar Solvent Extracted Flaxseed Oil

Satarupa Ghosh, D. K. Bhattacharyya, M. Ghosh

A Study of Drug-excipient Interaction and Drug Product Stability Using Dry (Powder) Film Coating in Comparison with Conventional (Aqueous) Film Coating

Derar Omari, Yazan Akkam

Enterovirus Inhibiting Activities of Two Lupane Triterpenoids and Anthraquinones from Senna Siamea Stem Bark Against Three Serotypes of Echovirus

Omonike Ogbale, Toluwanimi Akinleye, Temitope Faleye, Adekunle Adeniji

Two New Spectrophotometric Methods for the Determination of Isoniazid in Bulk form and Tablet Dosage Form

Olajire Adegoke, Olusegun Thomas, Deborah Babatunde, Oyindamola Oyelami, Adeyinka Adediran, Abayomi Omotosho

57^[3]

ACTA PHARMACEUTICA SCIENCIA

International Journal in Pharmaceutical Sciences, Published Quarterly

ISSN: 2636-8552

e-ISSN: 1307-2080,

Volume: 57, No: 3, 2019

Formerly: Eczacılık Bülteni

Acta Pharmaceutica Turcica

ACTA PHARMACEUTICA SCIENCIA

International Journal in Pharmaceutical Sciences
is Published Quarterly

ISSN: 2636-8552

e-ISSN: 1307-2080,

Volume: 57, No: 3, 2019

Formerly: Eczacılık Bülteni/Acta Pharmaceutica Turcica

Founded in 1953 by Kasım Cemal Güven

Editor

Şeref Demirayak

Associate Editors

Güliden Zehra Omurtag

Barkın Berk

Coordinators

M. Eşref Tatlıpınar

Gökberk Karabay

Language Editor

Recep Murat Nurlu

M. Eşref Tatlıpınar

Neda Taner

Biostatistics Editor

Pakize Yiğit

Address

İstanbul Medipol Üniversitesi

Kavacık Güney Kampüsü

Göztepe Mah. Atatürk Cad.

No: 40 34810 Beykoz/İSTANBUL

Tel: 0216 681 51 00

E-mail

editor@actapharmsci.com

secretary@actapharmsci.com

Web site

<http://www.actapharmsci.com>

Printing Office

Forart Basımevi

Ziya Gökalp Mah.

Süleyman Demirel Bulvarı

Simpaş İş Modern Zemin Kat A 17-18

İkitelli - İstanbul

Tel: (0212) 501 82 20

Editorial Board

Sabahattin Aydın

(İstanbul Medipol University, Turkey)

Ahmet Aydın (Yeditepe University, Turkey)

Ahmet Çağrı Karaburun (Anadolu University, Turkey)

Aristidis Tsatsakis (University of Crete, Greece)

Ayfer Beceren (Marmara University, Turkey)

Dilek Ak (Anadolu University, Turkey)

Ebrahim Razzazi-Fazeli (University of Veterinary

Medicine, Vienna)

Erem Memişoğlu Bilensoy

(Hacettepe University, Turkey)

Fatma Tosun

(İstanbul Medipol University, Turkey)

Fatih Demirci (Anadolu University, Turkey)

Hakan Göker (Ankara University, Turkey)

Hanefi Özbek

(İstanbul Medipol University, Turkey)

Hayati Çelik (Yeditepe University, Turkey)

İhsan Çaliş (Near East University, Cyprus)

Julide Akbuğa

(İstanbul Medipol University, Turkey)

Kenneth A. Jacobson

(National Institutes of Health, USA)

Leyla Yurttaş (Anadolu University, Turkey)

Mahmud Miski (İstanbul University, Turkey)

Mesut Sancar (Marmara University, Turkey)

Murat Duran

(Eskişehir Osmangazi University, Turkey)

Nesrin Emekli

(İstanbul Medipol University, Turkey)

Nilay Aksoy (Altınbaş University, Turkey)

Nurşen Başaran (Hacettepe University, Turkey)

Özgen Özer (Ege University, Turkey)

Roberta Ciccocioppo

(University of Camerino, Italy)

Selma Saraç Tarhan

(Hacettepe University, Turkey)

Semra Şardaş (İstinye University, Turkey)

Sevda Süzgeç Selçuk

(İstanbul University, Turkey)

Stefano Constanzi (American University, USA)

Süreyya Ölgün (Biruni University, Turkey)

Şule Apikoğlu Rabuş

(Marmara University, Turkey)

Tuncer Değim (Biruni University, Turkey)

Yıldız Özsoy (İstanbul University, Turkey)

Yusuf Öztürk (Anadolu University, Turkey)

Printing Office

Has Kopyalama Baskı ve Kirtasiye A.Ş.

Kavacık Mah. Ekinçiler Cad. No:19

Medipol Üniversitesi Kuzey Yerleşkesi

Tel: 0216 681 53 72

Contents

Aims and Scope of Acta Pharmaceutica Scientia	
Seref Demirayak	5
Instructions for Authors	6
ORIGINAL ARTICLES	20
Isolation of two homologous Triterpenes with Antimalarial Activities from the Leaf Extract of Combretum Zenkeri	
Wande Oluyemi, Babatunde Samuel, Kahlig Hans-Peter, Taramelli Donatella, Krenn Liselotte	21
Flax Seed Mucilage-chitosan Polyelectrolyte Complex Nanoparticles: Optimization, Characterization and Evaluation	
Meenakshi Bhatia, Sunidhi Lohan	31
Synthesis and Characterization of Novel Tetrazole Derivatives and Evaluation of their Anti-candidal Activity	
Hiba Maher Tawfeeq, Rasim Farraj Muslim, Obaid Hasan Abid, Mustafa Nadhim Owaid	45
Comparative Study of Chemical Characteristics, Phytochemical Contents and Antioxidant Activity of Polar and Non-polar Solvent Extracted Flaxseed Oil	
Satarupa Ghosh, D. K. Bhattacharyya, M. Ghosh	65
A Study of Drug-exciipient Interaction and Drug Product Stability Using Dry (Powder) Film Coating in Comparison with Conventional (Aqueous) Film Coating	
Derar Omari, Yazan Akkam	75
Enterovirus Inhibiting Activities of Two Lupane Triterpenoids and Anthraquinones from Senna Siamea Stem Bark Against Three Serotypes of Echovirus	
Omonike Ogbole, Toluwanimi Akinleye, Temitope Faleye, Adekunle Adeniji	105
Two New Spectrophotometric Methods for the Determination of Isoniazid in Bulk form and Tablet Dosage Form	
Olajire Adegoke, Olusegun Thomas, Deborah Babatunde, Oyindamola Oyelami, Adeyinka Adediran, Abayomi Omotosho	117

Aims and Scope of Acta Pharmaceutica Scientia

Acta Pharmaceutica Scientia is a continuation of the former “Eczacılık Bülteni” which was first published in 1953 by Prof. Dr. Kasım Cemal GÜVEN’s editorship. At that time, “Eczacılık Bülteni” hosted scientific papers from the School of Medicine-Pharmacy at Istanbul University, Turkey.

In 1984, the name of the journal was changed to “Acta Pharmaceutica Turcica” and it became a journal for national and international manuscripts, in all fields of pharmaceutical sciences in both English and Turkish. (1984-1995, edited by Prof. Dr. Kasım Cemal GÜVEN, 1995-2001, edited by Prof. Dr. Erden GÜLER, 2002-2011, edited by Prof. Dr. Kasım Cemal GÜVEN)

Since 2006, the journal has been published only in English with the name, “Acta Pharmaceutica Scientia” which represents internationally accepted high-level scientific standards. The journal has been published quarterly except for an interval from 2002 to 2009 in which its issues were released at intervals of four months. The publication was also temporarily discontinued at the end of 2011 but since 2016, Acta Pharmaceutica Scientia has continued publication with the reestablished Editorial Board and also with the support of you as precious scientists.

Yours Faithfully

Prof. Dr. Şeref DEMİRAYAK

Editor

INSTRUCTIONS FOR AUTHORS

1. Scope and Editorial Policy

1.1. Scope of the Journal

Acta Pharmaceutica Scientia (Acta Pharm. Sci.), formerly known as Bulletin of Pharmacy and Acta Pharmaceutica Turcica is a peer-reviewed scientific journal publishing current research and reviews covering all fields of pharmaceutical sciences since 1953.

The original studies accepted for publication must be unpublished work and should contain data that have not been published elsewhere as a whole or a part. The reviews must provide critical evaluation of the state of knowledge related with the subject.

All manuscripts has to be written in clear and concise English. Starting from 2016, the journal will be issued quarterly both in paper and on-line formates also publish special issues for national or international scientific meetings and activities in the coverage field.

1.2 Manuscript Categories

Manuscripts can be submitted as Research Articles and Reviews.

1.2.1 Research Articles are definitive accounts of significant, original studies. They are expected to present important new data or provide a fresh approach to an established subject.

1.2.2 Reviews integrate, correlate, and evaluate results from published literature on a particular subject. They expected to report new and up to date experimental findings. They have to have a well-defined theme, are usually critical, and may present novel theoretical interpretations. Up to date experimental procedures may be included. Reviews are usually submitted at the invitation of the Editors. However, experts are welcome to contact the Editors to ensure that a topic is suitable. Approval is recommended prior to submission.

1.3 Prior Publication

Authors should submit only original work that has not been previously published and is not under consideration for publication elsewhere. Academic theses, including those on the Web or at a college Web site, are not considered to be prior publication.

1.4 Patents and Intellectual Property

Authors need to resolve all patent and intellectual property issues. Acceptance

and publication will not be delayed for pending or unresolved issues of this type. Note that Accepted manuscripts and online manuscripts are considered as published documents.

1.5 Professional Ethics

Editors, reviewers, and authors are expected to adhere to internationally accepted criteria's for scientific publishing.

1.5.1 Author Consent. Submitting authors are reminded that consent of all coauthors must be obtained prior to submission of manuscripts. If an author is removed after submission, the submitting author must have the removed author consent to the change by e-mail or faxed letter to the assigned Editor.

1.5.2. Plagiarism. Manuscripts must be original with respect to concept, content, and writing. It is not appropriate for an author to reuse wording from other publications, including one's own previous publications, whether or not that publication is cited. Suspected plagiarism should be reported immediately to the editorial office. Report should specifically indicate the plagiarized material within the manuscripts. Acta Pharmaceutica Scientia uses iThenticate or Turnitin software to screen submitted manuscripts for similarity to published material. Note that your manuscript may be screened during the submission process.

1.5.3. Use of Human or Animal Subjects. For research involving biological samples obtained from animals or human subjects, editors reserve the right to request additional information from authors. Studies submitted for publication approval must present evidence that the described experimental activities have undergone local institutional review assessing safety and humane usage of study subject animals. In the case of human subjects authors must also provide a statement that study samples were obtained through the informed consent of the donors, or in lieu of that evidence, by the authority of the institutional board that licensed the use of such material. Authors are requested to declare the identification or case number of institution approval as well as the name of the licensing committee in a statement placed in the section describing the studies' Material and Methods.

1.6 Issue Frequency

The Journal publishes 4 issues per year.

2. Preparing the Manuscript

2.1 General Considerations

Manuscripts should be kept to a minimum length. Authors should write in clear,

concise English, employing an editing service if necessary. For professional assistance with improving the English, figures, or formatting in the manuscript before submission please contact to editorial office by e-mail for suggestions.

The responsibility for all aspects of manuscript preparation rests with the authors. Extensive changes or rewriting of the manuscript will not be undertaken by the Editors. A standard list of Abbreviations, Acronyms and Symbols is in section 5.

It is best to use the fonts “Times” and “Symbol.” Other fonts, particularly those that do not come bundled with the system software, may not translate properly. Ensure that all special characters (e.g., Greek characters, math symbols) are present in the body of the text as characters and not as graphic representations. Be sure that all characters are correctly represented throughout the manuscript—e.g., 1 (one) and l (letter l), o (zero) and O (letter o).

All text (including the title page, abstract, all sections of the body of the paper, figure captions, scheme or chart titles, and footnotes and references) and tables should be in one file. Graphics may be included with the text or uploaded as separate files. Manuscripts that do not adhere to the guidelines may be returned to authors for correction.

2.1.1 Articles of all kind. Use page size A4. Vertically orient all pages. Articles of all kind must be double-spaced including text, references, tables, and legends. This applies to figures, schemes, and tables as well as text. They do not have page limitations but should be kept to a minimum length. The experimental procedures for all of experimental steps must be clearly and fully included in the experimental section of the manuscripts.

2.1.2 Nomenclature. It is the responsibility of the authors to provide correct nomenclature. It is acceptable to use semisynthetic or generic names for certain specialized classes of compounds, such as steroids, peptides, carbohydrates, etc. In such a case, the name should conform to the generally accepted nomenclature conventions for the compound class. Chemical names for drugs are preferred. If these are not practical, generic names, or names approved by the World Health Organization, may be used.

Authors may find the following sources useful for recommended nomenclature:

- The ACS Style Guide; Coghill, A. M., Garson, L. R., Eds.; American Chemical Society: Washington DC, 2006.
- Enzyme Nomenclature; Webb, E. C., Ed.; Academic Press: Orlando, 1992.

· IUPHAR database of receptors and ion channels (<http://www.guidetopharmacology.org/>).

2.1.3 Compound Code Numbers. Code numbers (including peptides) assigned to a compound may be used as follows:

- Once in the manuscript title, when placed in parentheses AFTER the chemical or descriptive name.
- Once in the abstract.
- Once in the text (includes legends) and once to label a structure. Code numbers in the text must correspond to structures or, if used only once, the chemical name must be provided before the parenthesized code number, e.g., “chemical name (JEM-398).” If appearing a second time in the text, a bold Arabic number must be assigned on first usage, followed by the parenthesized code number, e.g., “1 (JEM-398).” Subsequently, only the bold Arabic number may be used. All code numbers in the text must have a citation to a publication or a patent on first appearance.

Compounds widely employed as research tools and recognized primarily by code numbers may be designated in the manuscript by code numbers without the above restrictions. Their chemical name or structure should be provided as above. Editors have the discretion of determining which code numbers are considered widely employed.

2.1.4 Trademark Names. Trademark names for reagents or drugs must be used only in the experimental section. Do not use trademark or service mark symbols.

2.1.5 Interference Compounds. Active compounds from any source must be examined for known classes of assay interference compounds and this analysis must be provided in the General Experimental section. Many of these compounds have been classified as Pan Assay Interference Compounds (PAINS; see Baell & Holloway, *J. Med. Chem.* 2010, 53, 2719-2740). These compounds shown to display misleading assay readouts by a variety of mechanisms by forming reactive compounds. Provide firm experimental evidence in at least two different assays that reported compounds with potential PAINS liability are specifically active and their apparent activity is not an artifact.

2.2 Manuscript Organization

2.2.1 Title Page. Title: The title of the manuscript should reflect the purposes and findings of the work in order to provide maximum information in a

computerized title search. Minimal use of nonfunctional words is encouraged. Only commonly employed abbreviations (e.g., DNA, RNA, ATP) are acceptable. Code numbers for compounds may be used in a manuscript title when placed in parentheses AFTER the chemical or descriptive name.

Authors' Names and Affiliations: The authors' full first names, middle initials, last names, and affiliations with addresses at time of work completion should be listed below the title. The name of the corresponding author should be marked with an asterisk (*).

2.2.2 Abstract and keywords. Articles of all types must have an abstract following the title page. The maximum length of the Abstract should be 150 words, organized in a findings-oriented format in which the most important results and conclusions are summarized. Code numbers may be used once in the abstract.

After the abstract, a section of Keywords not more than five has to be given. Be aware that the keywords, chosen according to the general concept, are very significant during searching and indexing of the manuscripts.

2.2.3 Introduction. The rationale and objectives of the research should be discussed in this section. The background material should be brief and relevant to the research described.

2.2.4. Methodology. Materials, synthetic, biological, demographic, statistical or experimental methods of the research should be given detailed in this section. The authors are free to subdivide this section in the logical flow of the study. For the experimental sections, authors should be as concise as possible in experimental descriptions. General reaction, isolation, preparation conditions should be given only once. The title of an experiment should include the chemical name and a bold Arabic identifier number; subsequently, only the bold Arabic number should be used. Experiments should be listed in numerical order. Molar equivalents of all reactants and percentage yields of products should be included. A general introductory section should include general procedures, standard techniques, and instruments employed (e.g., determination of purity, chromatography, NMR spectra, mass spectra, names of equipment) in the synthesis and characterization of compounds, isolates and preparations described subsequently in this section. Special attention should be called to hazardous reactions or toxic compounds. Provide analysis for known classes of assay interference compounds.

The preferred forms for some of the more commonly used abbreviations are mp, bp, °C, K, min, h, mL, µL, g, mg, µg, cm, mm, nm, mol, mmol, µmol, ppm,

TLC, GC, NMR, UV, and IR. Units are abbreviated in table column heads and when used with numbers, not otherwise. (See section 4 for more abbreviations)

2.2.5 Results and Discussion. This section could include preparation, isolation, synthetic schemes and tables of biological and statistical data. The discussions should be descriptive. Authors should discuss the analysis of the data together with the significance of results and conclusions. An optional conclusions section is not required.

2.2.6 Ancillary Information. Include pertinent information in the order listed immediately before the references.

PDB ID Codes: Include the PDB ID codes with assigned compound Arabic number. Include the statement “Authors will release the atomic coordinates and experimental data upon article publication.”

Homology Models: Include the PDB ID codes with assigned compound Arabic number. Include the statement “Authors will release the atomic coordinates upon article publication.”

Corresponding Author Information: Provide telephone numbers and email addresses for each of the designated corresponding authors.

Present/Current Author Addresses: Provide information for authors whose affiliations or addresses have changed.

Author Contributions: Include statement such as “These authors contributed equally.”

Acknowledgment: Authors may acknowledge people, organizations, and financial supporters in this section.

Abbreviations Used: Provide a list of nonstandard abbreviations and acronyms used in the paper, e.g., YFP, yellow fluorescent protein. Do not include compound code numbers in this list. It is not necessary to include abbreviations and acronyms from the Standard Abbreviations and Acronyms listed in section 4.

2.2.7 References and Notes. Number literature references and notes in one consecutive series by order of mention in the text. Numbers in the text are non-parenthesized superscripts. The accuracy of the references is the responsibility of the author. List all authors; do not use et al. Provide inclusive page numbers. Titles may have capitalization of first word only (excluding, for example, acronyms and trade names) or standard capitalization as shown below. The chosen style should be used consistently throughout the references. Double-space the references using the following format.

· For journals: Rich, D. H.; Green, J.; Toth, M. V.; Marshall, G. R.; Kent, S. B. H. Hydroxyethylamine Analogues of the p17/p24 Substrate Cleavage Site Are Tight Binding Inhibitors of HIV Protease. *J. Med. Chem.* **1990**, *33*, 1285-1288.

· For online early access: Rubner, G.; Bendsdorf, K.; Wellner, A.; Kircher, B.; Bergemann, S.; Ott, I.; Gust, R. Synthesis and Biological Activities of Transition Metal Complexes Based on Acetylsalicylic Acid as Neo-Anticancer Agents. *J. Med. Chem.* [Online early access]. DOI: 10.1021/jm101019j. Published Online: September 21, 2010.

· For periodicals published in electronic format only: Author 1; Author 2; Author 3; etc. Title of Article. *Journal Abbreviation* [Online] **Year**, *Volume*, Article Number or other identifying information.

· For monographs: Casy, A. F.; Parfitt, R. T. *Opioid Analgesics*; Plenum: New York, 1986.

· For edited books: Rall, T. W.; Schleifer, L. S. Drugs Effective in the Therapy of the Epilepsies. In *The Pharmacological Basis of Therapeutics*, 7th ed.; Gilman, A. G., Goodman, L. S., Rall, T. W., Murad, F., Eds.; Macmillan: New York, 1985; pp 446-472

List submitted manuscripts as “in press” only if formally accepted for publication. Manuscripts available on the Web with a DOI number are considered published. For manuscripts not accepted, use “unpublished results” after the names of authors. Incorporate notes in the correct numerical sequence with the references. Footnotes are not used.

2.2.8 Tables. Tabulation of experimental results is encouraged when this leads to more effective presentation or to more economical use of space. Tables should be numbered consecutively in order of citation in the text with Arabic numerals. Footnotes in tables should be given italic lowercase letter designations and cited in the tables as superscripts. The sequence of letters should proceed by row rather than by column. If a reference is cited in both table and text, insert a lettered footnote in the table to refer to the numbered reference in the text. Each table must be provided with a descriptive title that, together with column headings, should make the table self-explanatory. Titles and footnotes should be on the same page as the table. Tables may be created using a word processor’s text mode or table format feature. The table format feature is preferred. Ensure each data entry is in its own table cell. If the text mode is used, separate columns with a single tab and use a return at the end of each row. Tables may be inserted in the text where first mentioned or may be grouped after the references.

2.2.9 Figures, Schemes/Structures, and Charts. The use of illustrations to convey or clarify information is encouraged. Structures should be produced with the use of a drawing program such as ChemDraw. Authors using other drawing packages should, in as far as possible, modify their program's parameters so that they conform to ChemDraw preferences. Remove all color from illustrations, except for those you would like published in color. Illustrations may be inserted into the text where mentioned or may be consolidated at the end of the manuscript. If consolidated, legends should be grouped on a separate page(s). Include as part of the manuscript file.

To facilitate the publication process, please submit manuscript graphics using the following guidelines:

1. The preferred submission procedure is to embed graphic files in a Word document. It may help to print the manuscript on a laser printer to ensure all artwork is clear and legible.
2. Additional acceptable file formats are: TIFF, PDF, EPS (vector artwork) or CDX (ChemDraw file). If submitting individual graphic files in addition to them being embedded in a Word document, ensure the files are named based on graphic function (i.e. Scheme 1, Figure 2, Chart 3), not the scientific name. Labeling of all figure parts should be present and the parts should be assembled into a single graphic.

EPS files: Ensure that all fonts are converted to outlines or embedded in the graphic file. The document settings should be in RGB mode. **NOTE:** While EPS files are accepted, the vector-based graphics will be rasterized for production. Please see below for TIFF file production resolutions.

3. TIFF files (either embedded in a Word doc or submitted as individual files) should have the following resolution requirements:

- Black & White line art: 1200 dpi

- Grayscale art (a monochromatic image containing shades of gray): 600 dpi

- Color art (RGB color mode): 300 dpi

- The RGB and resolution requirements are essential for producing high-quality graphics within the published manuscript. Graphics submitted in CMYK or at lower resolutions may be used; however, the colors may not be consistent and graphics of poor quality may not be able to be improved.

- Most graphic programs provide an option for changing the resolution when you are saving the image. Best practice is to save the graphic file at the final resolution and size using the program used to create the graphic.

4. Graphics should be sized at the final production size when possible. Single column graphics are preferred and can be sized up to 240 points wide (8.38 cm.). Double column graphics must be sized between 300 and 504 points (10.584 and 17.78 cm's). All graphics have a maximum depth of 660 points (23.28 cm.) including the caption (please allow 12 points for each line of caption text).

Consistently sizing letters and labels in graphics throughout your manuscript will help ensure consistent graphic presentation for publication.

2.2.10 Image Manipulation. Images should be free from misleading manipulation. Images included in an account of research performed or in the data collection as part of the research require an accurate description of how the images were generated and produced. Apply digital processing uniformly to images, with both samples and controls. Cropping must be reported in the figure legend. For gels and blots, use of positive and negative controls is highly recommended. Avoid high contrast settings to avoid overexposure of gels and blots. For microscopy, apply color adjustment to entire image and note in the legend. When necessary, authors should include a section on equipment and settings to describe all image acquisition tools, techniques and settings, and software used. All final images must have resolutions of 300 dpi or higher. Authors should retain unprocessed data in the event that the Editors request them.

2.3 Specialized Data

2.3.1 Biological Data. Quantitative biological data are required for all tested compounds. Biological test methods must be referenced or described in sufficient detail to permit the experiments to be repeated by others. Detailed descriptions of biological methods should be placed in the experimental section. Standard compounds or established drugs should be tested in the same system for comparison. Data may be presented as numerical expressions or in graphical form; biological data for extensive series of compounds should be presented in tabular form.

Active compounds obtained from combinatorial syntheses should be resynthesized and retested to verify that the biology conforms to the initial observation. Statistical limits (statistical significance) for the biological data are usually required. If statistical limits cannot be provided, the number of determinations and some indication of the variability and reliability of the results should be given. References to statistical methods of calculation should be included.

Doses and concentrations should be expressed as molar quantities (e.g., mol/kg, $\mu\text{mol/kg}$, M, mM). The routes of administration of test compounds and vehicles used should be indicated, and any salt forms used (hydrochlorides, sulfates, etc.) should be noted. The physical state of the compound dosed (crystalline, amorphous; solution, suspension) and the formulation for dosing (micronized, jet-milled, nanoparticles) should be indicated. For those compounds found to be inactive, the highest concentration (in vitro) or dose level (in vivo) tested should be indicated.

If human cell lines are used, authors are strongly encouraged to include the following information in their manuscript:

- the cell line source, including when and from where it was obtained;
- whether the cell line has recently been authenticated and by what method;
- whether the cell line has recently been tested for mycoplasma contamination.

2.3.2 Purity of Tested Compounds.

Methods: All scientifically established methods of establishing purity are acceptable. If the target compounds are solvated, the quantity of solvent should be included in the compound formulas. No documentation is required unless asked by the editors.

Purity Percentage: All tested compounds, whether synthesized or purchased, should possess a purity of at least 95%. Target compounds must have a purity of at least 95%. In exceptional cases, authors can request a waiver when compounds are less than 95% pure. For solids, the melting point or melting point range should be reported as an indicator of purity.

Elemental analysis: Found values for carbon, hydrogen, and nitrogen (if present) should be within 0.4% of the calculated values for the proposed formula.

2.3.3 Confirmation of Structure. Adequate evidence to establish structural identity must accompany all new compounds that appear in the experimental section. Sufficient spectral data should be presented in the experimental section to allow for the identification of the same compound by comparison. Generally, a listing of ^1H or ^{13}C NMR peaks is sufficient. However, when the NMR data are used as a basis of structural identification, the peaks must be assigned.

List only infrared absorptions that are diagnostic for key functional groups. If a series contains very closely related compounds, it may be appropriate merely to list the spectral data for a single representative member when they share a common major structural component that has identical or very similar spectral features.

3. Submitting the Manuscript

3.1 Communication and log in to Author's Module All submissions to Acta Pharmaceutica Scientia should be made by using e-Collittera (Online Article Acceptance and Evaluation) system on the journal main page (www.actapharmsci.com)

3.2 Registration to System It is required to register into the e-Collittera system for the first time while entering by clicking "Create Account" button on the registration screen and the fill the opening form with real information. Some of the information required in form is absolutely necessary and the registration will not work if these fields are not completely filled.

After the registration, a "Welcome" mail is sent to the user by the system automatically reminding user name and password. Authors are expected to return to the entry screen and log on with their user name and password for the submission. Please use only English characters while determining your username and password.

If you already registered into the e-Collittera system and forget your password, you should click on "Forgot My Password" button and your user name and password will be mailed to your e-mail in a short while.

3.3 Submitting A New Article The main page of author module consists of various parts showing the situation of manuscripts in process. By clicking the New Manuscript button, authors create the beginning of new submission, a process with a total of 9 consecutive levels. In first 7 levels, information such as the article's kind, institutions, authors, title, summary, keywords etc. are asked respectively as entered. Authors can move back and forth while the information is saved automatically. If the transaction is discontinued, the system move the new submission to "Partially Submitted Manuscripts" part and the transaction can be continued from here.

3.1.1 Sort of Article Authors should first select the type of article from the drop down menu.

Warning. If "Return to Main Page" button is clicked after this level, the article automatically assigned as "Partially Submitted Manuscripts".

3.2.2 Institutions Authors should give their institutional information during submission.

3.2.3 Authors The authors' surnames, names, institutional information appear as entered order in the previous page. Filling all e-mail addresses are re-

quired. Institutional information is available in **Manuscript Details** table at the top of the screen. After filling all required fields, you may click the **Continue** button.

3.2.4 Title should be English, explaining the significance of the study. If the title includes some special characters such as alpha, beta, pi or gamma, they can easily be added by using the **Title** window. You may add the character by clicking the relevant button and the system will automatically add the required character to the text.

Warning. No additions to cornered parenthesis are allowed. Otherwise the system will not be able to show the special characters.

3.2.5 Abstract The summary of the article should be entered to **Abstract** window at this level. There must be an English summary for all articles and the quantity of words must be not more than 150. If special characters such as alpha, beta, pi or gamma are used in summary, they can be added by **Abstract** window. You may add the character by clicking the relevant button and the system will automatically add the required character to the text. The abstract of the articles are accessible for arbitrators; so you should not add any information related to the institutions and authors in this summary part. Otherwise the article will returned without evaluation. Authors will be required to comply with the rules.

Warning. No additions to cornered parenthesis are allowed. Otherwise the system will not be able to show the special characters.

3.2.6 Keywords There must be five words to define the article at the keywords window, which will diverged with commas. Authors should pay attention to use words, which are appropriate for “*Medical Subjects Headings*” list by National Library of Medicine (NLM).

3.2.7 Cover Letter If the submitting article was published as thesis and/or presented in a congress or elsewhere, all information of thesis, presented congress or elsewhere should be delivered to the editor and must be mentioned by the “Cover Letter” field.

3.3.1 Adding Article This process consists four different steps beginning with the loading of the article in to system. **Browse** button is used to reach the article file, under the **Choose a file to upload** tab. After finding the article you may click to **Choose File** and file will be attached.

Second step is to select the file category. Options are: Main Document, Black and White Figure, Color Figure and Video.

The explanation of the files (E.g., Figure 1, Full Text Word File, supplements etc.) should be added on third step and the last step is submitting the prepared article into the system. Therefore, **Download** button under the **Send your file by clicking on download button** tab is clicked.

Reminder If the prepared article includes more than one file (such as main document, black and white figure, video), the transaction will be continued by starting from the first step. The image files must be in previously defined format. After all required files were added, **Continue** button should be clicked. All details and features of the article might be reached from the **Article Information** page.

This page is the last step of the transaction which ensures that entered information is controlled.

3.3.2 Your Files After adding the article you may find all information related to article under **Your Files** window.

File Information This window includes file names, sizes, forming dates, categories, order numbers and explanations of files. The details about the files can be reached by clicking on **Information** button.

If you click on **Name of File**, the file download window will be opened to reach the copy of the file in system.

File Download This window submits two alternatives, one of them is to ensure the file to be opened in valid site and the second one is to ensure to download submitted file into the computer.

Opening the Category part on fourth column can change the category of the file.

Opening the Order column on fifth column can change the order of file.

The file can be deleted by clicking on **Delete** button on the last column. Before deleting, system will ask the user again if it's appropriate or not.

3.3.3 Sending Article Last level is submitting the article and the files into the system. Before continuing the transaction, **Article Information** window must be controlled where it is possible to return back; by using **Previous** button and required corrections can be made. If not, clicking the **Send the Article** button completes transaction.

3.3.4 Page to Follow The Article The Main Page of Author ensures possibility to follow the article. This page consists three different parts; some infor-

mation and bridges related to the sent articles, revision required articles and the articles that are not completed to be sent.

3.3.4.1 Articles Not Completed to be Sent After the sending transaction was started, if article is not able to continue until the ninth step or could not be sent due to technical problems shown at this part. Here you can find the information such as the article's number which is assigned by system, title and formation date. You may delete the articles by using **Delete** button on the right column, if the article is not considered to send into the system.

3.3.4.2 Articles That Require Revision Articles, which were evaluated by the referee and accepted by the editor with revision, continues to **Waiting for Revision** table.

The required revisions can be seen in “**Notes**” part by clicking the articles title.

In order to send any revision, **Submit Revision** button on the last column should be clicked. This connection will take the author to the first level of **Adding Article** and the author can complete the revision transaction by carrying out the steps one by one. All changes must be made in the registered file and this changed file must be resent. Author's most efficacious replies relating to the changes must be typed in “Cover Letter” part.

If the is transaction is discontinued, the system move the revised article to **Submitted Manuscripts** part and the transaction can be continued from here.

After the transaction was completed, the system moves the revised article to “Submitted Manuscripts” part.

3.3.5 Submitted Manuscripts Information related to articles can be followed through the **Submitted Manuscripts** line. Here you can find the information such as the article's number assigned by system, title, sending date and transaction situation. The **Manuscript Details** and summary files can be reached by clicking the title of the article and the **Processing Status** part makes it possible to follow the evaluation process of the article.

ORIGINAL ARTICLES

Isolation of Two Homologous Triterpenes with Antimalarial Activities from the Leaf Extract of *Combretum Zenkeri*

Wande Oluyemi^{1,2}, Babatunde Samuel^{1*}, Kahlig Hans-Peter³, Taramelli Donatella⁴, Krenn Liselotte²

1 University Of Ibadan, Pharmaceutical Chemistry Department, Ibadan/Oyo, Nigeria.

2 University of Vienna, Department of Pharmacognosy, Althanstrasse, Vienna, Austria.

3 University of Vienna, Department of Organic Chemistry, WähringerStrasse, Vienna, Austria.

4 Università degli Studi di Milano, Dipartimento di Scienze Farmacologiche, Milano, Milan, Italy.

ABSTRACT

Combretum genus (Combretaceae) is used locally in the treatment of various diseases including malaria. Current study aimed to investigate the antiplasmodial activities of methanol extract of *C. zenkeri* in *Plasmodium falciparum* chloroquine sensitive (D10) and resistant (W2) strains and identify the bioactive principles. Repeated chromatographic separation was carried out on the chloroform fraction to afford the isolation of bioactive compounds which was characterized by application of spectroscopic techniques (ESI-MS, HR-ESIMS, 1D and 2D NMR). Antiplasmodial activities of chloroform fraction (D10; $IC_{50} = 12.57 \pm 1.57 \mu\text{g/mL}$ and W2; $IC_{50} = 12.14 \pm 0.95 \mu\text{g/mL}$) showed more activity than the n-butanol fraction (D10; $IC_{50} = 61.98 \pm 3.25 \mu\text{g/mL}$ and W2; $IC_{50} = 61.26 \pm 8.64 \mu\text{g/mL}$). Phytochemical investigation of the extract afforded isolation of two triterpenes with antimalarial activities. This paper identified for the first time the antimalarial principles in *C. zenkeri* as ursolic and oleanolic acids; which justified the local use of the plant in the treatment of malaria.

Keywords: *C. zenkeri*, antimalarial, bioguided isolation, triterpenes, *Plasmodium falciparum*.

*Corresponding Author: Babatunde Samuel, e-mail: tundebsamuel@gmail.com

Wande Oluyemi ORCID Number: 0000-0003-3646-2488

Babatunde B. Samuel ORCID Number: 0000-0002-1834-9548

Kahlig Hans-Peter ORCID Number: 0000-0002-9526-4396

Taramelli Donatella ORCID Number: 0000-0001-5108-4492

Krenn Liselotte ORCID Number: 0000-0002-3898-6501

(Received 04 February 2019, accepted 24 March 2019)

INTRODUCTION

Infectious diseases, among which is malaria, are the serious problem and cause of morbidity and mortality worldwide, particularly in the developing countries. This accounts for approximately 50% of all deaths where access to health care is inadequate.¹ Medicinal plants as the backbone of traditional medicine have over the years been subjected to serious pharmacological investigations with a view to discovering new bioactive molecules.^{2,3} *Combretum* is the largest genus of the Combretaceae family with about 370 species.⁴ Several species of *Combretum* are used in traditional medicine for treating various kinds of diseases by many communities across Africa.⁵ Phytochemical studies of a number of *Combretum* species have led to the isolation of triterpenoids with different pharmacological actions such as antimicrobial, anti-inflammatory anticancer and many others.⁶⁻⁸ Triterpenoids, glycosides and acidic compounds were also identified as possible antimalarial agents in medicinal plants.⁹ *Combretum zenkeri* is a widely distributed climbing shrub used in tropical West Africa from Guinea to Southern Nigeria and Cameroon. The decoction preparation of the leaves of this plant is used as purgative, the twig is chewed by Ivory Coast women to relieve menstrual pain, treating intestinal worms and malaria treatment.¹⁰ In Western Nigeria, *Combretum zenkeri* leaves are used in the treatment of inflammatory diseases like rheumatoid–arthritis, and the roots used frequently in recipes for managing cancer.^{11,12} In previous studies, several pharmacological investigations for *Combretum zenkeri* such as nephro-protective effect,¹³ hepatoprotective effect,¹⁴ anti-oxidative activity and neuro-protective effect¹⁵ and cytotoxic activity¹² have been validated. In our more recent study, preliminary screening of 10 Combretaceae species showed that *Combretum zenkeri* possessed antimalarial activity.¹⁶ All these pharmacological effects show *Combretum zenkeri* as a promising and important phyto-agent in the search of bioactive compounds for the treatment of diseases. Until now, to the best of our knowledge, no bioactive constituent is reported to have been isolated from *Combretum zenkeri*, which prompted us to investigate its active constituents. Current study focus on the investigation of the antimalarial potential of *C. zenkeri* methanol extract and fractions which led to the isolation of two related triterpenes: ursolic acid (**1**) and oleanolic acid (**2**). This is the first time any bioactive principle is reported to have been identified from *C. zenkeri*.

METHODOLOGY

General experimental methods

1D and 2D Nuclear Magnetic Resonance (NMR) data were performed by using a Bruker 500 MHz NMR spectrometer. The samples were measured at 298 K

in fully deuterated methanol. The resonance frequency for ^1H and ^{13}C NMR was 700.40 MHz. Standard 1D and gradient-enhanced 2D experiments, such as, DEPT, COSY, TOCSY, NOESY, HSQC and HMBC were used. Electrospray ionization mass-spec (ESI-MS) and high-resolution mass spectrometric analyses were performed on a maxis mass spectrometer. The sum formulas of the ions were determined using Bruker Compass Data Analysis 4.1. Flash chromatography was performed on an InterchimPuriFlash 4250 system, equipped with an evaporative light scattering detector (ELSD), a photodiode array (PDA), and a fraction collector controlled by Interchim software. PuriFlash column 30 silica HG (120 g, 20 bar) served as stationary phase. The fractions obtained from all chromatographic steps were analyzed by TLC (mobile phase: $\text{CH}_3\text{Cl}/\text{MeOH}$, 95:5 or 97:3 depending on the polarity of all the fractions; stationary phase: Merck silica gel 60 F₂₅₄, detected after derivatization with anisaldehyde/ H_2SO_4 spray reagent under visible light, UV₂₅₄ and UV₃₆₆).

Plant material

Fresh leaves of *Combretum zenkeri* was collected in March 2017 from the Botanical Garden of the University of Ibadan. The plant was identified by Mr. Owolabi, the curator of the Botanical Garden. The authentication was done, and the Voucher specimen was deposited at Forestry Research Institute of Nigeria (FRIN), Ibadan and the Voucher number obtained as FHI/110277.

Plant extraction and isolation

The air-dried and ground leaf of *C. zenkeri* (500 g) was extracted with methanol using soxhlet apparatus. The extract was filtered and evaporated to dryness using rotary evaporator and afterwards placed inside a desiccator to remove residual solvent. Liquid-liquid partitioning was performed on the extract to give three different fractions (chloroform, n-butanol and aqueous). The dried methanol extract (10 g) was successively partitioned between CHCl_3 and H_2O and n-BuOH and H_2O . The different fractions obtained were also dried on Buchi rotary evaporator at 40 °C to yield 700 mg CHCl_3 fraction, 2.8 g n-BuOH fraction and 5.6 g water fraction. The CHCl_3 fraction was then selected for further phytochemical investigation according to its appropriate antiplasmodial properties (the lowest IC_{50}). To afford the major bioactive compound(s) of the plant, the CHCl_3 fraction (600 mg) was further sub-fractionated by silica column (PuriFlash column 30 silica HP 40G 20 bar) flash CC with a $\text{CHCl}_3/\text{MeOH}/\text{H}_2\text{O}$ gradient as mobile phase (36.54 mins 98%:2%:0%; 36.94 mins 90%:9%:1%; 36.94 mins 80%:17%:3%; 36.94 mins 70%:25%:5%; 18.94 mins 60%:35%:5%) to yield 301 fractions which were later pooled according to the similarities in their TLC profile to give 9 fractions (FCZ1 to FCZ9). The fractions were concentrated to

dryness under reduced pressure with Buchi rotary evaporator at 40 °C. FCZ2 (90 mg) was investigated further by means of chromatographic separation on a silica glass column (1cm x 60cm; 250 mL column vol.) filled with silica gel 60 (70-230 mesh) (Merck) and separated by isocratic elution with mixture of $\text{CHCl}_3/\text{MeOH}/\text{H}_2\text{O}$ 95+1.5+0.1. The flow rate was set at 2 mL/30 minutes on electronic automatic fraction collector. This produced 21 fractions (F1-F21). From the TLC profiles, F12-F15 as a result of their similarities in TLC pattern afforded compound **CZ-A** (5 mg), a white amorphous powder; a mixture of two isomers which could not be separated by chromatography.

Antiplasmodial test of extract and fractions

In vitro maintenance of *Plasmodium falciparum* strains

Two different strains of *P. falciparum*, W2 (chloroquine-resistant) and D10 (chloroquine-sensitive), were used for the chemosensitivity tests. Both strains were cultured according to the method described by Trager and Jensen with slight modifications^{17,18}. The parasites were cultured in human type A-positive erythrocytes at 5% hematocrit at 37°C in a standard gas mixture consisting of 1% O_2 , 5% CO_2 , 94% N_2 . The medium was RPMI-1640 (EuroClone, Celbio) with the addition of 1% AlbuMax (lipid-rich bovine serum albumin) (Invitrogen, Milan, Italy), 0.01% hypoxanthine (Sigma, Italy), 20mM Hepes (EuroClone, Celbio) and 2mM L-glutamine (EuroClone, Celbio). For routine parasite growth, the parasitemia was maintained within 1% and 5%, and evaluated in Giemsa colored smears, as the number of infected RBC with respect to the total number of erythrocytes counted.

Drug sensitivity assay

For the drug sensitivity assay, a colorimetric method was used based on the detection of parasite LDH¹⁹. Parasite growth was determined by measuring the activity of the parasite lactate dehydrogenase (pLDH), according to a modified version of Makler's method¹⁹. Antimalarial activity was determined and expressed as the 50% inhibitory concentrations (IC_{50} , concentration of drug required to inhibit 50% parasite growth). Each IC_{50} value is the mean \pm standard deviation of at least three separate experiments performed in duplicate.

RESULTS AND DISCUSSION

The methanol extract of the leaves of *C. zenkeri* was concentrated under a reduced pressure and then partitioned successively with CHCl_3 , n-BuOH and H_2O . The CHCl_3 soluble fraction, according to its appropriate antiplasmodial activity (lowest IC_{50}), was selected for silica flash CC followed by a glass column separation over a silica gel to afford compound **CZ-A** (5 mg). The structure of **CZ-A**

was unambiguously determined and elucidated by spectroscopic experiments including 1D (^1H and ^{13}C NMR), 2D NMR (COSY, TOCSY, NOESY, HSQC and HMBC), ESI-MS and HR-ESIMS, and by comparison with reported data in related literature. Compound **CZ-A** was found to be an isomeric mixture (1:0.4) as revealed from the spectroscopic information. The MS gave a molecular ion peak at m/z 456 (M-H) relating to $\text{C}_{30}\text{H}_{48}\text{O}_3$. The isomers were identified as ursolic acid (3β -hydroxyurs-12-en-28-oic acid) (**1**)²⁰ and oleanolic acid (3β -hydroxyolean-12-en-28-oic acid) (**2**)²¹ (figure 1). This study is one among others carried out on species of *Combretum* genus where compounds were isolated as mixtures of two isomers. From *C. nelsonii*, arjunolic acid with asiatic acid as mixtures of two isomers were isolated.²² Likewise in another study, ursolic acid with oleanolic acid as isomeric mixture, and maslinic acid with 2α , 3β -dihydroxyurs-12-en-28-oic acid as isomeric mixture were isolated from *C. zeyheri*.²³ Compound **2** showed a signal pattern very similar to those of **1** in both ^1H and ^{13}C experiments (Table 1), but with the main difference noted in the DEPT experiment, where **1** and **2** possessed seven and eight quaternary carbon atom (C), seven and six methine group (CH), nine and ten methylene group (CH_2), respectively, with seven methyl groups for each compound. The chemical shifts of olefinic carbons revealed on ^{13}C NMR signals help to unambiguously identify compounds **1** and **2**. Previous report has confirmed that for the olean-12-ene type, the chemical shifts of the double bond C_{12} and C_{13} are around 122.0 and 144.0, respectively, while those of its isomer urs-12-ene are around 125.0 and 139.0, respectively, for the same carbons.²⁴ This characteristic chemical shifts of oleanane and ursane triterpenes are consistent with ^{13}C NMR signals generated in this study; help to establish the difference between compound **1** and **2** and elucidate their structures in the mixture. 3β -hydroxyurs-12-en-28-oic acid and its isomer, 3β -hydroxyolean-12-en-28-oic acid are reported to have been isolated from *Combretum zenkeri* for the first time in this study.

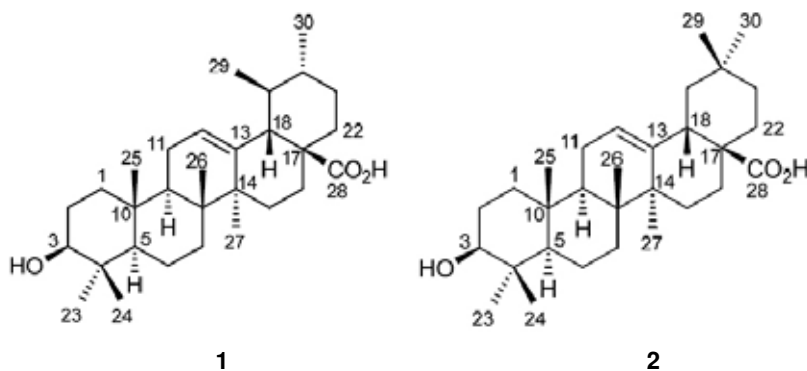


Figure 1. Compound 1 and 2, isomeric mixture identified in CZ-A isolated from *C. zenkeri*

Table 1. ^1H and ^{13}C NMR (700MHz) data generated for compound 1 and 2 in CD_3OD

	1		2	
	$\delta_{\text{H}}\text{m (J in Hz)}\delta_{\text{C}}$		$\delta_{\text{H}}\text{m (J in Hz)}\delta_{\text{C}}$	
1	1.67 m 1.01	39.99	1.63 m 0.99 m	39.83
2	1.63 m 1.56	27.90	1.63 m 1.56	27.87
3	3.15 dd (11.7, 4.6)	79.70	3.15 m	79.71
4	-	39.84	-	40.55
5	0.75 dd (11.8, 1.6)	56.74	0.76 m	56.76
6	1.56 m 1.42 m	19.47	1.56 m 1.42 m	19.50
7	1.55 m 1.34 m	34.33	1.51 m 1.32 m	34.02
8	-	40.78	-	40.78
9	1.55 m	49.06	1.59 m	49.10
10	-	38.10	-	38.17
11	1.93 m	24.36	1.93 m	24.52
12	5.23 t (3.7)	126.88	5.24 t (3.7)	123.62
13	-	139.66	-	145.25
14	-	43.25	-	42.89
15	1.93 m 1.09 m	29.22	1.78 m 1.08 m	28.85
16	2.04 m 1.65	25.33	1.74 m 1.26	24.06
17	-	49.10	-	47.67
18	2.20 dd (11.5, 1.0)	54.38	2.85 m	42.75
19	1.38 m	40.44	1.69 m 1.12 m	47.27
20	0.99 m	40.42	-	31.62
21	1.50 m 1.35 m	31.79	1.39 m 1.20 m	34.91
22	1.70 m 1.63 m	38.13	1.74 m 1.54 m	33.84
23	0.98 s	28.76	0.97 s	28.73
24	0.78 s	16.37	0.78 s	16.31
25	0.96 d (0.6)	16.02	0.95 d (0.6)	15.88
26	0.85 s	17.81	0.82 s	17.73
27	1.12 d (0.7)	24.08	1.16 d (0.7)	26.38
28	-	181.74	-	181.96
29	0.88 d (6.5)	17.64	0.94 s	23.98
30	0.96 m	21.57	0.91 s	33.57

Table 2. Antiplasmodial activity of *C. zenkeri* methanol extract and fraction in *P. falciparum* chloroquine sensitive (D10) and resistant (W2) strains.

	D10 (IC ₅₀ µg/mL) ^a	W2 (IC ₅₀ µg/mL) ^a
<i>C. zenkeri</i> MeOH extract	68.98 ± 1.00 ^c	69.68 ± 3.09 ^d
CHCl ₃ fraction	12.57 ± 1.57	12.14 ± 0.95
n-BuOH fraction	61.98 ± 3.25 ^b	61.26 ± 8.64 ^b
Chloroquine (ng/mL)	13.1 ± 2.4	217.0 ± 28.0

^aData are the mean ± SD of three different experiments in duplicate

^bThe activity of CHCl₃ fraction is significantly (P<0.05) higher compared with n-BuOH

^cThe activity of CHCl₃ fraction is significantly (P<0.001) higher compared with *C. zenkeri* MeOH extract

^dThe activity of CHCl₃ fraction is significantly (P<0.01) higher compared with *C. zenkeri* MeOH extract

Antiplasmodial test was carried out in *P. falciparum* chloroquine sensitive (D10) and resistant (W2) strains to check the activities of *C. zenkeri* extract and fractions obtained from solvent-solvent partitioning and the results are summarized in Table 2. The water fraction was not tested due to its high tannin content which interferes with the actual antimalarial activity. The *C. zenkeri* methanol extract showed good antiplasmodial activities (IC₅₀ = 68.98±1.00 µg/mL) and (IC₅₀ = 69.68±3.09 µg/mL) for both chloroquine sensitive D10 and resistant W2 strains respectively. In this experiment, the chloroform fraction showed promising activities (IC₅₀ = 12.57±1.57 µg/mL) and (IC₅₀ = 12.14±0.95 µg/mL) more than 5-folds active than the crude extract for both sensitive D10 and resistant W2 strains respectively. This observation is indicative of the fact that the major compound(s) responsible for the antimalarial activities in the *C. zenkeri* methanol extract situate in the chloroform soluble fraction. The anti-malarial activity of the extract would be partly or majorly due to the presence of ursolic acid because this compound isolated from *Morinda lucida* was shown to exhibit excellent *in vitro* and *in vivo* antimalarial activities.²⁵ Interesting *in vitro* antiplasmodial activities (IC₅₀ = 3.1±1.3 µg/mL), about 5-folds more active than oleanolic acid (IC₅₀ = 15.2±3.4 µg/mL) against a chloroquine sensitive *P. falciparum* strain was reported.²⁵ Likewise for *in vivo* test in the same study, ursolic acid produced 97.7% chemosuppression of parasitemia in mice infected with *Plasmodium berghei berghei*, greater reduction in parasitemia compared to oleanolic acid 37.5%. Although effort is currently ongoing to isolate and purify other compounds from the said chloroform fraction, as there may be other principles with related activities from this extract. In this study the activity test of their mixture (ursolic/oleanolic acids) was not possible as a result of insufficient amount isolated. Although, in a few cases the activity of their mixture in other pharmacological activities has shown to be greater than

that of the single compounds,^{26,27} and extensive data about the synergistic antimalarial activity of these two isomers is lacking. Some studies have recently described ursolic acid as a pentacyclic triterpenoid with a wide spectrum of pharmacological activities such as protective effect on lungs, kidneys, liver and brain, anti-inflammatory properties, anabolic effect on skeletal muscles, anti-osteoporosis, antimicrobial effect against numerous strains of bacteria, anti HIV and HCV viruses and antimalarial among others^{28,29,30} Consequently, it is plausible to suggest that the presence of ursolic acid in *C. zenkeri* contribute hugely to the different pharmacological actions¹³⁻¹⁶ exerted by the plant. However, it is important to widely explore *C. zenkeri* for its other bioactive constituents which may be useful lead compounds or scaffolds necessary for their synthesis for many other pharmacological investigations important. An analogue of ursolic acid, N-{3-[4-(3-aminopropyl)piperazinyl]propyl}-3-O-acetylursolamide, which reported showed better antimalarial activity (175 nM) than the aglycone.³¹ This report showed that the ursolic acid derivative which showed to be non-toxic demonstrated a new potent antimalarial prototype that disrupts plasmodium calcium homeostasis.

Ongoing studies in our laboratory is targeted at creating several derivatives of ursolic acid with a view to obtaining more potent and less toxic antimalarial agents. These studies further highlight the need for further investigation of unexplored *Combretum* species of Africa, particularly *Combretum zenkeri*.

The Combretaceae family is significant in the search for bioactive compounds useful in the treatment of malaria. This study showed the antimalarial potential of *Combretum zenkeri* and justified its use in traditional medicine. Triterpenoids have contributed largely to the antimalarial activities of several medicinal plants.

Two closely related triterpenes, ursolic acid and oleanolic acid were isolated as known antimalarial principles from *Combretum zenkeri*. Ursolic acid may contribute largely to the antimalarial effect of the extract. Further studies are ongoing on *Combretum zenkeri* to isolate more possible compounds which could possess antimalarial or other pharmacological activities.

ACKNOWLEDGEMENTS

The first author appreciates The Austrian Agency for International Cooperation in Education, Science and Research (OeAD-GmbH)- Ernst Mach for the scholarship awarded to complete this work in University of Vienna, Austria.

REFERENCES

1. Mosaffa-Jahromi, M.; Lankarani, K.B.; Pasala, M.; Afsharypuor, S.; Tamaddon, A.M. Efficacy and safety of enteric coated capsules of anise oil to treat irritable bowel syndrome. *J. Ethnopharmacol.* **2016**, *194*, 937-946.
2. Samuel, B.; Oluyemi, W. M.; Abiodun, O. Bio-guided investigation of the antimalarial activities of *Trema orientalis* (L.) Blume leaves. *Afr. J. Biotechnol.* **2015**, *14*, 2966-2971.
3. Makhafola, T.J.; Samuel, B.B.; Elgorashi, E.E.; Eloff, J.N. Ochnaflavone and Ochnaflavone 7-O-methyl Ether: two Antibacterial Biflavonoids from *Ochna pretoriensis* (Ochnaceae). *Nat. Prod. Commun.* **2012**, *7*, 1601-1604.
4. McGaw, L.J.; Rabe, T.; Sparg, S.G.; Jäger, A.K.; Eloff, J.N.; Van Staden, J. An investigation on the biological activity of *Combretum* species. *J. Ethnopharmacol.* **2001**, *75*, 45-50.
5. Eloff, J.N.; Katerere, D.R.P.; McGaw, L.J. The biological activity and chemistry of the southern African Combretaceae. *J. Ethnopharmacol.* **2008**, *119*, 686-699.
6. Eloff, J.N. The antibacterial activity of 27 southern African members of the Combretaceae. *S. Afr. J. Sci.* **1999**, *95*, 148-152.
7. Angeh, J.E.; Huang, X.; Sattler, I.; Swan, G.E.; Dahse, H.; Hartl, A.; Eloff, J.N. Antimicrobial and anti-inflammatory activity of four known and one new triterpenoid from *Combretum imberbe* (Combretaceae). *J. Ethnopharmacol.* **2007**, *110*, 56-60.
8. Pettit, G.R.; Singh, S.B.; Niven, M.L.; Schimdt, J.M. Cell growth inhibitory dihydrophenanthrene and phenanthrene constituents of the African tree *Combretum caffrum*. *Can. J. Chem.* **1988**, *66*, 406-413.
9. Dibua, U.M.; Okeke, C.C.; Ugwu, C.; Kenechukwu, F.C.; Okorie, A. *In vivo* antimalarial and cytotoxicity activity of ethanolic stem bark of *Petersianthus macrocarpus* and leaf of *Astonia boonei* in experimental mice model. *Int. J. Curr. Microbiol. App. Sci.* **2013**, *2*, 354-368.
10. Ujowundu, C.O.; Okafor, O.E.; Agha, N.C.; Nwaogu, L.A.; Igwe, K.O.; Igwe, C.U. Phytochemical and chemical composition of *C. zenkeri* leaves. *J. Med. Plant Res.* **2010**, *4*, 965-968.
11. Gbolade, A. A.; Ogbale, O. O.; Ajaiyeoba, E. O. Ethnobotanical Survey of Plants used in Treatment of Inflammatory Diseases in Ogun State of Nigeria. *Euro. J. Sc. Res.* **2010**, *43*, 183-191.
12. Sowemimo, A.; Van de Venter, M.; Baatjies, L.; Koekemoer, T. Cytotoxic activity of selected Nigerian plants. *Afr. J. Trad. CAM.* **2009**, *6*, 526-528.
13. Ogbonna, C.U.; Ujowundu, C.O.; Okwu, G.N.; Emejulu, A.A.; Alisi, C.S.; Igwe, K.O. Biochemical and histological evaluation of benzo[a]pyrene induced nephrotoxicity and therapeutic potentials of *C. zenkeri* leaf extract. *Afr. J. Pharm. and Pharmacol.* **2016**, *10*, 873-882.
14. Okwu, G.N.; Ogbonna, C.U.; Ujowundu, C.O.; Igwe, K.O.; Igwe, C.U.; Emejulu A.A. 2014. Protective effect of ethanol leaf extract of *C. zenkeri* on liver functions of Albino rats following benzo[a]pyrene exposure. *Biol. Chem. Res.* **2014**, 16-25.
15. Ujowundu, C.O.; Ogbonna, C.U.; Okwu, G.N.; Alisi, C.S. Free radicals scavenging and neuroprotective effects of ethanolic leaf extract of *Combretumzenkeri*. *Annu. Res. Rev. Bio.*, **2015**, *6*, 133-141.
16. Oluyemi, M. W.; Samuel, B. B. In vitro screening of ten Combretaceae plants for antimalarial activities applying the inhibition of beta-hematin formation. *Int. J. Biol. Chem. Sci.* **2017**, *11*, 2971-2981.

17. Trager, W.; Jensen, J. B. Human malaria parasites in continuous culture. *Science*, **1976**, *193*, 673–675.
18. Ilboudo, D.P.; Basilico, N.; Parapini, S.; Corbett, Y.; D'Alessandro, S.; Dell'Agli, M.; Coghi, P.; Karou, S.D.; Sawadogo, R.; Gnoula, C.; Simporé, J.; Nikiema, J.B.; Monti, D.; Bosisio, E.; Taramelli, D. Antiplasmodial and anti-inflammatory activities of *Canthium henriquesianum* (K. Schum), a plant used in traditional medicine in Burkina Faso. *J. Ethnopharmacol.* **2013**, *148*, 763–769.
19. Makler, M. T.; Ries, J. M.; Williams, J. A.; Bancroft, J. E.; Piper, R. C.; Gibbins, B. L.; Hinrichs, D. J. Parasite Lactate Dehydrogenase as an Assay for Plasmodium falciparum Drug Sensitivity. *Am. J. Trop. Med. Hyg.* **1993**, *48*, 739–741.
20. Venditti, A.; Lattanzi, C.; Ornano, L.; Maggi, F.; Sanna, C.; Ballero, M.; Alvinao, A.; Serafini, M.; Bianco, A. A new glucosidicphthalide from *Helichrysum microphyllum* sub sp. *Tyr-rhenicum* from La Maddalena Island (Sardinia, Italy), *Nat. Prod. Res.*, **2016**, *30*, 789–795.
21. Kipchakbaeva, A.K.; Eskalieva, B.K.; Burasheva, G.Sh.; Adikari, A.; Aisa, H.A.; Choudhary, M.I. Saponins from *Climacoptera subcrassa*. *Chem. Nat. Compds*, **2016**, *52*, 363–364.
22. Masoko, P.; Mdee, L.K.; Mampuru, L.J.; Eloff J.N. Biological activity of two related triterpenes isolated from *Combretum nelsonii* (Combretaceae) leaves. *Nat. Prod. Res.* **2008**, *22*, 1074–1084.
23. Runyoro, D.K.B.; Srivastava, S.K.; Darokar, M.P.; Olipa, N.D.; Joseph, C.C.; Matee, M.I.N. Anticandidiasis agents from a Tanzanian plant, *C. zeyheri*. *Med. Chem. Res.* **2013**, *22*, 1258–1262.
24. Mahato, S.B.; Kundu, A.P. ¹³C NMR spectra of pentacyclic triterpenoids—a compilation and some salient features. *Phytochemistry*, **1994**, *37*, 1517–1575.
25. Cimanga, R.K.; Tona, G.L.; Mesia, G.K.; Kambu, O.K.; Bakana, D.P.; Kalenda, P.D.T.; Penge, A.O.; Muyembe, J.T.; Totte, J.; Pieters, L.; Vlietinck, A.J. Bioassay-guided isolation of triterpenoid acids from the leaves of *Morinda lucida*. *Pharm Biol.* **2006**, *44*, 677–681.
26. Bisio, O.A.; Schito, A.M.; Parricchi, A.; Mele, G.; Romussi, G.; Malafrente, N.; Oliva, P.; Tommasi, N. Antibacterial activity of constituents from *Salvia buchananii* Hedge (Lamiaceae). *Phytochem. Lett.* **2015**, *14*, 170–177.
27. Jimenez-Arellanes, A.; Luna-Herrera, J.; Cornejo-Garrido, J.; Lopez-Garcia, S.; Castro-Mussot, M.E.; Meckes-Fischer, M.; Mata-Espinosa, D.; Marquina, B.; Torres, J.; Hernandez-Pando, R. Ursolic and oleanolic acids as antimicrobial and immunomodulatory compounds for tuberculosis treatment. *BMC Complement. Altern. Med.* **2013**, *13*, 258.
28. Wozniak, L.; Skapska, S.; Marszalek, K. Ursolic acid- A pentacyclic triterpenoid with a wide spectrum of pharmacological activities. *Molecules*, **2015**, *20*, 20614–20641.
29. Awan, Z.I.; Habib-Ur-Rehman, Minhas, F.A.; Awan, A.A. Antiplasmodial activity of compounds isolated from *Viburnum nervosum*. *Int. J. Pharm. Sci. Invent.* **2013**, *2*, 19–24.
30. Jie Liu. Oleanolic acid and ursolic acid: Research perspectives. *J. Ethnopharmacol.* **2005**, *100*, 92–94.
31. Innocente, A.M.; Silva, G.N.S.; Cruz, L.N.; Moraes, M.S.; Nakabashi, M.; Sonnet, P.; Gosmann, G.; Garcia, C.R.S.; Gnoatto, S.C.B. Synthesis and antiplasmodial activity of betulinic acid and ursolic acid analogues. *Molecules*, **2012**, *17*, 12003–12014.

Flax Seed Mucilage-chitosan Polyelectrolyte Complex Nanoparticles: Optimization, Characterization and Evaluation

Meenakshi Bhatia^{1*}, Sunidhi Lohan¹

¹ Guru Jambheshwar University of Science and Technology, Department of Pharmaceutical Sciences Hisar, India.

ABSTRACT

The aim of this study is to prepare flaxseed mucilage (FSM) and chitosan polyelectrolyte complex (PEC) nanoparticles by ionic gelation method for developing sustained release formulation. For the formation of PEC nanoparticles, the water extract of flax seed is obtained by soaking the seeds in water overnight followed by precipitation with ethanol and washing with distilled water. FSM was interacted with fully protonated chitosan (in acetic acid 2% v/v) using Isonicotinylhydrazide (INH) as a model drug. The results of optimization study reveals that lower level of chitosan and flaxseed mucilage favors the lowest particle size. The optimum quantum of FSM and chitosan were found to be 0.011% (w/v) and 0.011% (w/v) respectively, that produced nanometric particles of size 326 nm with poly-dispersity index (PdI) of 0.217. The *in vitro* release profile of INH from the optimized batch was determined using the dialysis sac and it was found that INH get released over a prolonged period of 20 hours following Higuchi's square root release kinetics with the combination of diffusion and erosion of matrix as release mechanism. It can be concluded from the present study that interaction between chitosan and FSM can be used for the formation of PEC nanoparticles and for developing sustained release formulation.

Keywords: Flaxseed, chitosan, polyelectrolyte, complex, nanoparticles.

INTRODUCTION

Flax (*Linum usitatissimum*), also known as common flax or linseed consists of the dried fully ripe seeds of the genus *Linum* belonging to family *Linaceae*¹. Chemically, it contains d-galacturonic acid, l-rhamnose, l-galactose, and d-xylose. It is gluten free and also rich in omega-3, omega-6, α -linolenic acid, lignans, high quality proteins and fibers. The flax seed mucilage has been widely

*Corresponding Author: Meenakshi Bhatia, e-mail: meenaxibhatia@gmail.com

Meenakshi Bhatia ORCID Number: 0000-0003-4568-7582

Sunidhi Lohan ORCID Number: 0000-0002-2085-8720

(Received 15 March 2019, accepted 20 May 2019)

explored in traditional herbal remedies, food and pharmaceutical industry. Flaxseed is a multi component system containing biologically-active plant substances like dietary fiber, oil, protein, soluble polysaccharides, phenolic compounds, minerals, vitamins and lignans². It also contains water soluble and insoluble fibers. Insoluble fibers help in improving laxation and preventing constipation, chiefly by increasing fecal mass and lowering bowel transit time³. Moreover, water-soluble fibers helps in maintaining glucose levels and lowering the cholesterol levels in blood⁴. Flax lignans is known to be effective in reducing the growth of particularly hormone sensitive cancerous tumors, such as those of the breast, endometrium and prostate⁵. Flaxseeds were also used as medicines since immemorial times to relieve the abdominal pain and as cough remedy. Flaxseeds possess significant health benefits besides the nutrition due to high content of ω -3 α -linolenic acid and of lignans having antioxidant properties².

Chitosan (CS) is commonly obtained from deacetylated (D-glucosamine) derivative of chitin, a cationic polysaccharide. It has already been explored for formulating nanoparticles with polyanions by ionotropic gelation method⁶. The complexes of chitosan with polyanions have been screened in effectively limiting the release of entrapped drug as compared to the polyanion or chitosan alone. PEC nanoparticles of chitosan with psyllium arabinosylan⁷, hyaluronic acid⁸, carboxymethyl gum kondagogu⁹, carboxymethyl amylopectin¹⁰, gum ghatti¹¹ and sodium alginate¹² have been reported in literature. Isonicotinylhydrazide (INH) is an antibiotic that is used in the treatment of tuberculosis¹³. It is used in combination with other tuberculosis drugs to prevent the development of drug resistance and also act as bactericidal and bacteriostatic drug. It also acts as a source of free radicals by inhibiting the cytochrome P450 system. The solubility of INH in water is 125mg/ml at room temp. It is on the border line of BCS Class I & III¹⁴. In this piece of research work PEC nanoparticles of CS-FSM were prepared by ionotropic gelation method using INH as a model drug. The PEC nanoparticles was characterized by fourier-transform infra-red spectroscopy, X-ray diffraction analysis, thermo gravimetric analysis and scanning electron microscopy. The interaction of Chitosan-FSM in preparing PEC nanoparticles was optimized by using two-factor, three-level central composite experimental design. *In-vitro* release behaviour of drug INH from the optimised batch of PEC nanoparticles was evaluated by release rate study.

METHODOLOGY

Flax seeds were purchased from Patanjali mega store, Hisar, India. Chitosan was purchased from Sisco Research Laboratories Pvt. Ltd. Mumbai, India.

Isonicotinylhydrazide (INH) was generously provided as a gift sample from Aventis Pharma Ltd (Ankleshwar, India). All other chemicals like ethanol and acetic acid (SD Fine Chemical Ltd.) used in this study were of analytical grade and utilised as received.

Isolation of flaxseed mucilage

The water extract of flax seed was obtained by soaking the seeds in distilled water (1:50) overnight. The insoluble fraction was removed by passing it through the muslin cloth. To isolate the mucilage, equal volume of ethanol was added for precipitation under continuous stirring. The separated mucilage is then washed with distilled water and collected through filtration by muslin cloth. The mucilage so obtained was kept at -80°C for 4 h followed by lyophilization in a laboratory model freeze drier at -90°C under a pressure of 0.0010 mbar for 24 h.

Preparation of flaxseed mucilage–chitosan PEC nanoparticles

FSM was interacted with fully protonated chitosan (in acetic acid 2% v/v) using INH as a model drug for the preparation of PEC nanoparticles. Aqueous chitosan solutions were prepared in acetic acid (2% w/v) under stirring while aqueous solutions of FSM were prepared by adding the required quantity of FSM as per the design protocol in distilled water followed by stirring. The polyelectrolyte complex nanoparticles of FSM-CS were prepared by drop wise addition of aqueous solution of CS (0.010 to 0.020% w/v) containing INH (50 % of the total polymer weight) to the aqueous solution of FSM (0.010 to 0.020% w/v) under strong agitation at room temperature⁷.

Experimental design

The preparation of FSM-CS polyelectrolyte nanoparticles was optimised using 2-factor,3-level central composite experimental design (Table I). It was discerned from the preliminary trials that concentration of FSM and CS affect the p-size, polydispersity index (PdI) and entrapment efficiency. Therefore, the concentration of chitosan (X_1) and FSM (X_2) were taken as the formulation variables whereas particle size (Y_1), PdI (Y_2) and entrapment efficiency (Y_3) were selected as response variables. Each of the independent variable was investigated at three levels (i.e. -1 , 0 , $+1$). Design Expert software (Version 11.0) was used for the experimental design and statistical analysis of data⁷.

Table 1. Particle size, Pdl and entrapment efficiency of different batches of CS-FSM polyelectrolyte complex nanoparticles.

Batch	Conc. of chitosan (% w/v) (X_1)	Conc. of FSM (% w/v) (X_2)	P- size (d-nm) (Y_1)	Pdl (Y_2)	Entrapment efficiency (%) (Y_3)
1	0.015	0.015	425	0.312	87.5
2	0.015	0.010	377	0.256	87.3
3	0.010	0.015	350	0.249	87.0
4	0.010	0.010	327	0.230	85.2
5	0.015	0.020	413	0.391	88.9
6	0.015	0.015	442	0.307	87.8
7	0.015	0.015	456	0.289	86.8
8	0.010	0.020	372	0.235	85.7
9	0.020	0.020	712	0.472	92.0
10	0.015	0.015	468	0.338	87.2
11	0.020	0.015	565	0.464	91.0
12	0.020	0.010	532	0.391	89.0
13	0.015	0.015	481	0.374	86.7

Characterization of flaxseed mucilage and chitosan PEC nanoparticles:

The polyelectrolyte complex nanoparticles of flaxseed mucilage–chitosan containing INH drug were characterised by Fourier transform infra-red spectroscopy (FT-IR), Differential scanning calorimeter (DSC), Powder X-ray diffraction analysis (PXRD) and Scanning electron microscopy (SEM) studies and further evaluated for particle size (d, nm), polydispersity index (PdI), and drug entrapment efficiency.

Particle size analysis

Average particle size and polydispersity index (PdI) of nanoparticles was measured by using Zetasizer (Nano ZS90, Malvern Instrument, UK). The measurements were done in automated mode at 25°C after equilibrating for 120 s.

Entrapment efficiency

The amount of drug entrapped in nanoparticles was calculated by separating the untrapped drug by centrifuging the sample at 15000 rpm for 40 min by cooling centrifuge (C-24 BL, Remi Instruments, and Mumbai, India). The supernatant was analyzed for the contents of untrapped INH by measuring the absorbance at 262 nm in a UV-Vis spectrophotometer (Cary 5000, Varian Australia). The entrapment efficiency (%) was calculated as follows:

Where, INH_t is the total amount of isoniazid used in the preparation of polyelectrolyte complex nanoparticles and INH_s is the untrapped isoniazid present in the supernatant.

Fourier transform infra-red spectroscopy (FT-IR)

FSM-CS PEC nanoparticles were subjected to FT-IR spectroscopy in a FTIR spectrophotometer (Perkin-Elmer, Spectrum, US) in range of 4000cm^{-1} to 400cm^{-1} using KBr pellet method, to detect interaction between drug and polymer.

Powder X-ray diffraction analysis (PXRD)

Powder X-ray diffraction analysis was carried out to study the structure, composition and physical properties of samples. The CS, FSM, INH and PEC powder samples were examined using an X-ray diffractometer (Miniflex 2, Rigaku, Japan) from 0° to 80° diffraction angle (2Θ) range under the following measurement conditions: source, nickel filtered Cu-K α radiation; voltage 30 kV; current 25 mA; scan speed 0.05 min^{-1} , division slit 1.25° , receiving slit 0.3 mm.

Differential scanning calorimeter

Differential scanning calorimetric analysis was carried out to confirm the physical state and purity of the samples. The DSC of CS, FSM, INH and PEC were carried out in the temp. range of 25°C to 250°C under constant nitrogen purge of 100ml/min with heating rate of 10°C per minute using DSC (Perkin Elmer USA).

Scanning electron microscopy

The surface and shape of the polyelectrolyte complex was examined using scanning electron microscopy. The sample was mounted using double sided adhesive tape on metal grids and coated with gold under vacuum prior to observation.

***In-vitro* drug release study**

The drug release from the optimized batch formulation and drug solution was determined using dialysis sac method using USP-II dissolution apparatus. An accurately measured volume of nanoparticles (5ml) and equivalent amount of drug solution were placed in the dialysis tubing (cut off 10,000 kDa) separately. The dialysis tubing was tied up to the paddle of USP type II dissolution apparatus (TDL-08L, Electro lab, India) and immersed in 300 ml of dissolution fluid (phosphate buffer pH 7.4). The temp. of dissolution media was maintained at $37^{\circ}\text{C} \pm 0.5^{\circ}\text{C}$ with continuous stirring at 50 rpm. An aliquot of 5 ml sample was withdrawn at various time intervals and the media volume was maintained by replacing equal volumes of fresh media i.e. buffer pH 7.4. The concentration of INH in the samples was determined in UV-visible spectrophotometer by measuring absorbance at 262 nm. The release data was then fitted into various release kinetic models to estimate the kinetic and mechanism of release.

RESULTS AND DISCUSSION

CS-FSM PEC nanoparticles prepared by ionic gelation method were optimized using 2-factor,3-level central composite design (Design expert version 11.0) and characterized by FTIR, DSC, XRD and SEM studies. The *in-vitro* release pattern of optimized batch was estimated using USP type II dissolution apparatus using dialysis sac.

Figure 1 exhibits the FT-IR spectra of PEC, CS, INH, and FSM respectively in the frequency range of $4000\text{-}400\text{cm}^{-1}$. The spectra of CS show a broad absorption band at 3422.04 cm^{-1} which may be attributed to -OH stretching of alcohols. The peak appearing at 2874.61 cm^{-1} can be ascribed to -CH stretch of alkanes, while the peak at 2145.70 cm^{-1} is due to $\text{-C}\equiv\text{C-}$ stretch of alkynes, whereas peak at 1602.93 cm^{-1} is due to -NH bending whereas peaks at 1420.62 cm^{-1} and 1384.11 cm^{-1} are due to -CH bending of alkanes. The spectra of FSM exhibit a broad absorption band at 3423.63 cm^{-1} is due to -OH stretching of alcohols. The peak appearing at 2933 cm^{-1} is due to -CH stretching of alkane, while the peaks appearing at 2345.45 cm^{-1} and 2364.71 cm^{-1} may be ascribed to -CH stretch of alkane. The peaks at 1618.03 cm^{-1} and 1420.42 cm^{-1} are due to -NH bending and -CH bending, respectively. The spectra of pure drug INH shows a sharp absorption peak at 3304.06 cm^{-1} due to presence of (-NH_2) amine group and other peak at 3114.02 cm^{-1} is due to -NH stretch of amine group and other peak -CH on 2862.74 cm^{-1} , -C=O stretch on 1666.53 cm^{-1} , -NH bending on 1602.55 cm^{-1} and 1556.24 cm^{-1} shows presence of amide group. Peak at 1411.93 cm^{-1} shows -CH bending of alkane, while peak at 1334.23 cm^{-1} , 1221.32 cm^{-1} and 1141.62 cm^{-1} are due to -CN stretch of amine. The spectra of

CS-FSM PEC displayed characteristic peak of drug at 1648 cm^{-1} that is attributed to amide carbonyl structure of hydrazide in PEC and the peak appearing at 1087.02 cm^{-1} may be ascribed to $-\text{CN}$ stretch of amine whereas peak appearing at 1024.20 cm^{-1} is due to $-\text{C}-\text{O}$ stretch of ether. The peaks at 889.87 cm^{-1} and 672.51 cm^{-1} are due to $=\text{C}-\text{H}$ bending of alkene appeared in PEC. The spectra of CS-FSM polyelectrolyte complex demonstrated a slight shift of the peak at 3292.27 cm^{-1} due to interaction between drug INH and carriers that confirms the formation of complex.

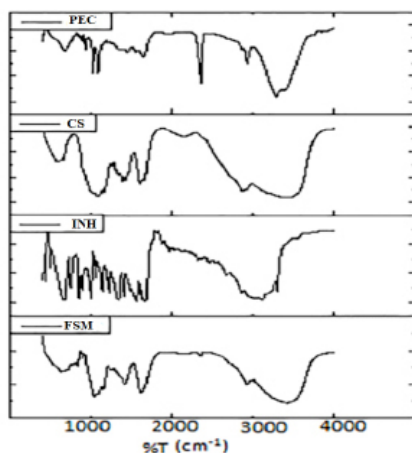


Figure 1. FT-IR spectra of PEC, CS, INH and FSM

Figure 2 represent the thermogram of differential scanning calorimetry (DSC) analysis of PEC, INH, FSM and CS. DSC of samples was carried out by heating the sample from room temperature to 250°C under constant nitrogen purge of 10 ml/min at a heating rate of 10°C per minute. The thermogram of INH shows sharp endothermic peak at 173.03°C that corresponds to its melting point, having AUC $45.0049\text{ (w/g)}^{\circ}\text{C}$ with heat of fusion of 232.62 J/g . The thermograms of FSM and CS are of typical amorphous material showing broad endothermic peak at 78.04°C and 75.92°C having AUC $105.767\text{ (w/g)}^{\circ}\text{C}$ and $64.0613\text{ (w/g)}^{\circ}\text{C}$ and heat of fusion of 355.63 J/g and 178.79 J/g , respectively. However, the thermogram of PEC shows two endothermic peaks at 150.95°C and 163.38°C with heat of fusion of 49.614 J/g and 97.591 J/g respectively. There is a disappearance of broad endotherm and a shift in the endothermic peak with decreased intensity is noticed that indicates that modification has been taken place in the formation of electrolyte complex.

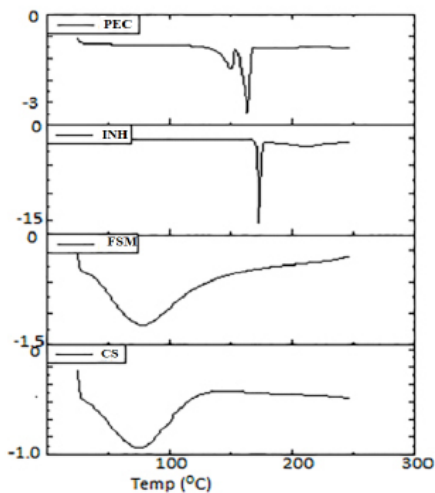


Figure 2. Thermogram of PEC, INH, FSM and CS

Figure 3 displays the X-ray diffraction spectra of PEC, CS, INH and FSM respectively. X-ray diffractogram of CS and FSM is of typical amorphous materials with no sharp peaks. The X-ray diffractogram of INH shows sharp peaks at 15.192° , 16.344° , 19.416° , 24.84° , 27.528° 2θ corresponding to its crystalline structure. However, X-ray pattern of PEC nanoparticles shows appearance of peaks 19.824° , 24.84° , 28.296° , 36.024° , 40.656° , 45.672° 2θ that indicates crystalline nature of final product.

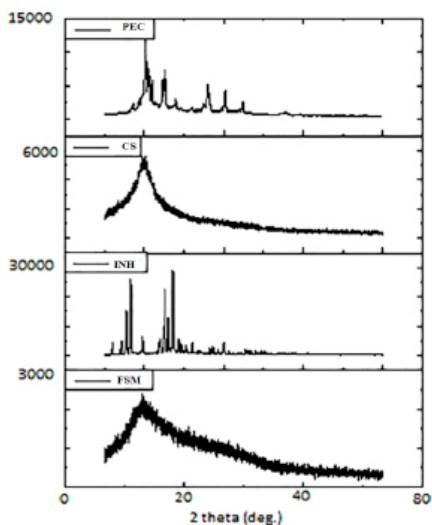


Figure 3. X-ray diffraction spectra of PEC, CS, INH and FSM

Scanning electron microscopy is used to obtain information about the surface topography and composition. Fig. 4 displays the surface morphology of PEC nanoparticles scanned under scanning electron microscope (SEM). A close examination of surface morphology of INH loaded CS-FSM PEC nanoparticles reveals that surface of CS-FSM PEC nanoparticles is rough and granular.

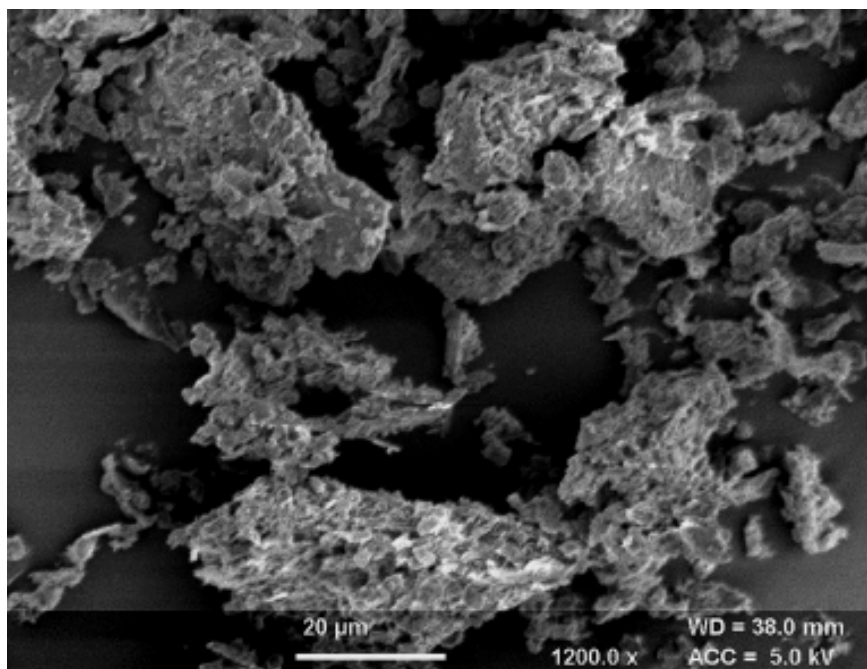


Figure 4. Surface morphology of PEC nanoparticles

Impact of critical process parameter and critical material attributes on the average particle size, PdI and entrapment efficiency of PEC nanoparticles between the FSM and CS was optimized for the formation of nanometric polyelectrolyte complex. The preliminary trial data suggested that concentration of chitosan and flax seed gum influence the p-size of polyelectrolyte particles and PdI. Accordingly, the concentration of chitosan (X_1) and FSM (X_2) were chosen as formulation variables whereas p-size (Y_1), PdI (Y_2) and entrapment efficiency (Y_3) were fixed as response variables to optimize the preparation of polyelectrolyte particles with constraints of minimum p-size and PdI and maximum entrapment efficiency of drug. Table 1 shows the result of PS(Y_1), PdI(Y_2) and EE (Y_3) of PEC nanoparticles prepared as per the design protocol. The response data was fitted into various polynomial models using the experimental design. It was discovered that the responses PdI (Y_2) and entrapment efficiency (Y_3) were fitted best into linear model with none transformation while the response p-

size (Y_1), was fitted best in to linear response surface model with square root transformation.

The polynomial models for the responses Y_1 , Y_2 and Y_3 can be expressed by the equation:

$$\text{Sqrt}(Y_1) = 21.22 + 2.91X_1 + 0.9547X_2 \quad (1)$$

$$(Y_2) = 0.3314 + 0.1022X_1 + 0.0368X_2 \quad (2)$$

$$(Y_3) = 87.85 + 2.35X_1 + 0.8500X_2 \quad (3)$$

The results of ANOVA are summarised in Table II. The polynomial model was found to be significant ($P < 0.0500$) with non-significant lack of fit ($P > 0.05$). The correlation between the experimental and predicted response is determined by the value of $R^2 (> 0.8)$. This value indicated good correlation between the experimental and predicted response. The measurement of signal to noise ratio i.e. adequate precision is much above the required value of 4 indicating the adequate signal and lend the model fit to navigate the design space.

Table 2. Model summary statistics

Response factors	Model					Lack of fit	
	F-value (%)	Prob.> f	R ²	Adeq. Prec	C.V.	F-value	Prob.>f
Y_1 (PS)	32.51	0.0001	0.8667	17.2978	4.38	4.78	0.0759
Y_2 (Pdl)	34.14	0.0001	0.8723	17.9753	9.72	0.9203	0.5592
Y_3 (EE)	24.20	0.0001	0.8288	15.1410	1.00	5.34	0.0635

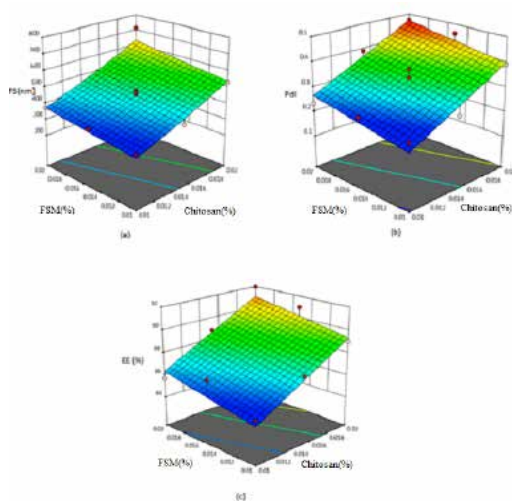


Figure 5. Effect of concentration of CS and FSM on (a) p-size, (b) Pdl and (c) entrapment efficiency (%).

Figure 5 (a,b,c) exhibits the combined effect of concentration of CS and FSM on p-size, PdI and entrapment efficiency (%), respectively. It can be deduced from the plot that a linear relationship exists between dependent and independent variables. It is also observed from the plot that lower concentration of CS and FSM favors the lower particle size with more prominent effect of concentration of CS. This may be described by the fact that higher concentration of CS increases the viscosity of CS dispersion thus resulting in increased droplet size on spraying chitosan on FSM solution and thereby leading to increase in size of polyelectrolyte complex particles. To develop an optimized formulation of INH loaded PEC nanoparticles a numerical optimization technique along with desirability approach was used. The optimization of the CS/FSM concentration was done with the goal of preparing PEC nanoparticles with minimum particle size and minimum PdI and maximum entrapment efficiency. The optimization tool provided different sets of solution. An optimized batch of INH loaded PEC nanoparticle was prepared and analyzed for entrapment efficiency and *in-vitro* release. The recommended parameters were concentration of CS (0.011%w/v) and FSM (0.011 %w/v) that dispensed INH loaded CS-FSM PEC nanoparticles of size 361nm (predicted 326nm) and PdI 0.302 (predicted 0.217) and entrapment efficiency is 82.06 % (predicted 85%). The closer agreement between the predicted and observed values indicates the high prognostic/predictive ability of polynomial model. The optimized batch of INH loaded CS-FSM nano particulate system was evaluated for drug release behavior.

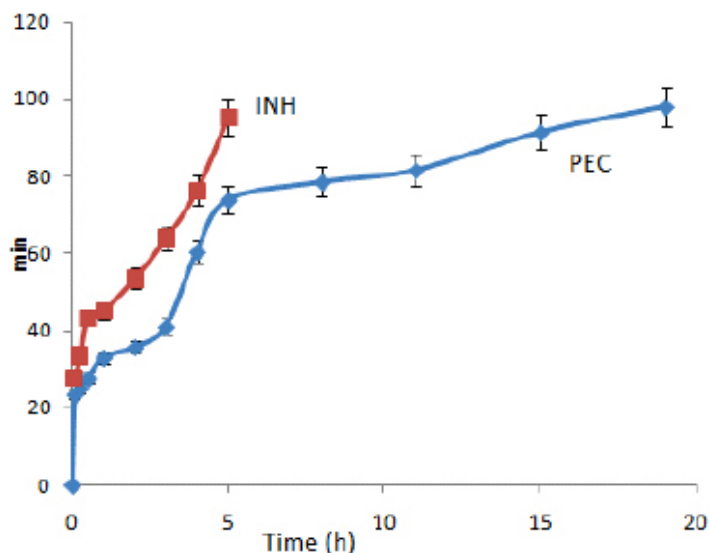


Figure 6. *In vitro* release profile of INH from polyelectrolyte complex and drug solution

Figure 6 is displaying the *in-vitro* release profile of INH nanoparticulate system. The nanoparticulate preparation provided a prolonged release of INH with approximate 98% of drug released in a period of 20h. The limiting effect of dialysis membrane was studied by comparing the release behavior of nanoparticulate system with equivalent concentration of drug solution that showed more than 90 % release in less than 5 h. The release of INH from nanoparticulate system and from drug solution was fitted into various kinetic models to estimate their kinetics and mechanism of release mechanism (Table 3).

Table 3. Modeling and release kinetics of isoniazid from polyelectrolyte nano particulate suspension.

Formulation	Zero Order R ²	First Order R ²	Higuchi R ²	Korsemeier – Peppas	
				R ²	n
Isoniazid solution	0.9021	0.4133	0.9857	0.3168	0.4787
PEC	0.8938	0.4354	0.9658	0.3193	0.4512

The outcomes of release rate data of the formulations were found to be fitted best into Higuchi model (with R² =0.9658) of release kinetics. Further the value of 'n' is 0.4512 (0.43<n<0.85), the release exponent of korsemeier and Peppas equation, indicated that the release of INH from nanoparticulate system occurs by diffusion and erosion mechanism from the matrix.

The interaction between cationic CS and anionic FSG was used to formulate polyelectrolyte complex. The DSC and XRD studies confirm the crystallinity of the product. The optimization study showed that lower level of chitosan (0.011%) and flaxseed gum (0.011%) favors the minimum particle size with more prominent effect of concentration of chitosan. The release of drug INH from PEC nanoparticles occurred over a prolonged period of time following Higuchi square root kinetics model and release occurs by mechanism of diffusion and erosion from the matrix. It can be concluded from the present study that interaction between chitosan and FSG can be used for the formation of PEC nanoparticles and for developing sustained release formulation.

ACKNOWLEDGEMENTS

The authors are thankful to Department of Pharmaceutical sciences, Guru Jambheshwar University of Science & Technology, Hisar for providing necessary facilities.

REFERENCES

1. Dubey, S. D.; Srivastava, N.; Singh, P. K.; Narian, V. Genetic variability in yield and quality traits of linseed at different locations. *J. Oilseed Res.* **2009**, *26*, 161-163.
2. Goyal, A.; Sharma, V.; Upadhyay, N.; Gill, S.; Sihag, M. Flax and flaxseed oil: an ancient medicine and modern functional food. *J. Food Sci. Technol.* **2014**, *51*, 1633-1653.
3. Greenwald, P.; Clifford, C. K.; Milner, J. A. Diet and cancer prevention. *Eur. J. Cancer*, **2001**, *37*, 948-965.
4. Kristensen, M.; Jensen, M. G.; Aarestrup, J.; Petersen, K. E.; **Søndergaard, L.**; Mikkelsen, M. S.; Astrup, A. Flaxseed dietary fibers lower cholesterol and increase fecal fat excretion, but magnitude of effect depend on food type. *Nutr. Metab.* **2012**, *9*, 8.
5. Touré, A.; Xueming, X. Flaxseed lignans: source, biosynthesis, metabolism, antioxidant activity, bio-active components, and health benefits. *Compr. Rev. Food Sci. F.* **2010**, *9*, 261-269.
6. Avadi, M. R.; Sadeghi, A. M. M.; Mohammadpour, N.; Abedin, S.; Atyabi, F.; Dinarvand, R.; Rafiee-Tehrani, M. Preparation and characterization of insulin nanoparticles using chitosan and Arabic gum with ionic gelation method. *Nanomedicine: NBM*, **2010**, *6*, 58-63.
7. Bhatia, M.; Ahuja, M. Psylliumarabinoxylan: Carboxymethylation, characterization and evaluation for nanoparticulate drug delivery. *Int. J. Biol. Macromol.* **2015**, *72*, 495-501.
8. Lim, S. T.; Martin, G. P.; Berry, D. J.; Brown, M. B. Preparation and evaluation of the in vitro drug release properties and mucoadhesion of novel microspheres of hyaluronic acid and chitosan. *J. Control. Release*, **2000**, *66*, 281-292.
9. Kumar, A.; Ahuja, M. Carboxymethyl gum kondagogu–chitosan polyelectrolyte complex nanoparticles: Preparation and characterization. *Int. J. Biol. Macromol.* **2013**, *62*, 80-84.
10. Thakur, K.; Ahuja, M.; Kumar, A. Carboxymethyl functionalization of amylopectin and its evaluation as a nanometric drug carrier. *Int. J. Biol. Macromol.* **2013**, *62*, 25-29.
11. Ahuja, M.; Kumar, A. Gum ghatti–chitosan polyelectrolyte nanoparticles: Preparation and characterization. *Int. J. Biol. Macromol.* **2013**, *61*, 411-415.
12. Motwani, S. K.; Chopra, S.; Talegaonkar, S.; Kohli, K.; Ahmad, F. J.; Khar, R. K. Chitosan–sodium alginate nanoparticles as submicroscopic reservoirs for ocular delivery: Formulation, optimisation and in vitro characterisation. *Eur. J. Pharm. Biopharm.* **2008**, *68*, 513-525.
13. Lougheed, K. E.; Taylor, D. L.; Osborne, S. A.; Bryans, J. S.; Buxton, R. S. New anti-tuberculosis agents amongst known drugs. *Tuberculosis*, **2009**, *89*, 364-370.
14. Becker, C., Dressman, J.B., Amidon, G.L., Junginger, H.E., Kopp, S., Midha, K.K., Shah, V.P., Stavchansky, S., Barends, D.M. (2007). Biowaiver Monographs for Immediate Release Solid Oral Dosage Forms: Isoniazid. *J. Pharm. Sci.* **2007**, *96*, 522-531.

Synthesis and Characterization of Novel Tetrazole Derivatives and Evaluation of Their Anti-candidal Activity

Hiba Maher Tawfeeq¹, Rasim Farraj Muslim^{2*}, Obaid Hasan Abid³,
Mustafa Nadhim Owaid⁴

¹ University Of Anbar, Department of Chemistry, College of Education for Pure Sciences, Anbar/Ramadi, Iraq

² University Of Anbar, Department of Ecology, College of Applied Sciences, Anbar/Hit, Iraq

³ University of Fallujah, Department of Scientific Affairs and Graduate Studies, Anbar/Fallujah, Iraq

⁴ Ministry of Education, Department of Heet Education, Anbar/Hit, Iraq

ABSTRACT

This research includes synthesis of new heterocycles containing disubstituted Tetrazole derivatives. Imine compounds were synthesized by reaction of primary aromatic amines with various substituted benzaldehydes in the presence of glacial acetic acid as catalyst in absolute ethanol to obtain new imine compounds O₁-O₅. The novel five-membered heterocycles as Tetrazole derivatives O₆-O₁₀ were obtained from treatment of each new imine compounds with sodium azide compound. Newly synthesized compounds were identified via spectral methods (FT-IR, ¹H-NMR and ¹³C-NMR) spectra and some physical properties. O₆ is the best derivative that has significantly ($p < 0.01$) recorded a stronger influence to inhibit the growth of *Candida guilliermondii* at an average of the zone of inhibition 14.0 mm. While, O₉ derivative recorded the lowest zone of inhibition 7.3 mm toward the same clinical fungal pathogen. The present work may be helpful in designing more potential antibacterial and antifungal agents for therapeutic use in the future.

Keywords: Tetrazole, *Candida* sp., anti-candidal, imine compounds, sodium azide.

INTRODUCTION

Imine compounds are class of the compounds which contain -HC=N- group, they are usually synthesizing by the condensation of a primary aromatic amino

*Corresponding Author: Mustafa Nadhim Owaid, e-mail: dr.rasim92hmts@gmail.com

Hiba Maher Tawfeeq ORCID Number: 0000-0002-5525-568X

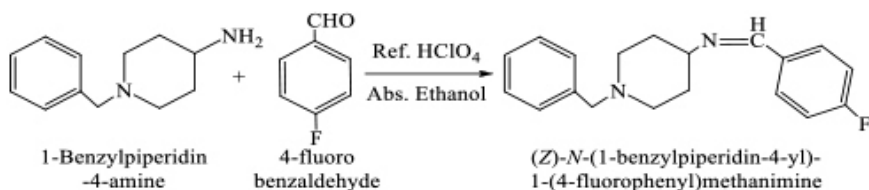
Rasim Farraj Muslim ORCID Number: 0000-0002-8273-2429

Obaid Hasan Abid ORCID Number: 0000-0001-8473-4842

Mustafa Nadhim Owaid ORCID Number: 0000-0001-9005-4368

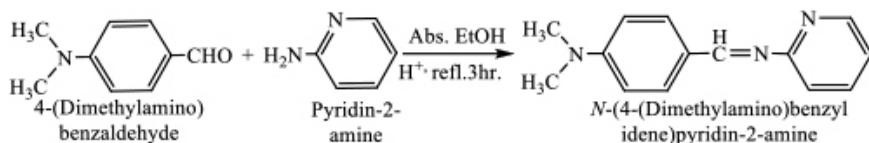
(Received 14 January 2019, accepted 20 May 2019)

group with an active carbonyl aromatic aldehyde. They are versatile precursors in the synthesis of organic, bio-organic, organometallic and industrial compounds via ring closure, cycloaddition and replacement reactions.¹⁻⁴ Imine compounds were discovered by a German chemist, Nobel prize winner, Hugo Schiff in 1864.⁵ Imine compounds produced from the reaction between ketone or aldehyde compounds with amine compounds.⁶ In the presence of perchloric acid (**Scheme 1**) the reaction of 4-fluorobenzaldehyde with 1-benzylpiperidin-4-amine gives the next product.⁷



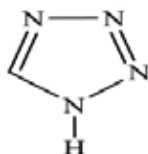
Scheme 1. The effect of perchloric acid on imine compound formation

The reaction of pyridine-2-amine with 4-(dimethyl amino) benzaldehyde (**Scheme 2**) produces the imine compound.⁸



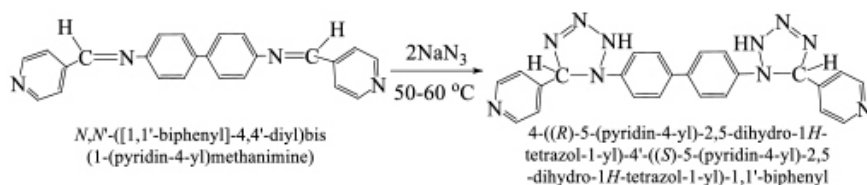
Scheme 2. Using glacial acetic acid to prepare the imine compound

One of the most important chemical compounds is sodium azide, which has been used in many fields including its effect on germination.⁹ Due to its great importance, it was used in the preparation of compounds called tetrazoles. Tetrazoles are a class of synthetic organic heterocyclic compounds consist of five-member ring of four nitrogen atoms and one carbon atom (**Scheme 3**).¹⁰



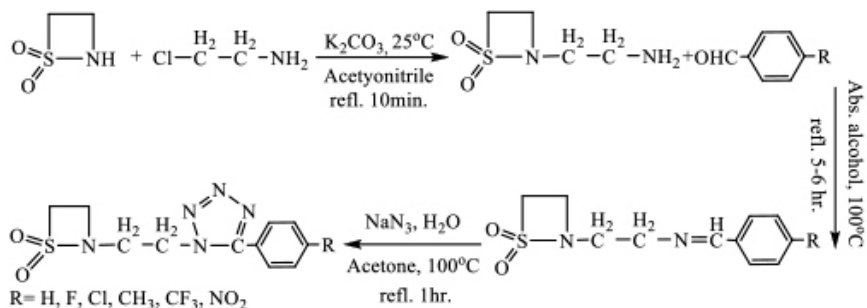
Scheme 3. Structure of tetrazole ring

Synthesis of tetrazole derivatives is an important task in modern medicinal chemistry.¹¹ Tetrazoles are class of heterocycles that have received attention due to their wide range of applications.¹² Pharmacologically, because of the effect of gram-negative or gram-positive bacteria on the health of human, thus some potential drugs/products must be synthesized.^{13,14} Tetrazole contains compounds reported to possess diverse chemotherapeutic activities as antibacterial,¹⁵ and antifungal.¹⁶ Example of one of tetrazole derivatives is the product from the reaction between imine compound (N,N'-([1,1'-biphenyl]-4,4'-diyl) bis (1-(pyridin-4-yl)methanimine)) and sodium azide (**Scheme 4**).¹⁷



Scheme 4. Synthesized of 2,5-dihydro-1H-tetrazol derivative

Tetrazole derivatives of type of 5-phenyl-1H-tetrazol-1-yl) thiazetidine dioxide prepared from the next reaction (**Scheme 5**),¹⁸ below:



Scheme 5. Potassium carbonate in tetrazole derivatives synthesis

This study aims to prepare tetrazole derivatives for first time and investigate their activity against pathogenic fungi, *Candida* spp. *in vitro*.

METHODOLOGY

Materials

All chemicals were obtained and purchased from Sigma Aldrich.

General procedure for the synthesis of imine compounds O₁-O₅

Equimolar mixtures 0.02 mole of aldehydes and aromatic amines and trace of glacial acetic acid dissolved in 25 ml absolute ethanol was placed in a 100-ml round-bottom flask equipped with condenser and stirrer bar. The mixture was allowed to react at reflux (at the boiling temperature of absolute ethanol) for 4hr, then allowed to cool down to the room temperature, whereby a crystalline solid was separated out. The solid product was recrystallized twice from absolute ethanol.¹⁹⁻²² The structural formulae, names, melting points, colors, and percentage of yields for the synthesized imine compounds are recorded in Table 1.

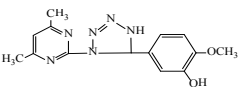
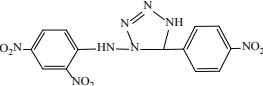
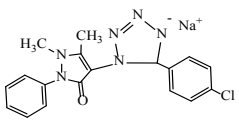
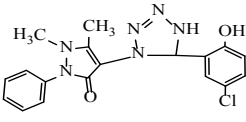
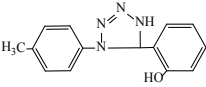
Table 1. Structural formula, nomenclature, melting points, percentages of yield and colors of imine compounds O₁-O₅

Comp. Code	Structural formula	Nomenclature	Yield %	m.p. °C	Color
O ₁		(E)-5-((4,6-dimethylpyrimidin-2-ylimino)methyl)-2-methoxyphenol	68%	78-80	Tan
O ₂		(E)-1-(2,4-dinitrophenyl)-2-(4-nitrobenzylidene)hydrazine	81%	291-293	Orange
O ₃		(E)-4-(4-ethoxybenzylideneamino)-1,5-dimethyl-2-phenyl-1H-pyrazol-3(2H)-one	90%	212-214	Bright yellow
O ₄		4-(5-chloro-2-hydroxybenzylideneamino)-1,5-dimethyl-2-phenyl-1H-pyrazol-3(2H)-one	89%	138-140	Bright pale yellow
O ₅		(E)-2-((p-tolylimino)methyl)phenol	87%	94-96	Bright yellow

General procedure for the synthesis of tetrazole derivatives O₆-O₁₀

Equimolar mixtures 0.01 mole of imine compounds and sodium azide dissolved in 20 ml of tetrahydrofuran and 2 ml of distilled water and refluxed the mixture (at the boiling temperature of tetrahydrofuran and distilled water) for 4 hr and left to stand for 24 hr. The solid product was precipitated, filtered off and recrystallized from absolute ethanol.^{23,24} The structural formulae, names, melting points, colors, and percentage yields for the synthesized tetrazole derivatives are presented in table 2. Melting points were recorded on electrothermal melting point apparatus (uncorrected). FT-IR spectra were recorded at the room temperature from (4000-400) cm⁻¹ with KBr disc by infrared spectrophotometer model tensor 27 Bruker Co., Germany. The ¹H-NMR and ¹³C-NMR spectra were recorded by Bruker Ac-300MHz spectrometer, it making sure from the purity and reaction occur of synthesized derivatives O₆-O₁₀ by the comparison between the physical measurements (Table 1) of O₁-O₅ and the physical measurements of O₆-O₁₀ (Table 2) and between FT-IR spectra of O₁-O₅ (Table 3) and FT-IR spectra of O₆-O₁₀ (Table 4).

Table 2. Structural formula, nomenclature, melting points, percentages of yield and colors of tetrazole derivatives O₆-O₁₀

Comp. code	Structural formula	Nomenclature	Yield %	m.p. °C	Color
O ₆		5-(1-(4,6-dimethylpyrimidin-2-yl)-4,5-dihydro-1H-tetrazol-5-yl)-2-methoxyphenol	81%	107-109	Bright Pale yellow
O ₇		N-(2,4-dinitrophenyl)-5-(4-nitrophenyl)-4,5-dihydro-1H-tetrazol-1-amine	89%	> 300	Pale Orange
O ₈		5-(4-chlorophenyl)-4-(1,5-dimethyl-3-oxo-2-phenyl-2,3-dihydro-1H-pyrazol-4-yl)-4,5-dihydro-1H-tetrazol-1-ide	93%	242-244	Pale yellow
O ₉		4-(5-(5-chloro-2-hydroxyphenyl)-4,5-dihydro-1H-tetrazol-1-yl)-1,5-dimethyl-2-phenyl-1H-pyrazol-3(2H)-one	85%	169-171	Pale yellow
O ₁₀		R)-2-(1-p-tolyl-4,5-dihydro-1H-tetrazol-5-yl)phenol	84%	119-120	Bright Golden

Anti-Candidal activity

This test was achieved *in vitro* to investigate inhibitory effects of the synthesized tetrazole derivatives using well diffusion method on Muller-Hinton agar. This experiment was done as mentioned by Owaed et al.^{25,26} Four milligrams of each tetrazole derivative was dissolved in DMSO and applied separately as 4 mg/well (6 mm-well). After 18 hr of incubation at 37 °C, the zone of inhibition was taken using the ruler in millimeters.

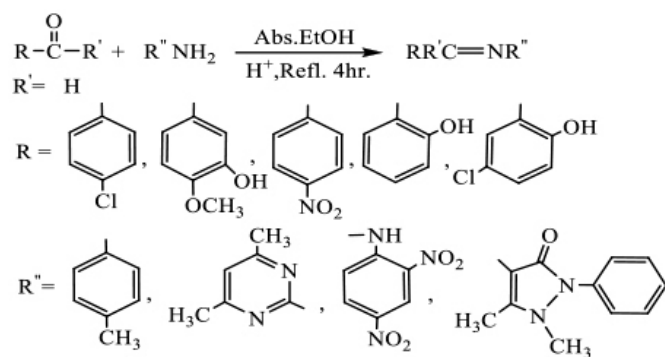
Statistical Analysis

The data (triplicates) were analyzed by one-way analysis of variance using ANOVA table by SAS program for Windows, version 9.0, SAS Institute Inc., USA. The significance of differences was calculated using Duncan's Multiple Range Test (DMRT). Probability value least than 1% was considered to be statistically significant.

RESULTS AND DISCUSSION

Imine compounds O₁-O₅

Imine compounds (**Scheme 6**) were synthesized from commercially available aromatic aldehydes and primary amines and identified by their melting points, and FT-IR. The FT-IR spectra showed the appearance of the stretching absorption bands of azomethine (C=N) at 1591-1669 cm⁻¹,^{27,28} beside the characteristic bands of the residual groups in the structure Table 3. See Figs. 1 and 2.



Scheme 6. Structure of the synthesized imine compounds

Table 3. FT-IR spectra of imine compounds O₁-O₅

FT-IR, $\nu(\text{cm}^{-1})$							
Comp. Code	C=N	C=C Aromatic	C-H		C-H Ali.		Others
			Aromatic	Alkene	Asymmetric	symmetric	
O ₁	1669	1510	3000	3045	2974	2941	O-H b3309, C=N yrimidine1547
O ₂	1610	1572	3042	3089	--	--	NO ₂ 1505, 1322 N-H 3277
O ₃	1591	1569	3044	3067	2983	2875	C=O 1645, C-Cl 829
O ₄	1594	1559	3044	3075	2983	2874	C=O 1634, C-Cl 815 O-H b3450
O ₅	1614	1566	3046	3079	2980	2867	O-H b3375

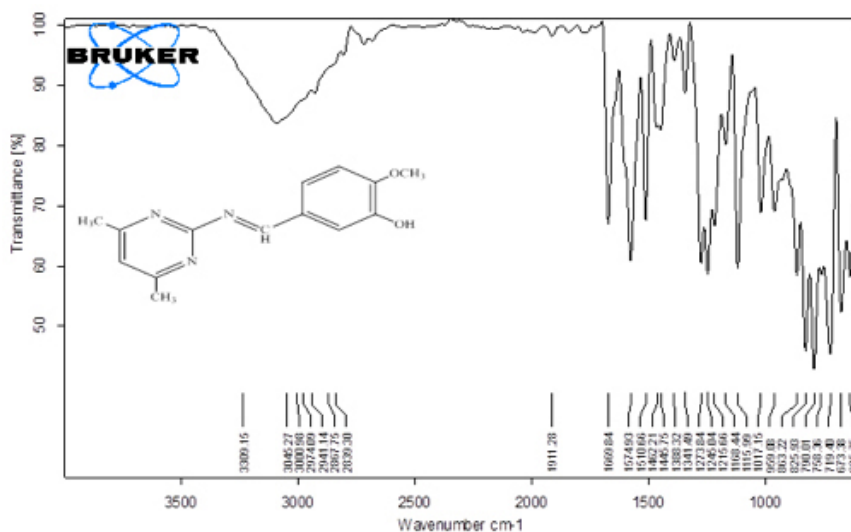


Figure 1. FT-IR spectra of O₁

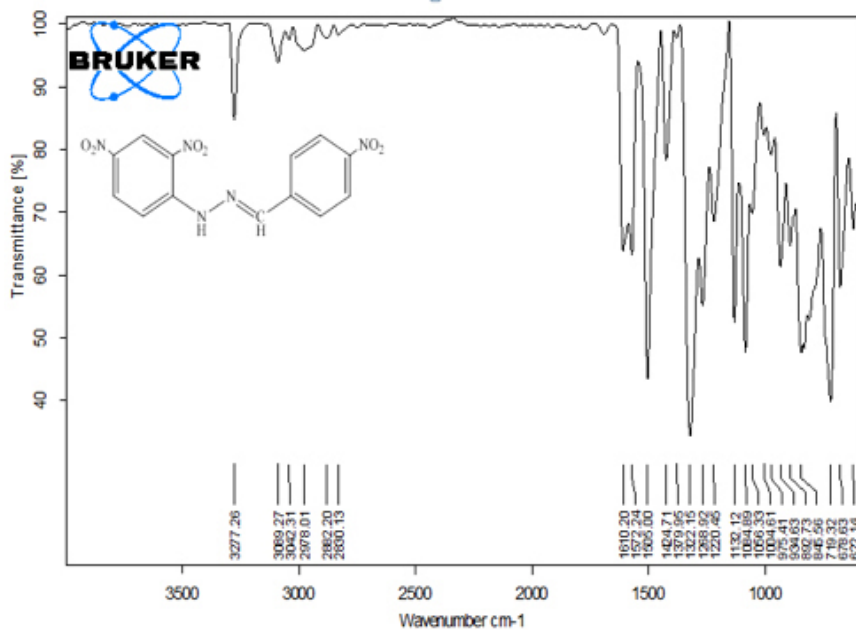
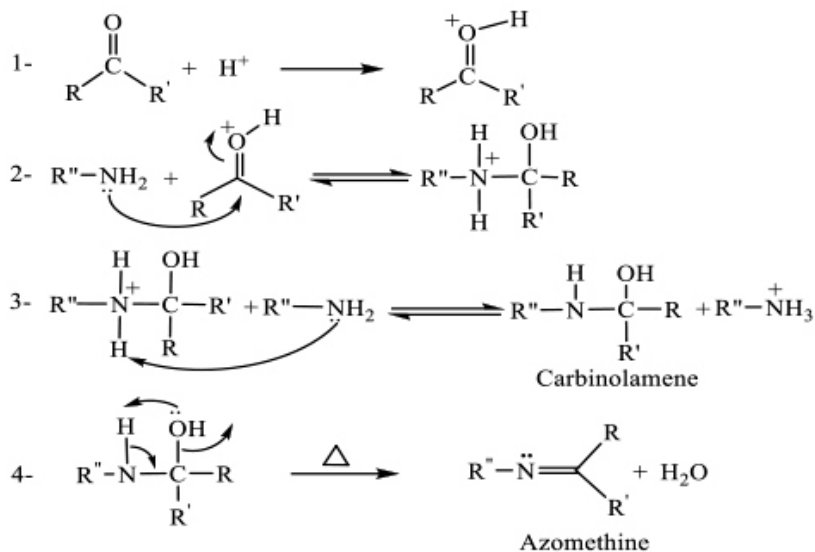


Figure 2. FT-IR spectra of O_2

The physical properties and FT-IR spectra of imine compounds O_1-O_5 prove the synthesis processes, Mechanism of imine compounds formation represented in the following reaction.^{29,30} See **scheme 7**.



Scheme 7. Mechanism of imine compounds formation

Tetrazole derivatives O₆-O₁₀

The synthesis of tetrazole derivatives was achieved by the reaction of imine and sodium azide. Their melting points identified the resulted products. FT-IR spectra of the products (table 4) showed characteristic absorption band at 1272-1301, 1022-1089 and 1484-1509 cm⁻¹ as an indicative of C-N, N-N and N=N bonds of tetrazole rings formation beside the characteristic bands of the residual groups in the structure as presented in Figs. 3 and 4.²⁸

Table 4. FT-IR spectra of tetrazole derivatives O₆-O₁₀

Comp. code	FT-IR n(cm ⁻¹)									
	N-H	N-N	N=N	C-N	C=C Aromatic	C-H Aromatic	C-H Ali.		Others	
							Asymmetric	Symmetric		
O ₆	3229	1022	1512	1278	1578	3082	2937	2875	O-H b 3627	
O ₇	3279	1089	1509	1272	1594	3091	2968	2877	NO ₂ 1575, 1331	
O ₈	--	1086	1484	1301	1594	3060	2941	2865	C=O 1650 C-Cl 768	
O ₉	3280	1087	1484	1273	1564	3055	2954	2874	O-H b 3491 C=O 1638	
O ₁₀	3320	1033	1499	1283	1598	3053	2920	2855	C-Cl 772 O-H b 3446	

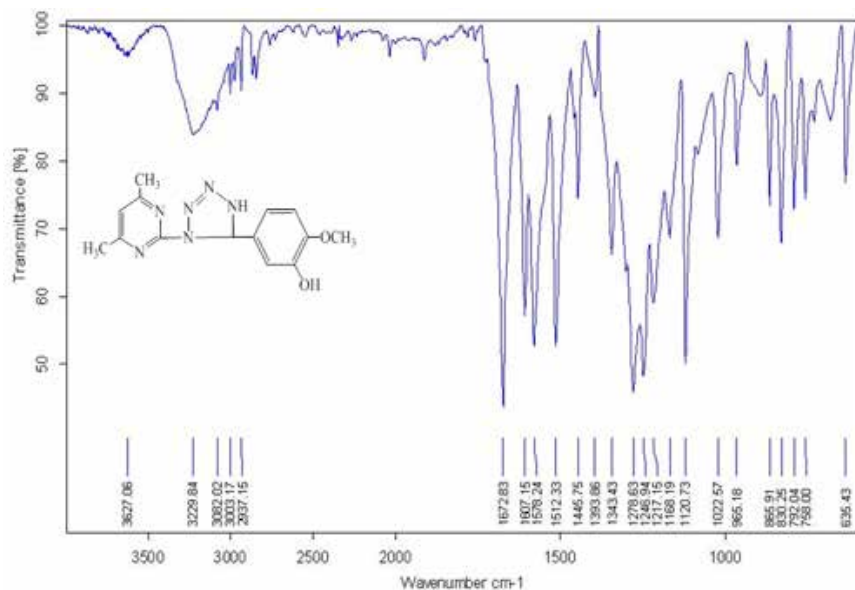


Figure 3. FT-IR spectra of O_6

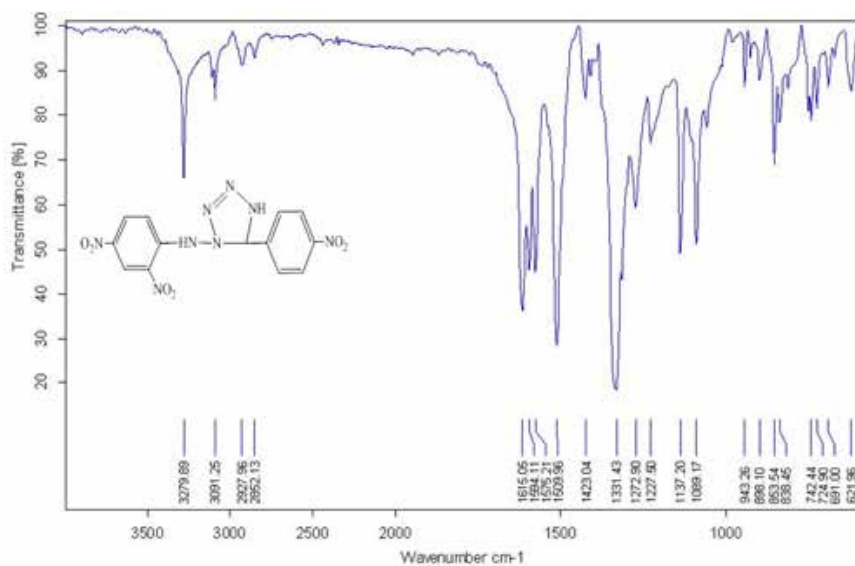


Figure 4. FT-IR spectra of O_7

The $^1\text{H-NMR}$ spectrum of compound O_8 in DMSO solvent (Fig. 5) showed chemical shifts, $\delta(\text{ppm})$, singlet in 2.46 indicates the presence 3H of the (N-CH_3) group, singlet in 3.20 indicates the presence 3H of the ($=\text{C-CH}_3$) group, singlet in 9.57 indicates the presence 1H of the (N-CH) group, multiplet and doublet of doublet in 7.85-7.36 indicates the presence 9H of the aromatic pro-

tons. Spectrum of compound O₉ (Fig. 6) showed chemical shifts, δ (ppm) at: singlet in 2.42 indicates the presence 3H of the (N-CH₃) group, singlet in 3.23 indicates the presence 3H of the (=C-CH₃) group, singlet in 6.78 indicates the presence 1H of the (-NH) group, singlet in 9.67 indicates the presence 1H (N-CH) group, singlet in 12.73 indicates the presence 1H of the (-OH) group, multiplet in 7.64-6.93 indicates the presence 8H of the aromatic protons.³¹ Other chemical shifts of O₆, O₇ and O₁₀, δ (ppm) are presented in table 5.

Table 5. The ¹H-NMR Spectra of tetrazole derivatives O₆-O₁₀ in DMSO

Comp. code	Chemical Shift δ ppm
O ₆	Singlet in 2.40 (6H, 2 <u>CH</u> ₂), singlet in 3.34 (3H, O- <u>CH</u> ₃), singlet in 7.11 (1H, - <u>NH</u>), singlet in 9.58 (1H, N- <u>CH</u>), singlet in 9.77 (1H, - <u>OH</u>), multiplet and singlet in 7.42-7.11 (4H, aromatic protons)
O ₇	Singlet in 3.57 (1H, <u>NH</u> out), singlet in 8.89 (1H, <u>NH</u> in), singlet in 11.86 (1H, N- <u>CH</u>) and multiplet and doublet of doublet in 8.82-8.05 (7H, aromatic protons)
O ₈	Singlet in 2.46 (3H, N- <u>CH</u> ₃), singlet in 3.20 (3H, =C- <u>CH</u> ₃), singlet in 9.57 (1H, N- <u>CH</u>), multiplet and doublet of doublet in 7.85-7.36 (9H, aromatic protons)
O ₉	Singlet in 2.42 (3H, N- <u>CH</u> ₃), singlet in 3.23 (3H, =C- <u>CH</u> ₃), singlet in 6.78 (1H, - <u>NH</u>), singlet in 9.67 (1H, N- <u>CH</u>), singlet in 12.73 (1H, - <u>OH</u>), multiplet in 7.64-6.93 (8H, aromatic protons)
O ₁₀	Singlet in 2.34 (3H, <u>CH</u> ₃), singlet in 6.80 (1H, - <u>NH</u>), singlet in 8.67 (H, N- <u>CH</u>), singlet in 13.25 (1H, - <u>OH</u>), multiplet and doublet of doublet in 7.66-6.95 (8H, aromatic protons)

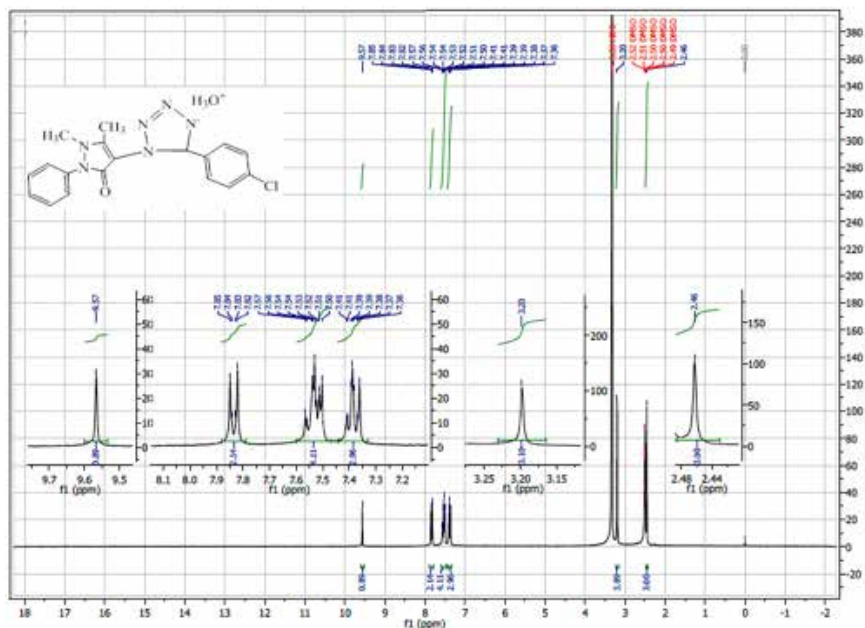


Figure 5. ¹H-NMR Spectra of O₉

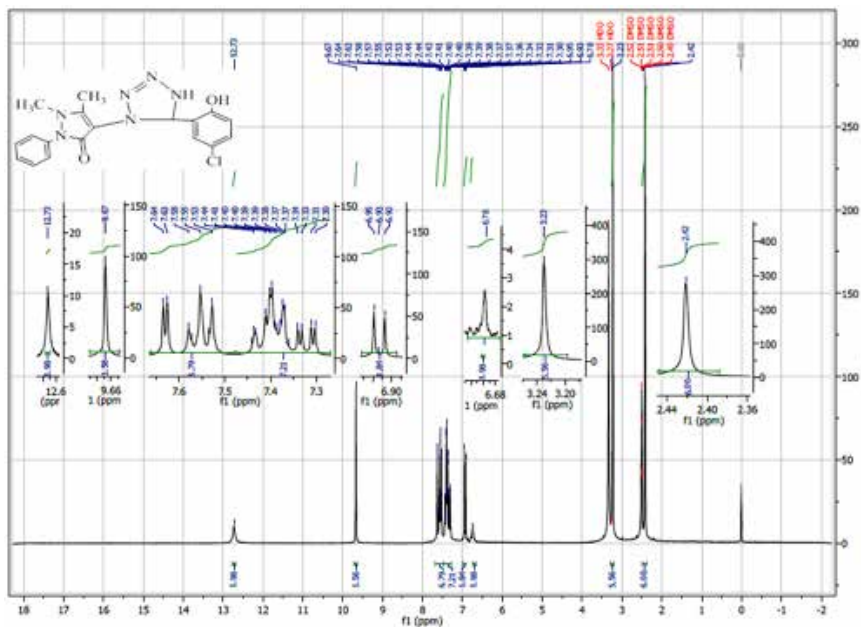


Figure 6. $^1\text{H-NMR}$ Spectra of O_9

The $^{13}\text{C-NMR}$ spectrum of compound O_6 in DMSO solvent (Fig. 7) showed chemical shifts, $\delta(\text{ppm})$, 37.47 indicates the presence two groups of (C-CH_3), 56.27 indicates the presence one group of (O-CH_3) group, 191.91 indicates the presence one group of (N-CH), 112.04-124.94 indicates the presence of aromatic carbons, 130.29-153.80 indicates the presence of pyrimidine carbons. While the spectrum of compound O_9 (Fig. 8) exhibited chemical shifts, $\delta(\text{ppm})$, 9.79 indicates the presence one group of (N-CH_3) group, 35.01 indicates the presence one group of ($=\text{C-CH}_3$), 150.46 indicates the presence one group of ($\text{CH}_3-\text{C}\equiv$), 154.78 indicates the presence one group of ($\text{CO-C}\equiv$), 157.80 indicates the presence one group of (N-CH), 158.59 indicates the presence one group of (N-CO), 113.96-134.10 indicates the presence of aromatic carbons.³² Other chemical Shifts of O_7 , O_8 , O_{10} , $\delta(\text{ppm})$ are displayed in table 6.

Table 6. The ^{13}C -NMR spectra of tetrazole derivatives O_6 - O_{10} in DMSO

Comp. code	Chemical Shift δ ppm
O_6	37.47 (2 C_{H_3}), 56.27 ($\text{O}-\text{C}_{\text{H}_3}$), 191.91 ($\text{N}-\text{C}_{\text{H}}$), 112.04-124.94 (Aromatic Carbons), 130.29-153.80 (Pyrimidine Carbons)
O_7	182.49 ($\text{N}-\text{C}_{\text{H}}$), 118.96-125.56 (Aromatic Carbons)
O_8	10.33 ($\text{N}-\text{C}_{\text{H}_3}$), 35.83 ($=\text{C}-\text{C}_{\text{H}_3}$), 144.11 ($\text{C}_{\text{H}_3}-\text{C}=\text{C}$), 152.34 ($\text{CO}-\text{C}=\text{C}$), 159.99 ($\text{N}-\text{C}_{\text{H}}$), 162.47 ($\text{N}-\text{C}_{\text{O}}$), 115.08-128.22 (Aromatic Carbons)
O_9	9.79 ($\text{N}-\text{C}_{\text{H}_3}$), 35.01 ($=\text{C}-\text{C}_{\text{H}_3}$), 150.46 ($\text{C}_{\text{H}_3}-\text{C}=\text{C}$), 154.78 ($\text{CO}-\text{C}=\text{C}$), 157.80 ($\text{N}-\text{C}_{\text{H}}$), 158.59 ($\text{N}-\text{C}_{\text{O}}$), 113.96-134.10 (Aromatic Carbons)
O_{10}	21.07 (C_{H_3}), 163.00 ($\text{N}-\text{C}_{\text{H}}$), 117.00-136.95 (Aromatic Carbons)

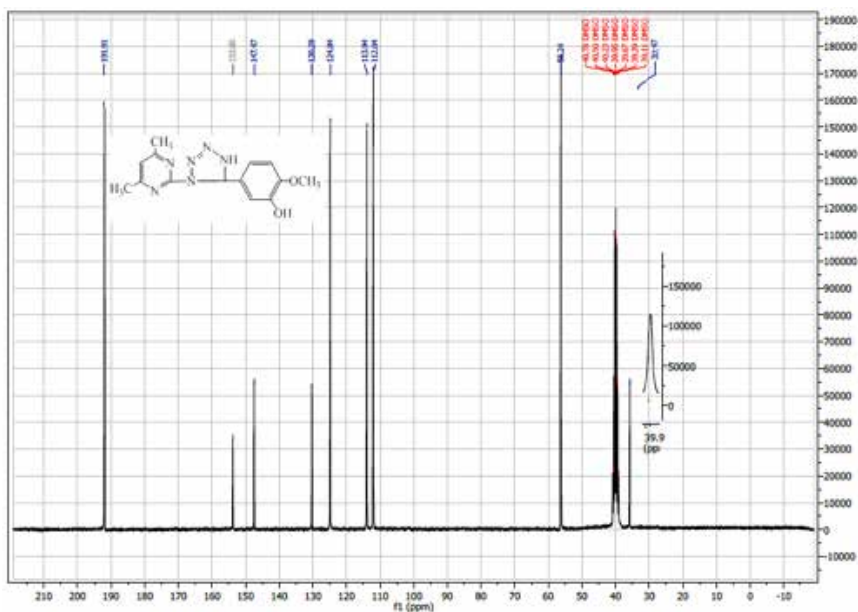
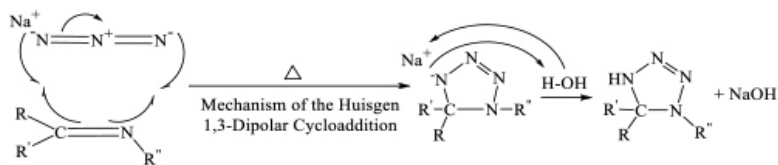


Figure 7. ^{13}C -NMR Spectra of O_6



Scheme 9. Mechanism of tetrazole derivatives formation

The results of FT-IR ^{13}C -NMR and ^1H -NMR showed that the five-ringed compounds were the least obstructed in all preparation processes. Because of the complete clarity in infrared beams and clear signals separated from each another by the resonance spectrum nuclear magnetic of hydrogen and carbon, this is the basis of organic preparation processes.

Anti-Candidal activity

Zone of inhibition of some human pathogenic fungi was done well-diffusion method to test the potential of the tetrazole derivatives O_6 - O_{10} as shown in Figs. 8 and 9. O_6 is the best derivative that has significantly ($p < 0.01$) recorded a stronger influence to inhibit the growth of *Candida guilliermondii* at an average of the zone of inhibition 14.0 mm. However, O_9 derivative recorded the lowest zone of inhibition 7.3 mm toward the same clinical fungal pathogen. From another hand, O_6 showed zone of inhibition 12.0 mm against *Candida zeylanoides*. Furthermore, O_6 derivative recorded zone of inhibition 11.3 mm against *Candida krusei* and *Candida albicans*. O_{10} did not inhibit the growth of *Candida albicans* as shown in Fig. 9. The resistance mechanisms depend on which specific pathways are inhibited by the drugs and the alternative ways available for those pathways that the organisms can modify to get a way around to survive.³⁴ Many new metal complexes and new 1,3-oxazepine derivatives had good antibacterial activity. Tetrazole derivatives are important to synthesize inflammatory agents.³⁵

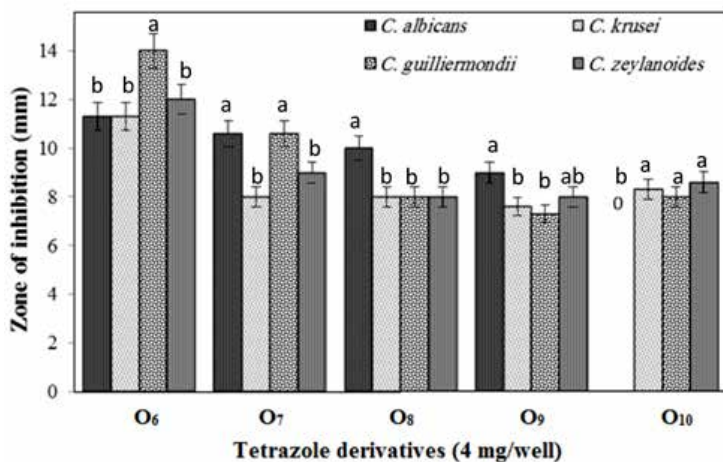


Figure 8. Zone of inhibition of *Candida* sp. using the synthesized tetrazole derivatives O₆-O₁₀, LDS ($p < 0.01$)

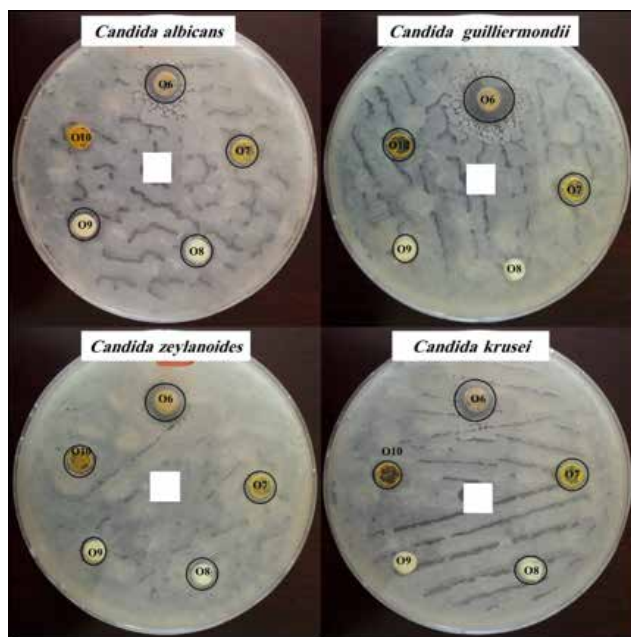


Figure 9. Anti-Candidal activity of the synthesized tetrazole derivatives O₆-O₁₀

This study referees to that preparing derivatives of tetrazole are possible. The results of FT-IR, ¹³C-NMR and ¹H-NMR showed that the five-ringed compounds were the least obstructed in all preparation processes. Because of the complete clarity in infrared beams and clear signals separated from each by

the resonance spectrum nuclear magnetic of hydrogen and carbon, this is the basis of organic preparation processes. O_6 is the best derivative that has significantly ($p < 0.01$) recorded a stronger influence to inhibit the growth of *Candida guilliermondii* at an average of the zone of inhibition 14.0 mm. However, O_9 derivative recorded the lowest zone of inhibition 7.3 mm against *Candida guilliermondii*. The present work may be helpful in designing more potential antifungal agents for the therapeutic use in the future.

ACKNOWLEDGEMENTS

Special thanks to Anbar University's President Professor Dr. Khalid Battal Najim for his continuous support to publishing the research in certified international journals. Also, grateful is for Dr. Abdullah Hussein Kshash, Department of Chemistry, College of Education for Pure Sciences, University of Anbar for helping to measurement the FT-IR spectra.

REFERENCES

1. Adabiardakani, A.; Hakimi, M.; Kargar, H.; Cinnamaldehyde Schiff Base Derivatives: a Short Review. *WA P Journal*. **2012**, *2*, 472–476.
2. Brodowska, K.; Chruścińska, E. Schiff bases – interesting range of applications in various fields of science. *CHEMIK*. **2014**, *68*, 129–134.
3. Qin, W.; Long, S.; Panunzio, M.; Biondi, S. Schiff Bases: A Short Survey on an Evergreen Chemistry Tool. *Molecules*. **2013**, *18*, 12264–12289.
4. Abid, O.; Muslim, R.; Mohammed, K. Synthesis and Characterization of Novel 1,3,4,9a-Tetrahydrobenzo[e][1,3]Oxazepin- 5(5aH)-One Derivatives via Cycloaddition Reactions of Schiff Bases *J. Uni. Al-Anbar Pure Sci*. **2016**, *10*, 8–18.
5. Ashraf, M.; Mahmood, K.; Wajid, A. Synthesis, Characterization and Biological Activity of Schiff Bases *IPCBE*. **2011**, *10*, 1-7.
6. Hussain, Z.; Fadhil, Z.; Adil, H.; Khalaf, M.; Abdullah, B.; Yousif, E. Schiff's Bases Containing Sulphamethoxazole Nucleus *RJPBCS*. **2016**, *7*, 1500–1510.
7. Mayavel, P.; Thirumurthy, K.; Dineshkumar, S.; Thirunarayanan, G. Perchloric acid catalyzed condensation of amine and aldehydes: Synthesis and antibacterial activities of some aryl (E)-imines, *Umcschem. lxix* **2014**, 159–179.
8. Al-Jamali, N.; Jameel, M.; Al-Haidari, A. Preparation and invitigation of diazipene, oxazipen compounds through condensation reaction, *IJLS*. **2013**, *1*, 13–15.
9. Dahot, M.; Rind, E.; Rafiq, M. Physical and biochemical analysis of sodium azide treated *sorghum bicolor* (L.) monech, *Pak. J. Biotechnol*. **2011**, *8*, 67–72.
10. Mohammed, J. Biological activities importance of tetrazole derivatives, *DRJI*. **2016**, *3*, 12796–12804.
11. Varadarasi, D.; Suban, S.; Ramasamy, V.; Kubendirran, K.; Raguraman, J.; Nalilu, S.; Pati, H. Synthesis and evaluation of a series of 1-substituted tetrazole derivatives as antimicrobial agents. *Org. Comm*. **2010**, *3*, 45–56.
12. Babu, K.; Prabhakar, V.; Ravindranath, L.; Kishore, N.; Latha, J. Synthesis, Characterization and Study of Antibacterial Activity of Some Novel Substituted Sulphonamide Pthalazine-Tetrazole Derivatives. *Res. J. Chem. Environ. Sci*. **2016**, *4*, 51–63.
13. Al-Hakak, Z. A pilot study for the treatment of microbial skin infections caused by bacteria *Pseudomonas aeruginosa* bacteria that resistance to antibiotic in human and animal by (ND: YAG LASER) technology. *Pak. J. Biotechnol*. **2017**, *14*, 417–422.
14. Sial, N.; Abro, S.; Shah, J.; Memon, M. Response of different doses of phosphate fertilizer and phosphate solubilizing_bacteria and mycorrhiza in mungbean (*VIGNA RADIATA* L.), *Pak. J. Biotechnol*. **2016**, *1*, 67–71.
15. El-Sayed, W.; Abdel Megeid, R.; Abbas, H. Synthesis and antimicrobial activity of new 1-[(tetrazol-5-yl)methyl] indole derivatives, their 1,2,4-triazole thioglycosides and acyclic analogs. *Arch. Pharm. Res.*, **2011**, *34*, 1085–1096.
16. Malik M.; Al-Thabaiti, S. Structure Optimization and Antifungal Screening of Novel Tetrazole Ring Bearing Acyl-Hydrazones, *Int. J. Mol. Sci*. **2012**, *13*, 10880–10898.
17. Al-Juburi, R. Synthesis and Characterization of Some Heterocyclic Compounds (Oxazepine, Tetrazole) Derived from Schiff Bases. *ANJS*. **2012**, *15*, 60–67.
18. Babu, P.; Ravindranath, L.; Rajesh, D.; Saritha, B. Synthesis of Novel Sultams Containing

Tetrazole Heterocycles. *World J. Pharm. Pharm. Sci.* **2016**, *5*, 929–940.

19. Abid, O.; Tawfeeq, H.; Muslim, R. Synthesis and Characterization of Novel 1,3-Oxazepin-5(1H)-One Derivatives via Reaction of Imine Compounds with Isobenzofuran-1(3H)-One. *Acta Pharm. Sci.* **2017**, *55*, 43–55.

20. Murhekar, M.; Khadsan, R. Synthesis of Schiff bases by organic free solvent method. *J. Chem. Pharm. Res.* **2011**, *3*, 846–849.

21. Sabah, H. Synthesis, spectroscopic characterization of schiff bases derived from 4,4'-methylen di aniline. *Der Pharma Chemica.* **2014**, *6*, 38–41.

22. Berk, B.; Ertaş, M.; Biltekin, S. Synthesis, Antimicrobial Activity Studies and Molecular Property Predictions of Schiff Bases Derived from ortho-Vanillin. *Acta Pharm. Sci.* **2017**, *55*, 83–96.

23. Srinivas, B.; Prasanna, B.; Ravinder, M. Synthesis and anti-microbial activity of novel series of N-(substituted phenyl-1H-tetrazol-1-yl)-7-substituted tetrazolo[1,5-a] quinoxalin-4-yl-amine Derivatives. *Der Pharma Chemica.* **2016**, *8*, 84–93.

24. Ravula, P.; Vamaraju, H.; Paturi, M.; Chandra, N.; Kolli, S. Synthesis, in Silico Toxicity Prediction, Molecular Docking, and Evaluation of Novel Pyrazole Derivatives as Potential Antiproliferative Agents. *EXCLI Journal.* **2016**, *15*, 187–202.

25. Owaid, M. N.; Raman, J.; Lakshmanan, H.; Al-Saeedi, S. S. S.; Sabaratnam, V.; Al-Assaffii, I. A. Mycosynthesis of silver nanoparticles from *Pleurotus cornucopiae* var. *citrinopileatus* and its inhibitory effects against *Candida* sp. *Mater. Lett.* **2015**, *153*, 186–190.

26. Owaid, M.; Muslim, R.; Hamad, H. Mycosynthesis of Silver Nanoparticles using *Terminia* sp. Desert Truffle, Pezizaceae, and their Antibacterial Activity. *JJBS.* **2018**, *11*, 401–405.

27. Muslim, R.; Tawfeeq, H.; Owaid, M.; Abid, O. Synthesis, Characterization and Evaluation of Antifungal Activity of Seven-Membered Heterocycles. *Acta Pharm. Sci.* **2018**, *56*, 39–57.

28. Silverstein, R.; Webster, F.; Kiemle, D. Spectrometric identification of organic compounds, 7th edition, John Wiley and sons, Inc., **2005**, 72–126.

29. J. Simek, Organic Chemistry, 8th edition, Pearson education, Inc., **2013**, 412–414.

30. Abid, O.; Muslim, R.; Mohammed, K. Synthesis and Characterization of Novel 1,3-Oxazepin-4-Ones Derivatives via Schiff Bases Reactions with Phthalide. *J. Uni. Anbar Pure Sci.* **2016**, *10*, 1–9.

31. Silverstein, R.; Webster, F.; Kiemle, D. Spectrometric identification of organic compounds, 7th edition, John Wiley and sons, Inc., **2005**, 127–202.

32. Mistry, B. A Handbook of spectroscopic Data chemistry, edition 2009, Oxford book company Jaipur India, Mehra Offset Printers, Delhi, **2009**, 99–127.

33. Das, R.; Majumdar, N.; Lahiri, A. A review on 1,3-dipolar cycloaddition reactions in bio-conjugation and its importance in pharmaceutical chemistry. *IJRPC.* **2014**, *4*, 467–472.

34. Tenover, F. Mechanisms of antimicrobial resistance in bacteria, *Am. J. Med.* **2006**, *119*, 3–10.

35. M. F. El Shehry, J. Balzarini, C. Meier, Synthesis of 3-((2, 4-dichlorophenoxy) methyl)-1, 2, 4-triazolo (thiadiazoles and thiadiazines) as anti-inflammatory and molluscicidal agents., *Synthesis.* **2009**, *5*, 841–847.

Comparative Study of Chemical Characteristics, Phytochemical Contents and Antioxidant Activity of Polar and Non-polar Solvent Extracted Flaxseed Oil

Satarupa Ghosh¹, D.K. Bhattacharyya^{1*}, M. Ghosh¹

¹ Indian Institute of Engineering Science and Technology, School of Community Science and Technology, Howrah, India

ABSTRACT

This study investigated the chemical characteristics and antioxidant activity of flax seed oil extracted by polar (isopropanol) and non-polar (hexane) solvent. The fatty acid profiles of the extracted oils were determined by Gas Chromatography. Flax seed oil was found to contain high level of linolenic acid around (57%), followed by oleic acid (18%) and linoleic acid (19%), while the saturated acids were palmitic acid (6%) and stearic acid (4%). Analytical values such as acid value, peroxide value, iodine number, saponification value were determined and total phenolic and flavonoid content were performed. The antioxidant activity of flax seed oil extracted by polar and non-polar solvent, based on the determination of DPPH Free radical scavenging activity, FRAP assay, ABTS assay was evaluated.

Keywords: Flaxseed, chemical characteristics, phytochemical, antioxidant, activity.

INTRODUCTION

Flax seed (*Linum usitatissimum*) is used as a food source for having many valuable nutrients¹. It contains near about 45 % oil, 30 % dietary fiber and 25% protein. The oil is rich in essential fatty acids mainly omega 3 fatty acid, which is higher than any other vegetable oils², vitamin and minerals. Around 73% of the fatty acids in flaxseed are PUFA. Approximately 50% of the total fatty acid consists of α -Linolenic acid (ALA)³. The α -Linolenic acid and related chemicals in flaxseed oil seem to decrease inflammation. That is why flaxseed oil is thought to be useful for rheumatoid arthritis and other inflammatory

*Corresponding Author: D. K. Bhattacharyya, e-mail: dkb_oiltech@yahoo.co.in
D.K. Bhattacharyya ORCID Number: 0000-0001-7145-3654
M. Ghosh ORCID Number: 0000-0002-5360-4874
(Received 03 March 2019, accepted 20 May 2019)

(swelling) diseases. Flaxseed is also a rich source of lignan component such as secoisolariciresinol di glucoside (SDG). SDG is known for its high antioxidant activity, and also for anticarcinogenic and phytoestrogenic properties ⁴. Clinical and large-scale population studies show that flax improves laxation, lowers blood cholesterol, aids in blood glucose control, and blocks inflammation⁵. There has been a growing interest for the probiotic properties of flaxseed and its beneficial effects in coronary heart disease, some kinds of cancer, neurological and hormonal disorders⁶. Mainly flaxseeds are produced in Canada, Argentina, U.S.A, China, India and Europe ⁷. Flaxseed oil also has various industrial applications like linoleum and paints manufacture and in preserving wood and concrete ⁸. Flaxseed oil is normally extracted by cold pressing⁹ and also by a combination of pressing and solvent extraction for almost complete recovery of flaxseed oil ¹⁰. The use of bio renewable solvents like super critical CO₂, ethanol, acetone, isopropanol and water has been gaining interest for extraction of vegetable oils. The use of polar and non-polar solvent may indicate significant difference in both content and properties (physical and chemical).

The aim of the study is to examine the chemical characteristics, phytochemical content and antioxidant activity of polar and non-polar solvent extracted flaxseed oil.

METHODOLOGY

Sample and Chemicals

Flaxseed was bought from local market of Sealdah, Kolkata (West Bengal, India). All chemicals were purchased from MERCK, INDIA.

Oil Extraction

To obtain oil by solvent extraction method, flaxseed powder of known weight was extracted with polar (iso propanol) and non-polar (hexane) solvents separately using Soxhlet apparatus (Borocil) for 5 hours on a steam bath at 70-degree Celsius temperature. After extraction the remaining solvent was evaporated by rotary evaporator (BUCHI).

Analytical Characteristics of Flaxseed Oil

Acid value, peroxide value, saponification value and iodine value of flaxseed oil extracted by both polar and non-polar solvents were estimated according to the AOAC official method.

Phytochemical Content of Flaxseed Oil

Total Phenolic Content

Total Phenolic content was determined spectrophotometrically using Folin–Ciocalteu reagent ¹¹. A calibration curve of gallic acid was prepared and the results were expressed as gallic acid equivalents (mg GAE/gm). An aliquot of the extract (100 µl) was mixed with 250 µl of Folin Ciocalteu's reagent and incubated in room temperature for 5 minutes. Then 1.5 ml of 20% sodium bi carbonate was added to the mixture and the absorbance was measured at 765 nm., against a blank, which was composed of the same reagents except test extract. A calibration curve of gallic acid was prepared and the results were expressed as gallic acid equivalents (mg GAE/100 ml) and were calculated by the formula:

$T = (C \times V) / M$ Where, T=Total content of phenolic compounds, milligram per gram dry weight of plant extract, in GAE; C=the concentration of gallic Acid established from the calibration curve, milligram per milliliter; V=the volume of extract, milliliter; M=the weight of plant extract, gram.

Total Flavonoid Content

The total flavonoids content was measured using the aluminium chloride colorimetric method ¹². The sample extract (250µl) was added to 4.5 ml distilled water followed by 5% NaNO₂ (.03 ml). After incubation for 5 minutes AlCl₃ (0.03 ml, 10 %) was added at 25°C. The reaction mixture was treated with 2 ml of 1 M NaOH. The reaction mixture was then diluted to 10 ml distilled water and absorbance was measured at 510 nm against a blank which was composed of the same reagents except the test extract. A calibration curve of catechin was prepared and the results were expressed as catechin equivalents (µg CE/100 ml) and were calculated by the formula:

$T = (C \times V) / M$ Where; T = total content of flavonoid compounds, mg per gram dry weight of plant extract, in Catechin equivalent, C = concentration of Quercetin established from the calibration curve in mg/ml, V = volume of extract in ml and M = weight of plant extract in gram.

Fatty Acids Profiles

The fatty acids composition of flaxseed oil was analyzed by Gas Chromatography (Agilent technologies, Model NO-7890B) after converting the fatty acids of the oil into their methyl esters according to AOCS official method Ce 2-66. Here DB-Wax capillary column (30 mL, 0.25 mm I.D., 0.25 µm F.T.) and FID (Flame Ionization detector) were used. The carrier gas was nitrogen, at a flow rate of 1 ml/minute. Injector and detector temperatures were 200° C and 240°

C respectively. Column temperature was maintained from 150° C to 240° C. Samples of 1 µl were injected by manually, in the split mode.

Antioxidant Activity

Antioxidant activity of the flaxseed oil was measured by the following standard assay methods:

DPPH Free radical scavenging activity assay

The oil was assessed using 1, 1-diphenyl 2-picryl hydrazyl (DPPH) radical scavenging assay¹³. 0.1mM solution of DPPH in methanol was prepared. An aliquot of .2 ml of sample was added to 2.8 ml of this solution and kept in the dark place for 30 minutes. The absorbance was measured at 517 nm. The ability to scavenge the DPPH radical was calculated with the following equation.

Inhibition percentage (I %) = $(A_0 - A_1)/A_0$

(A_0 = Absorbance of the control, A_1 = Absorbance of the sample.)

Ferric reducing antioxidant power (FRAP)

The FRAP assay of the test samples were determined¹⁴. The FRAP reagent consists of 10 mM 2,4,6-Tripyridyl-s-triazine (TPTZ) in 40 mM HCL, 250 mM sodium acetate buffer (pH -3.6) and 20mM FeCl₃. The reagent was freshly prepared by mixing 2,4,6-Tripyridyl-s-triazine (TPTZ) solution, FeCl₃, 6H₂O solution and acetate buffer in a ratio of 1:1:10. An extract solution (100 µl) was mixed with 900µl of FRAP reagent. The mixture was incubated at 37° C for 4 minutes and the absorbance was measured at 593 nm.

2,2'-azino-bis(3-ethylbenzothiazoline-6-sulphonic acid) (ABTS) Free radical scavenging activity

2,2'-azino-bis(3-ethylbenzothiazoline-6-sulphonic acid) (ABTS) assay of flax seed oil was measured using the following method¹⁵. A solution of 2,2'-azino-bis(3-ethylbenzothiazoline-6-sulphonic acid) (ABTS) (7µM) was prepared in distilled water and mixed with the solution of potassium per sulphate (2.45 µM). The mixture was kept in the dark place for 16 hours at room temperature. The resulting intense color matches the 2,2'-azino-bis(3-ethylbenzothiazoline-6-sulphonic acid) (ABTS) radical cations. The solution was obtained subsequently diluted with distilled water and absorbance was measured at 734 nm. 1 ml of ABTS diluted solution was mixed with 10 µl of sample at different concentration and the reaction mixture was kept for 6 minutes before measuring the absorbance. 2,2'-azino-bis(3-ethylbenzothiazoline-6-sulphonic acid) (ABTS) scavenging activity was calculated by the following equation.

Inhibition Percentage (I %) = $(1-A/A_0) \times 100$.

(A=Absorbance of the sample. A_0 = Absorbance of the ABTS solution.)

Statistical Analysis

Results were expressed as mean value \pm standard deviation of three replications. Statistical differences were analyzed using one-way ANOVA followed by post-hoc Tukey HSD (Honestly Significant Difference) at level $p \leq 0.05$.

RESULTS AND DISCUSSION

Oil Extraction

Many polar and non-polar solvents can be used to extract oil from oil seeds including flaxseed. In this study iso-propanol, a biorenewable solvent which is also food grade, was used as a polar solvent and n- hexane was used as a non-polar solvent. As much as 35% (w/w) of flaxseed oil was extracted by iso-propanol (polar solvent) while 40% (w/w) flaxseed oil was obtained by hexane (non-polar solvent). Table 1 shows the respective oil yield in percentage by weight of seeds with polar and non-polar solvents. The less yield of flaxseed oil with iso propanol compared to n-hexane was due to the effect of water content of the seed .It could be that water became gradually miscible with iso propanol and reduced the solubility of the oil in iso propanol and ultimately extracting less amount of oil.On the other hand ,oil seeds with as much as 14% water can be almost wholly extracted with n-hexane^{16,17}. Generally flaxseed oil of good quality for food and pharmaceutical uses is produced commercially by cold pressing process with single pressing as flaxseed as flaxseed contains fairly high percentage of oil.Because of the importance of this oil from nutrition and health views the oil is not extracted by solvent process.However the soaring price of flaxseed oil and other edible oils demands for maximum recovery by extraction with organic food grade solvents.Infact ,both polar and non-polar solvents are in use or can be used in extracting vegetable oils.

Table 1. Oil content in flaxseed as extracted by polar and non-polar solvents

Solvent	Oil Content (% w/w)
Polar solvent (iso propanol)	35% \pm 0.79
Non-polar solvent (hexane)	40% \pm 0.92

Correlation is significant at the $p \leq 0.05$ level.

Analytical Characteristics of Flaxseed Oil

The analytical characteristics such as acid value, peroxide value, iodine number and saponification value of flaxseed oil extracted by polar and non-polar solvent were determined and included in the Table 2.

Table 2. Analytical Characteristics of Flaxseed oil

Test	Polar solvent extracted oil	Nonpolar solvent extracted oil
Acid value	0.80 ±0.25 mg KOH/gm oil	0.84 ±0.14 mg KOH/gm oil
Peroxide value	0.95 ±0.19 meq/kg oil	0.99 ±0.21 meq/kg oil
Iodine number	172 ±0.98 iodine/kg oil	180 ±0.79 iodine/kg oil
Saponification value	180 ±0.87 KOH/gm oil	192 ±0.91 KOH/gm oil

Correlation is significant at the $p \leq .05$ level.

Acid value, peroxide value, iodine number, saponification value of flax seed oil extracted by the polar solvent had acid value 0.80 mg KOH/g oil, peroxide value 0.95 meq/kg oil, iodine value 172 g iodine/100 g oil and saponification value 180 mg KOH/g oil, where as acid value, peroxide value, iodine number and saponification value of flax seed oil extracted by the non-polar solvent were 0.84 mg KOH/g oil, 0.99 meq/kg oil, 180 g iodine/100 gm oil and 192 mg KOH/g oil respectively.

Phytochemical Content

The phytochemical analysis revealed the presence and content of phenolics and flavonoids content shown in Table 3. Phenolics, main secondary metabolite of plant origin. They have multiple biological effects including antioxidant properties. They are not only essential for plant growth but also produced as a response against injury of plant from pathogens.

Table 3. Phytochemical Content of Flaxseed oil

Phytochemical Content	Polar solvent extracted oil	Nonpolar solvent extracted oil
Total phenolic content	1975±1.11 mg GAE/100 ^a gm	2120±1.07 mg GAE/100 ^a gm
Total flavonoid content	402±0.95 ^b µg CE/mg sample	441±0.87 ^c µg CE/mg sample

The data are presented as mean value ± standard deviation of triplet analyses. Different letters in the same column indicate statistically significant values ($p \leq .05$)

Flavonoids are important for normal growth and development of plant and they give protection from infection and injury. It also contains anti cancer, anti allergic, anti inflammatory and anti microbial properties.

Phenolic content of flaxseed oil obtained by polar and non-polar solvent extraction were 1975 mg GAE/100 ml sample and 2120 mg GAE/100 ml sample respectively and total flavonoids content in the non-polar extracted flaxseed oil were 402 µg CE/100 ml sample and 441 µg CE/100 ml sample. From the above result, it can be stated that the analytical characteristics are nearly same for both polar and non-polar solvent extracted flax seed oil. However, the phytochemical content of flaxseed oil extracted by non-polar solvent was more than polar solvent extracted flaxseed oil.

Fatty acid profile

The fatty acid composition of flaxseed oil extracted by polar and non-polar solvent was presented in Table 4. There were five fatty acids found in the profile including palmitic acid(C16:0), stearic acid (C18:0),oleic acid (C18:0), linoleic acid (C18:2) and linolenic acid(C18:3).The major saturated fatty acids found in the flaxseed oil whether extracted by polar and non-polar solvent were palmitic acid (C16:0), stearic acid (C18:0),oleic acid (C18:1) with the concentration of 6.58%-6.97% ,4.39%-4.43% and 18.53%-18.51% respectively.Poly unsaturated fatty acids found in both polar and non-polar solvent extracted flaxseed oil were linoleic acid (C18:2) at 19.78 -19.82 % and linolenic acid (C18:3) and 53.29-57.35% respectively.

Table 4. Fatty acids Composition of Flaxseed Oil

Fatty acids	Polar solvent	Non-polar solvent
Palmitic acid (C16: 0)	6.58 %	6.97 %
Stearic acid (C18:0)	4.39 %	4.43 %
Oleic acid (C18:1)	18.53 %	18.51 %
Linoleic acid (C18:2)	19.78 %	19.89 %
Linolenic acid (C18 :3)	53.29 %	57.35 %

Antioxidant Activity

The antioxidant activity of flaxseed oil samples was evaluated using DPPH, FRAP, ABTS assay and the results are shown in the Table 5. DPPH value of the non-polar solvent extracted flaxseed oil was slightly higher compared to the polar solvent extracted flax seed oil. FRAP value and ABTS value were near about same for flaxseed oil when extracted by both polar and non-polar solvent.

Table 5. Antioxidant Activity of Flaxseed Oil

Test	Polar solvent	Non-polar solvent
DPPH	80 %± 0.34	82 %± 0.21
FRAP (µmol/ml)	10 ± 0.03	11 ± 0.39
ABTS	43 % ± 0.52	44%± 0.42

Correlation is significant at the $p \leq .05$ level.

Flaxseed oil could be extracted effectively and satisfactorily by both polar and non-polar solvent. The polar solvent would be a better choice from nutritional and health or medicinal point of views.

The results of this study indicated that the chemical characteristics of both polar and non-polar solvent extracted flaxseed oils were nearly same. But the phytochemicals content and antioxidant activity appeared to be slightly more in case of the non-polar solvent extracted flaxseed oil compared to the polar solvent extracted flaxseed oil.

ACKNOWLEDGEMENTS

I would like to acknowledge my institute Indian Institute of Engineering Science and Technology (IEST), Shibpur, Howrah, West Bengal, India for providing laboratory facilities.

REFERENCES

1. Herchi, W.; Bahashwan, S.; Sebei, K.; Ben Seleh, H.; Kallel, H.; Boukhchina, S. Effects of germination on chemical composition and antioxidant activity of flaxseed (*Linum usitatissimum* L.) oil. *Grasas Aceites*, **2015**, *66*, 1-8.
2. Herchi, W.; Arraez-Roman, D.; Trabelsi, H.; Bouali, I.; Boukhchina, S.; Kalle, H.; Segura-Carretero, A.; Fernandez-Gutierrez, A. Phenolic compounds in a flaxseed: A review of their properties and analytical methods. An overview of the last decade. *J. Oleo. Sci.* **2014**, *63*, 7-14.
3. Sebei, K.; Debez, A.; Herchi, W.; Boukhchina, S.; Kallel, H. Germination kinetics and seed reserve mobilization in two flax (*Linum usitatissimum* L.) cultivars under moderate salt stress. *J Plant Biol.* **2007**, *50*, 447-454.
4. Touré, A.; Xueming, X. Flaxseed Lignans: Source, Biosynthesis, Metabolism, Antioxidant Activity, Bio-Active Components, and Health Benefits. *Compr. Rev. Food. Sci.* **2010**, *9*, 261-269
5. Winnipeg, MB, Flax Council of Canada. *Flax—A Health and Nutrition Primer*. **2003**, *134*, 1806-1811.
6. Simopoulos, A.P. The importance of the ratio of omega-6/omega-3 essential fatty acids. *Biomed. and Pharmacother.* **2002**, *56*, 365-379.
7. Alander, J.; Lidelfelt J. O. Vegetable oils and fats. *Karlshamn: AB.* **2002**
8. Vaisey-Genser, M.; Morris, D. H. History of cultivation and uses of flaxseed. In *Flax, the genus Linum*. Edited by: Muir A, Westscott N. *Amsterdam: Hardwood Academic Publishers*, **2001**, 1-21.
9. Tanska, M.; Roszkowska, B.; Skrajda M.; Dabrowski, G. Commercial cold pressed flaxseed oils quality and oxidative stability at the beginning and end of their shelf life. *J Oleo Sci.* **2016**, *65*, 111-121.
10. Kulkarni, N. G.; Kar, J. R.; Singhal, R. S. Extraction of Flaxseed Oil: A Comparative Study of Three-Phase Partitioning and Supercritical Carbon Dioxide Using Response Surface Methodology, *Food Bioproc Tech.* **2017**, *10*, 940-948.
11. McDonald, S.; Prenzler, P. D.; Antolovich, M.; Robards, K. Phenolic content and antioxidant activity of olive extract. *Food Chem.* **2001**, *73*, 73-84.
12. Chang, C.; Yang, M.; Wen, H.; Chern, J. Estimation of total flavonoid content in propolis by two complementary colorimetric methods. *J. Food Drug. Anal.* **2002**, *10*, 178-182.
13. Gorinstein, S.; Vargas, O. J. M.; Jaramillo, N. O.; Salas, I. A.; Ayala, A. L. M.; Arancibia-Avila, P.; Toledo, F.; Katrich, E.; Trakhtenberg, S. The total polyphenols and the antioxidant potentials of some selected cereals and pseudocereals. *Eur. Food Res. and Technol.* **2007**, *225*, 321-328.
14. Benzie, I.F.F.; Strain, J.J. The ferric reducing ability of plasma (FRAP) AS A MEASURE OF "antioxidant power" the FRAP assay. *Anal Biochem.* **1996**, *239*, 70-76.
15. Ghosh, S.; Bhattacharya, D. K.; Ghosh, M. Study on proximate composition, phytochemical content, oxidative stability, antioxidant activity and fatty acid composition of enzyme aided aqueous extraction of flax seed oil. *ASNH*, **2019**, *3*, 5-9.
16. Fan, H. P.; Morris, J. C.; Wakeham, H. Diffusion phenomena in solvent extraction of peanut oil: Effect of cellular structure. *Ind. Eng. Chem. RES.* **1948**, *40*, 195-199.
17. Wingard, M. R.; Shand, W. C. The determination of the rate of extraction of crude lipids from oil seeds with solvents. *J. Am. Oil Chem. Soc.* **1949**, *26*, 422-426.

18. Prescha, A.; Grajzer, M.; Dedyk, M.; Grajeta, H. The Antioxidant Activity and Oxidative Stability of Cold-Pressed oils. *J. Am. Oil Chem. Soc.* **2014**, *91*, 1291-1301.
19. AOAC International, Official methods of analysis of AOAC International, 16th ed., Gaithersburg, **1999**.
20. Litchfield, C. Analysis of Triglycerides, Academic Press, New York, **1972**. pp: 17- 35.
21. Choo, W. S.; Birch, J.; Dufour J. P. Physico chemical and quality characteristics of cold-pressed flax seed oils. *J. Food Compos. Anal.* **2007**, *20*, 202-211.
22. Gorinstein, S.; Cvikrova, M.; Machackova, I.; Haruenkit, R.; Park, Y. S.; Jung, S. T.; Yamamoto, K.; Ayala, A. L. M.; Katrich, E.; Trakhtenberg, S. Characterization of antioxidant compounds in Jaffa sweeties and white grape fruits. *Food Chem.* **2004**, *84*, 503-510.
23. El-Beltagi, H. S.; Salama, Z. A.; El-Hariri, D. M. Evaluation of fatty acids profile and the content of some secondary metabolites in seeds of different flax cultivars (*Linum usitatissimum* L.), *Gen. Appl. Plant Physiol.* **2007**, *33*, 187-202.
24. Gutfinger, T. Polyphenols in olive oils. *J. Am. Oil Chem. Soc.* **1981**, *58*, 966-968.
25. Silva, C.; Garcia, V. A. S.; Zanetle, C. M. Chia (*Salvia hispanica* L.) Oil extraction using different organic solvents: oil yield, fatty acids profile and technological analysis of defatted meal. *Int Food Res. J.* **2016**, *23*, 998-1004.
26. Mingyai, S.; Kettawan, A.; Srikaeo, K.; Singanusong, R. Physico chemical and antioxidant properties of rice bran oils produced from coloured rice using different extraction methods. *J Oleo sci.* **2017**, *66*, 565-572.
27. Barthet, V. J.; Klensprof –Pawlik, D.; Przybylski, R. Antioxidant Activity of Flax seed meal components. *Can. J. of Plant Sci.* **2014**, *94*, 593-602.
28. Bouaziz, F.; Koubaa, M.; Barba, F. J.; Roohinejad, S.; Chaabouni, S. E. Antioxidant properties of water-soluble gum from flax seed hull, *Antioxidants (Basel)*, **2016**, *5*, 1-10.

A Study of Drug-Excipient Interaction and Drug Product Stability Using Dry (Powder) Film Coating in Comparison with Conventional (Aqueous) Film Coating

Derar M. Omari^{1*}, Yazan Akkam¹

¹ Yarmouk University, Faculty of Pharmacy, Pharmaceutical Sciences, Irbid, Jordan

ABSTRACT

The objective of this work was to study drug-excipient interactions in solid dosage forms when coated with dry powder film-coat compared with conventional aqueous film. Free films of Eudragit RL, (ERL) with or without drugs (Metoprolol Succinate or Diclofenac sodium) were prepared by casting method and characterized by FTIR, NMR, or DSC. Tablets of either drugs were prepared by wet granulation and coated in a fluidized-bed by ERL aqueous dispersion or micronized powder. Dissolution behavior and color change study were carried out for tablet batches on zero time and after 3 months of storage in stability chambers. The results of free films showed a greater possibility of drug polymer interaction in the aqueous dispersion than dry powder films. The results of dissolution rate revealed a greater rate change in aqueous- than in dry-coated tablets. This was confirmed by the Color change study which showed more intense yellowing in aqueous-coated tablets.

Keywords: Drug-excipient interaction, eudragit RL, diclofenac sodium, dry powder, coating.

INTRODUCTION

Solid pharmaceutical dosage forms like tablets, capsules, granules, pellets etc. are coated for many purposes such as protection from moisture, light or oxygen; masking of odor or taste; acid resistance in gastric fluids; and to modify drug release from these dosage forms as controlled or delayed action. Traditionally, coating is carried out using either organic solution or aqueous solution or dispersion of certain polymers sprayed, after mixing with other substances

*Corresponding Author: Derar M. Omari, e-mail: derar.m@yu.edu.jo

Derar Omari ORCID Number: 0000-0002-1939-8640

Yazan Akkam ORCID Number: 0000-0003-0699-0060

(Received 15 March 2019, accepted 20 May 2019)

such as plasticizers, onto dosage forms¹⁻⁴. However, solvent-based coatings suffer from many potential disadvantages such as toxicity, air pollution or residual remnants of organic solvents. Also, the removal of solvents is highly energy consuming and takes longer processing time⁵⁻⁶. These all reflected as an increase in the cost of the process as well as the drug product per se.

Among serious efforts to overcome the above-mentioned problems of solvent-based coating, many recent works have been published regarding new coating technologies which are independent of solvent referred to as “solventless” coating. These may include, but not limited to, compression coating, hot melt coating, supercritical fluid spray coating, photocurable coating and dry powder coating⁷. However, the later, dry powder coating, was the most widely investigated. In this process, powdered (micronized) coating materials are directly applied, with or without wetting, onto solid dosage forms, and then heat-cured to form a coat⁸. Several dry coating technologies, including plasticizer-dry-coating, electrostatic-dry-coating, heat-dry-coating and plasticizer-electrostatic-heat-dry-coating have been developed and extensively reported⁸⁻¹⁰.

Drug-exipient interaction, among other factors, may affect drug product quality and performance¹¹⁻¹³. One example of such interactions is the action of the drug as a plasticizer for the polymeric film¹⁴⁻¹⁵. Plasticizers are generally added to polymers to increase their flexibility and hence durability, increase the permeability for the drug and promote film formation^{3,11}. Therefore, the action of drug as a plasticizer is an extra- or over-plasticization and should be seriously taken in consideration and extensively investigated^{11,15}. Sieppmann et al (2006) studied the plasticization effect of 3 different drugs, namely, chlorpheniramine, metoprolol tartrate and ibuprofen and found that they acted as good plasticizers for Eudragit RS polymers, and this effect was directly proportional to drug load¹⁶. The presence of solvent (ex. water) may complicate physical interaction between drug and polymer¹⁷. This type of interaction may simply occur during coating process due to the presence of solvent or even after coating (i.e. within the final dosage form) by solvent migration from core to coat¹¹. In critical cases such as enteric coating of gastric antiulcer drugs, ex. proton pump inhibitors (PPIs), which are sensitive to acidic materials (ex. Eudragit L-100-55), a subcoat of different polymer have been applied¹⁸⁻²⁰.

Eudragit RL (ERL), generically referred to as Polymethacrylate, is widely used as film former for controlled release dosage forms²¹⁻²². Polymethacrylate polymers include ERL and Eudragit RS (ERS). However, ERL possesses higher permeability and hydrophilicity than ERS, since the content of quaternary ammonium moieties is greater in ERL²³. These polymers are weakly cationic in nature and therefore are prone to interaction with anionic drug moieties^{2, 16, 24,25}.

It has recently been shown that metoprolol free base and metoprolol tartrate act as plasticizers for Eudragit RL based networks in the dry state^{17, 18, 26}. Omari (1995), studied the interaction of diclofenac sodium (DS) with Eudragit RL and RS films prepared either from organic solutions or aqueous dispersions of these polymers²⁴. Except for the study by Adeyeye et al (2004), who reported that solid state mixtures of DS and Eudragit polymers (RS or L100-55) showed lower extent of interaction than in liquid state²⁷, drug excipient interaction was not investigated particularly during powder dry coating.

In this work, both metoprolol succinate (MS) and diclofenac sodium (DS) were selected as model drugs. The objective was to study drug-excipient interaction as well as the effect of certain processing parameters on the performance and stability of dosage forms when coated by dry ERL powder in comparison with conventional aqueous coating technique. In first part, free films of ERL alone or with drugs were prepared by casting method using aqueous dispersion or dry powder of the polymer. Free films were characterized using Fourier-transform infrared spectroscopy (FTIR), Nuclear magnetic resonance (NMR) and Differential scanning calorimetry (DSC). In the second part, tablets of either MS or DS, were prepared by wet granulation method and coated with ERL polymers using dry powder coating or conventional aqueous coating techniques. The tablets were tested for physical properties and drug release behavior. A stability (aging) study also was conducted for up to 3 months under different storage conditions during which tablets were retested for their dissolution behavior at predetermined periods. A color change study was also performed using adobe photoshop.

METHODOLOGY

Metoprolol Succinate (MS) and Diclofenac sodium (DS) were donated by Hikma Pharma PLC, Amman, Jordan; Eudragit RL 100 was donated by Evonik industries AG, Germany; Triethyl citrate (TEC) was purchased from Parchem, NY, USA; Lactose anhydrous was donated by Al-Taqaddom Pharm. Co. Amman, Jordan; microcrystalline cellulose (Avicel) was donated by FMC, PA, USA; Polyvinylpyrrolidone (PVP) was purchased from BASF Corp. (Mt. Olive, NJ, USA), Magnesium stearate and talc were purchased from Spectrum Chemical Mfg. Corp. (Gardena, CA, USA). Other solvents and reagents are of pharmaceutical grades.

Free films preparation

Free films of ERL aqueous dispersion, were prepared by casting technique reported by Lehman (1997)²⁸. A 5g ERL plus 1g (20% of dry polymer) triethyl

citrate (TC) as a plasticizer were added to 20g of distilled water (DW) (termed later as Aqueous Dispersion Film, ADF) and stirred, using high sheer propeller (IKA, Germany) for at least 3hr in a hot water bath ($>80^{\circ}\text{C}$). The weight then was corrected by DW under stirring until cooling to room temperature (RT). The mixture was dried on a Teflon tape (Taixing Chuanda Plastic Co., Ltd., China) at RT for 24 hr. The casting area was 15cm x 15cm and the casting volume was 25-30ml. ADF was then cured in an oven at 60°C for 2 hr which then peeled off, labeled and stored in double plastic cases at RT until further use. Free films containing drugs were prepared in the same way except that a 0.5g of either MS or DS was added to ADF and equilibrated using magnetic stirrer for 2 hr prior to casting.

Free films of polymer powder (termed later as dry powder film, DPF) was prepared by micronization of ERL100 pellets using an electric chopper (Moulinex Co. France). The particle size under 60μ -sieve (5g) was taken, mixed well with TC (1g=20% of polymer), using mortar and pestle, distributed evenly by a ruler on Teflon tape and cured in an oven at 75 - 80°C for 6 hr. The film was then peeled off and stored in double plastic cases until further use. For DPF with drugs, 0.5 g of either MS or DS was added to the polymer-plasticized mixture and further mixed homogeneously and continue with the same procedure.

Free Film Characterization

NMR

Proton Nuclear magnetic resonance (H^1 -NMR) spectra for the free films prepared were determined using NMR spectrometer (Bruker 400MHz Avance III, USA). Samples were dissolved in DMSO or CDCl_3 as a solvent and tetramethylsilane (TMS) as an internal standard.

DSC

The glass transition temperature (T_g) of the polymeric systems was determined by differential scanning calorimetry (DSC 821; Mettler Toledo AG, Giesen, Germany). Film

samples of approximately 6 mg were accurately weighed into aluminum pans, which were sealed and perforated. The samples were heated (at $5^{\circ}\text{C}/\text{min}$) under a nitrogen atmosphere from 0 to 100°C . The T_g and heat flow energy (mJ) were determined.

FTIR

FTIR spectra were determined Using FTIR spectrometer (Bruker, Billerica,

MA, USA) and KBr pellets. The scanning range was 4000-400 cm^{-1} . Spectra for drugs, ERL polymer, free films of polymer with or without drugs were obtained.

Tablets Preparation

Tablets of either MS or DS were prepared by wet granulation method using PVP solution (10%) as a binder. Formulae are shown in Table 1. Granules were mixed with appropriate amount of magnesium stearate and compressed into tablets using single punch tableting machine (Korsch, GMPH, Germany) tooled with 12mm shallow concave punch. Tablets were characterized for their content and weight uniformity, hardness, friability and disintegration time. Table 2 shows tablet properties.

Table 1. Tablet formula of either Diclofenac sodium or metoprolol succinate.

Ingredients	Wt (mg/tab)
MS or DS	50
Lactose anhydrous	200
Microcrystalline cellulose	200
PVP (as 10% solution)	~2
Mg stearate	~1%
Total	~450

Table 2. Physical properties of tablets prepared from DS or MS.

Tablet properties	Value
Hardness (N)	20-35
Friability (%)	< 1
Disintegration time (min)	5-10
Weight uniformity (mg) \pm 5%	450
Content Uniformity (mg) \pm 5%	50

Tablets Coating

Tablets prepared in the previous section were coated with ERL aqueous dispersion using fluid bed (Wurster) system (Aeromatic STREA1, AG, Switzerland). Coating formulation and conditions were as reported in a previous work ²⁹. In brief, a certain weight of tablets was loaded in the coating chamber and after preheating the weight was taken again as initial weight (Wi). The process then started at a low spray rate which increased gradually under a suitable atomizing and fluidizing air rates. The coated tablets were then cured in a static tray-

oven at 60°C for 24 hours. The final weight (W_f) was taken and the amount of coat was calculated as percentage coat to core ratio (%CCR=[$W_f - W_i / W_i$] $\times 100$).

Dry powder coating was conducted in the same coating apparatus, with a simple modification. A side hole (6mm in diameter) was drilled in the lower side of the Wurster chamber to facilitate powder delivery (see fig1). ERL micronized powder (<60 micron) was fed using powder feeder (AccuRate® Tuf-Flex™ feeders, Schenck Co. USA) connected via silicon tubing, 15mm in diameter from feeder side and 5mm from the other side to fit the drilled hole. Powder delivery was performed with the aid of compressed air via a separate airway hose (2mm in diameter) inserted directly in the silicon tubing. The process was carried out by spraying TEC -as a plasticizer- by the Wurster's bottom spray nozzle, using a peristaltic pump (VELP Scientifica, SRL, Italy), onto tablets to wet their surfaces, followed immediately by direct powder application. These 2 steps were repeated in a reciprocal intermittent way till the end of predetermined quantity of coat. Feeding rate and other coating conditions are shown in Table 3. At the end of the process, the tablets were cured in a static oven on Teflon-lined trays at 60°C for 24 hours. To prevent sticking during the curing step (and later in stability test), the cured tablets were dusted with 1-2% talc based on the weight of the coated tablets. Percentage CCR was calculated as in aqueous process.

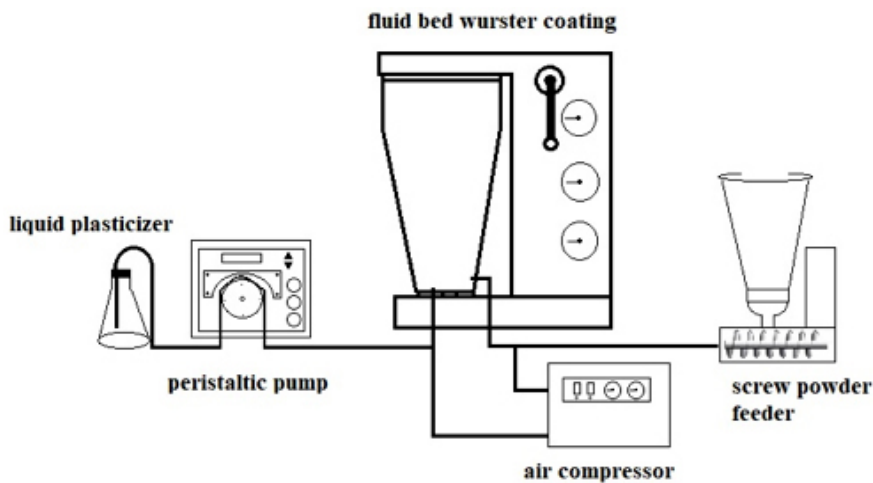


Figure 1. Fluid bed coating system with modifications for dry powder coating.

Table 3. Conditions employed during dry coating process

Condition	Values
Tablets batch weight (g)	250
Plasticizer Spray rate (ml/min)	1-2
Atomizing air pressure (bar)	1.5
Fluidizing air rate (m ³ /hr)	50
Inlet air temperature (°C)	55
Outlet air temperature (°C)	45
Powder feeding rate (g/min)	2-5

A total of eight tablet batches were prepared of both DS (4 batches) and MS (4 batches) coated with ERL-ADF or ERL-DPF. Table 4 shows these batches and their CCR percentages. It is noteworthy that the objective of this work is to study interaction of drugs with excipient (coating polymer or other additives) using either solvent-dependent (aqueous dispersion) or solventless (dry powder) techniques irrespective of coat ratio. Therefore, the CCR value will not be considered as an investigating parameter in this research.

Table 4. Tablet batches of DS or MS prepared in this work and coated with either ERL-ADF or ERL-DPF of different coat-to-core ratios (%CCR).

No	DS tablets		MS tablets	
	Coated with	%CCR	Coated with	%CCR
1	ERL-ADF	2.7	ERL-ADF	1.0
2	ERL-ADF	4.0	ERL-ADF	4.0
3	ERL-DPF	2.4	ERL-DPF	1.6
4	ERL-DPF	3.0	ERL-DPF	4.4

Dissolution of coated tablets

Dissolution of coted tablets was conducted in 1000ml of gradient pH profile dissolution media corresponding to pH 1.2 (0.1N HCl) (for 2 hr) and 6.8 (phosphate buffer) using USP II (paddle) method apparatus (Esico International, India) operated at 75 rpm (± 3 rpm) and 37°C (± 1 °C). The change in pH was done *in situ* by addition a precalculated amount of concentrated solution of tribasic sodium phosphate directly to the medium ³⁰. Five milliliter samples were withdrawn at predetermined intervals up to 20-24hr, replaced immediately with fresh medium, filtered through Millipore filter (Merck, Germany) and analyzed spectrophotometrically (SCO-TECH, GmbH, Germany) at λ_{\max} 276 nm and 222 nm for DS and MS, respectively. Average of at least 3 replicates was calculated.

Dissolution Kinetics

The percentage of drug released was first calculated, then the average of three independent replicates along with standard deviation were measured. Data was then fitted to 2 kinetic models: zero order and first order equations. For zero order, the linear regression and linear equation was calculated for the first 6 time points. In case of first order, the percentage of drug released transformed to natural Logarithm then the linear regression was conducted. linear equation was used is $y = ax + b$, where a is the slope and b is the intercept with the y axis. Both a and b were calculated for all data points using Microsoft Excel.

Stability study of coated tablets

All tablet batches prepared in this work (see Table 4) were included in stability study. Adequate quantities of tablets from each batch were filled in plastic (HDPE) bottles, closed and stored in a closed cabinet at room temperature (RT, $20 \pm 3^\circ\text{C}$), or in stability chambers (Binder GmbH, Germany) at 40°C ($\pm 3^\circ\text{C}$) and 50°C ($\pm 3^\circ\text{C}$) for 3 months. After 1, 2 and 3 months, samples of tablets were withdrawn and inspected visually for any change in surface appearance, analyzed for color changes (see next section) and retested for their dissolution behavior and compared with the initial data (at zero time).

Color change study

Two batches of each of MS or DS tablets coated with either ADF or DPF were selected; namely: MS tablets of CCR 1% and 4.0% ADF and 1.6% and 4.4% DPF and DS tablets of CCR 2.7% and 4% ADF and 2.4% and 3% DPF. As a row of three tablets, a photo using camera was taken (Fig 2). Two different types of analysis were then conducted: qualitative and quantitative.

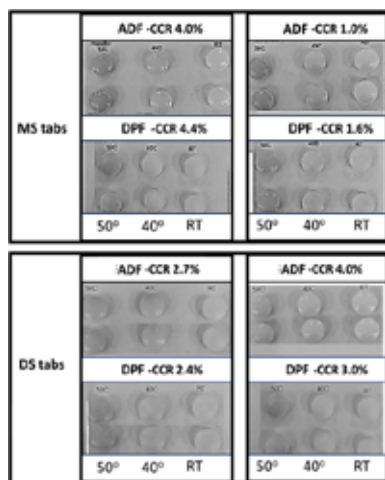


Figure 2. Images (in black and white) for selective tablets of different CCR and at different storage conditions to study color variation.

Qualitative analysis: an image processing was conducted using Adobe Photoshop to show the density of yellow color in black and white images. The images were split into the original channels (red, blue and green).

Quantitative analysis: To endorse the variation of yellow color between the tablets, the intensity of yellow color was measured. The procedure is summarized in Fig 3. Using unprocessed colored images, the hexadecimal code of the tablet color was identified using color picker tool from Adobe photoshop. The regions with extreme shadow and light have been excluded. The hexadecimal code was then applied on ColorHexa website (www.colorhexa.com) to get the intensity of red, blue, green, yellow and black color. The average yellow color was then calculated for multiple images of the same formulation. Later, the averages of three independent images were graphed using Microsoft excel.

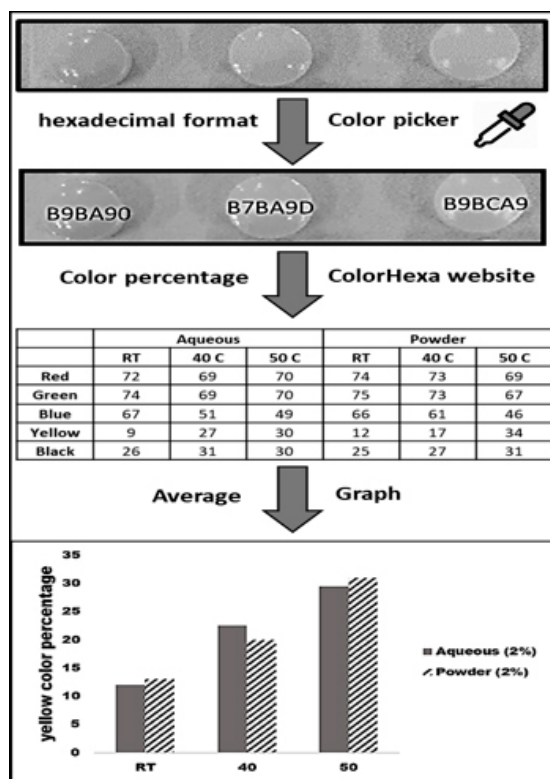


Figure 3. The image analysis steps. the hexadecimal format of each tablet color was identified using color picker from Adobe illustrator, then the percentages of colors (Red, Green, Blue, Yellow, Black) for each hexadecimal name were identified using Colorhexa website (www.colorhexa.com).

RESULTS AND DISCUSSION

Free films characterization

The functional groups of Eudragit polymers (and in some cases, the charges associated) make them readily reactive with drug substances³¹. Interaction of

the Ammoniomathacrylate copolymers (ex. ERL) (Fig 4) with other molecules is, most probably, attributed to their quaternary ammonium groups (QAGs) content^{22,24,31}. In coating technology, studying the effect of such interactions on different properties of the final polymer films and later on the drug dosage form, free film (vs applied film) technique is usually adopted. Such technique has been established as a successful tool in the development of a film coating systems³²⁻³³. In this work, free films of ERL either from aqueous dispersion or dry powder with or without drugs were prepared using casting method and characterized for drug- polymer interactions using methods such as FTIR, NMR and DSC.

In a previous work²⁴, a stoichiometric ionic interaction was detected between DS solution and ERL powder and ERL aqueous dispersion and was supported by evidences from FTIR spectroscopy and X-Ray diffraction. However, the interaction was slower in case of powder than aqueous dispersion due to particle surface area difference²⁴.

In this work, ADF and DPF of DS were prepared in 1:10 ratio and characterized using FTIR, NMR and DSC. Fig 5 shows the FTIR spectrum of ERL-DS ADF and ERL-DS DPF (the complete spectra of the 2 drugs as well as pure polymer were shown in the associated supplement file). In aqueous films two peaks were appeared at 1557 and 1574 cm^{-1} which, most probably, correspond to secondary amine in DS molecule (see structure in Fig 4). In dry films these peaks were not shown or insignificant. This could be explained as follows: the ionic interaction between carboxylate anions of DS and quaternary ammonium cations of ERL in case of ADF, introduce some modification (such as deshielding) to the secondary amine of DS made it detectable by the FTIR spectrometer. This did not happen in DPF. In FTIR of ERL with MS (see supplement file), some small peaks appeared, however, not significant.

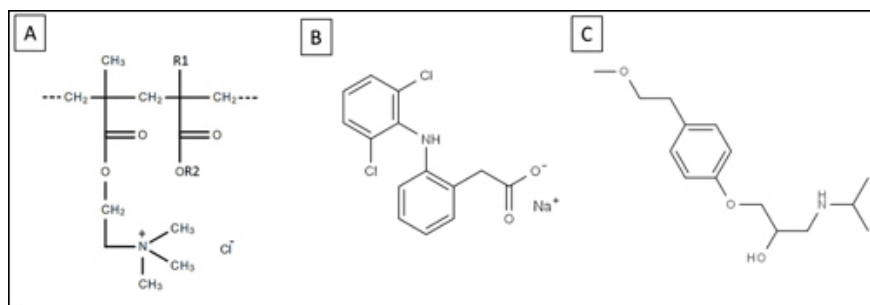


Figure 4. Chemical structure of (A) ERL polymer, (B) Diclofenac Sodium (C) Metoprolol Succinate

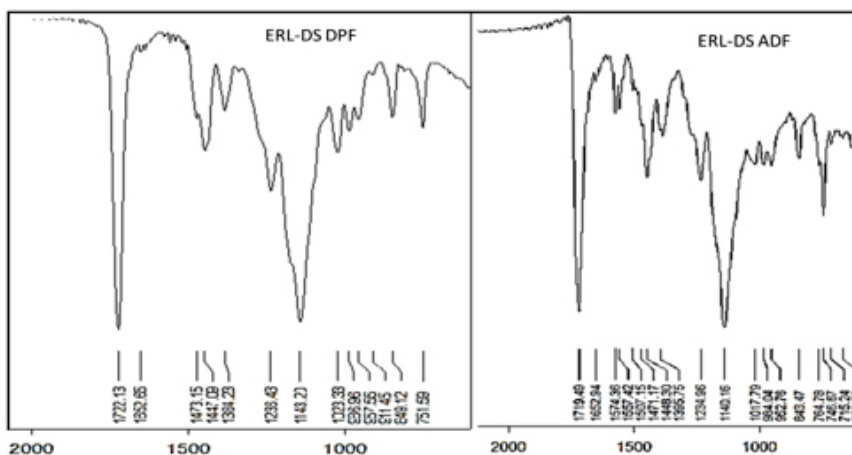


Figure 5. FTIR spectra of ERL free films: A) ERL-DS DPF B) ERL-DS ADF

Metoprolol interaction with polymethacrylate polymers was extensively investigated by Siepmann et al (2006) and Glaessel et al (2009, 2010)^{16-17, 26}. They found that metoprolol tartrate (and chlorpheniramine maleate and ibuprofen) act as efficient plasticizers for Eudragit RS as indicated by the significantly decreased Tg with increasing drug loading, irrespective of the type of drug²⁶. In this work, MS were added in 1:5 ratio to ERL aqueous dispersion (without TEC) and cast on Teflon tape for 24hr. A clear transparent film was obtained (see Fig 1 A in supplement file) which is in agreement with the results reported in literature¹⁶⁻¹⁷. DS in a similar experiment, failed to form a film (see Fig 1 B in supplement file). Attempts to prepare a dry powder film containing drug and polymer only were unsuccessful even at higher temperatures (up to 80°C).

A strong evidence on MS interaction with the polymer was obtained using proton NMR spectroscopy of the free films (Fig 6). In spectrum of ERL-MS ADF (Fig 6B) in the region around 3.5 ppm where the protons of QAGs are expected to resonate, 2 peaks were depicted at 3.55 and 3.59 ppm. In the spectrum of the DPF (Fig 6A) only one peak is obtained at 3.59 ppm. In aqueous films, MS as a water-soluble drug, will dissolve and an electrostatic or hydrophilic interaction with the polymer is expected. This interaction led up to formation of a new peak in that region. In the DPF no new peak observed. The same can be said for interaction of DS with ERL NMR spectrum, however not in the same degree of clarity (Fig 6 C and D).

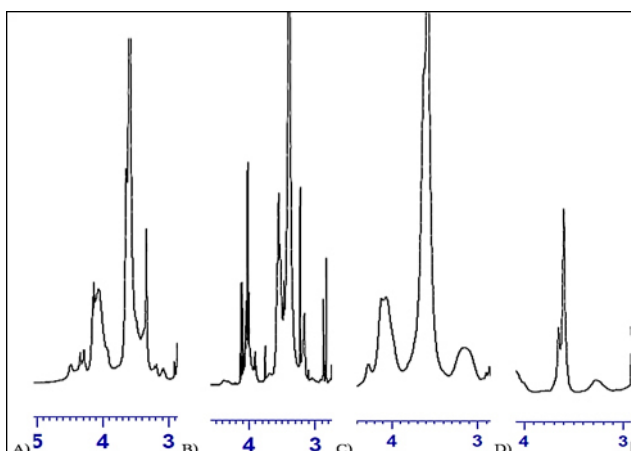


Figure 6. Proton NMR spectra of free films: A) ERL-MS DPF, B) ERL-MS ADF, C) ERL-DS DPF and D) ERL-DS ADF.

Thermal study using DSC for free films of ERL alone or containing drugs showed that the transition behavior of these films was different in aqueous from that in dry films (Fig 7 and table 5). The glass transition temperature (T_g) of ERL100 was reported to be $58-68^\circ\text{C}$ ³⁴⁻³⁵. In this work, DSC thermograms showed that in aqueous films T_g was reduced by TEC to 54°C and further reduced to 48 and 53°C after interaction with DS and MS, respectively (Table 5). In dry films TEC reduced T_g to below 50°C , however addition of either drugs (with TEC) increased it to 53°C and 54°C for DS and MS, respectively. The explanation to this behavior is that, in the aqueous systems, drugs may synergize plasticization effect of the TEC while in dry films antiplasticization effect occurs³⁶. This may also explain the difference in heat flow magnitudes during transition which was significantly higher in aqueous in comparison to dry films as shown in Table 5.

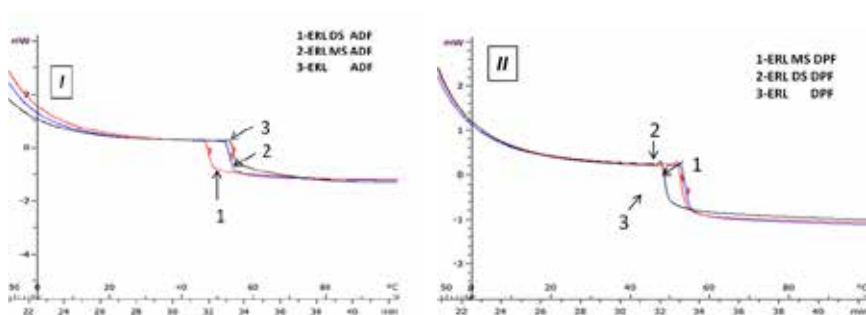


Figure 7. DSC thermograms of free films of ERL with or without drugs. I) aqueous dispersion films (ADF). II) dry powder films (DPF).

Table 5. Glass transition temperature (T_g) and Heat flow of ERL free films with or without drugs according to method of preparation (aqueous or dry)

Film Preparation	T _g Midpoint (°C)	Heat Flow (mJ)
ERL ADF	54	- 46
ERL-DS ADF	48	- 24
ERL-MS ADF	53	- 21
ERL DPF	49	- 15
ERL-DS DPF	53	- 18
ERL-MS DPF	54	- 25

Coating Process of Tablets with ERL ADF or DPF

The coating process was performed using fluid bed (Wurster) system for both aqueous conventional coating and powder dry coating. However, to suit the technique for dry coating, a modification in the apparatus (see experimental section) was done in order to facilitate dry powder feeding to coating chamber. In literature, several trial investigations have been published. Some of these include fluid bed system and centrifugal granulator⁹, modified Wurster apparatus³⁷, rotary fluid bed³⁸ and modified lab scale spheronizer³⁹⁻⁴¹. In most of these studies, modifications were made to the original apparatus without technique standardizations. In our work, since (up to the authors' knowledge) no standard apparatus can be obtained, the introduced modifications to fluid bed system helped to reach good success. However, standardization and validation of such technique still required.

All tablet batches prepared in this work (see Table 4 in experimental section) were investigated for coat uniformity, color changes and stickiness during coating. In general, all batches were of good coat and color uniformity, however, dry coated tablets showed somewhat more stickiness than those coated with aqueous dispersion. This might be attributed to high percentage (40%) of the highly hydrophilic plasticizer (TEC) used in case of dry process. Therefore, use of dusting talc has become an essential requirement in order to minimize this phenomenon. All batches also were tested for their dissolution behavior (i.e. at zero time) for the purpose of initial drug release performance and as a reference for comparison in later studies (see results in the next section).

Stability Study

Stability is the extent to which a product retains, within the specified limits, throughout its period of storage and use, the same properties and characteristics possessed at the time of its manufacturing. Stability testing thus evaluates the effect of environmental factors on the quality of the drug substance or a

formulated product⁴²⁻⁴³. In this study, different tablet batches prepared (Table 4) were stored at different conditions as explained in experimental section. Tablets were tested for color changes and dissolution behavior.

Color Change Study

Many recent articles were published using color change as stability indicator⁴⁴⁻⁴⁶. In this study the discoloration of tablets via the formation of yellow color was studied qualitatively and quantitatively.

In the qualitative color analysis, as shown in Fig 2, black and white picture doesn't represent the real case, as the change in tablets color is undistinguished specially between 40°C and room temperature (RT), as well as between aqueous and dry (see Fig 2). Therefore, image processing was conducted by splitting images into the original channels. As seen in Fig 8 there is a distinct change in color using blue filter between the stored tablets at different temperatures, while no differences were observed using red and green filter. Yellow color appears as black color under blue filter. Therefore, it's clear that the intensity of yellow color is proportional to the heat; as the storage temperature increases, the yellow color intensity increases (Fig 8 blue filter).

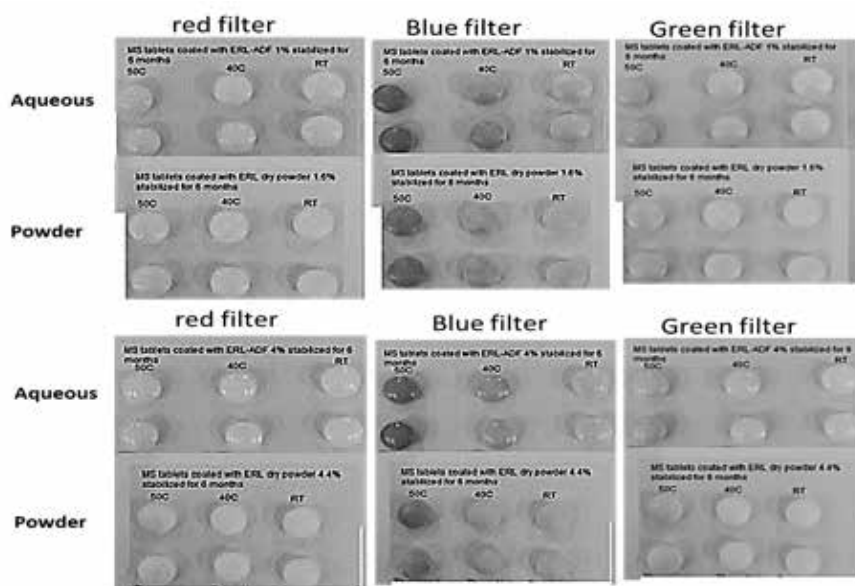


Figure 8. Tablet images after split into red blue and green channel. The upper image is MS tablets coated with 1% ERL-ADF (Aqueous) and 1.6 % ERL-DPF (Powder), the lower image is MS tablets coated with 4.0% ERL-ADF (Aqueous) and 4.4% ERL-DPF (Powder).

The quantitative analysis of yellow color is needed to differentiate the effect of coating method on the discoloration of tablets. As has been illustrated in Fig 9 (A and B), in case of MS, the yellow color was more intense in aqueous coating than in dry coating across the range of temperatures. The analysis suggests potential benefits of using dry over aqueous coating. Meanwhile, it was not the case with DS (Fig 9 C and D), the intensity of yellow color was somewhat similar between aqueous and dry coating.

The source of yellow-brown color is highly suggested due to a Maillard reaction (browning reaction), which has been observed in several drug formulations^{18,47-49} including metoprolol⁴⁷. Browning reaction is initiated by the heat, and that explains the increasing in the intensity of yellow color was associated with the elevating of the storage temperature. All formulations in this study contained lactose and polyvinylpyrrolidone which play parts of Maillard reaction under the stress of temperatures⁵⁰. Also, this reaction peaks in the presence of water and occurs better in alkaline than in acid conditions. This explains the higher color intensity in aqueous coating systems than dry powder coating systems. Meanwhile explains why the MS tablets with aqueous coat (Metoprolol pKa=9.5), has more intense yellow color than DS tablets (Diclofenac pKa=4.5)⁵⁰.

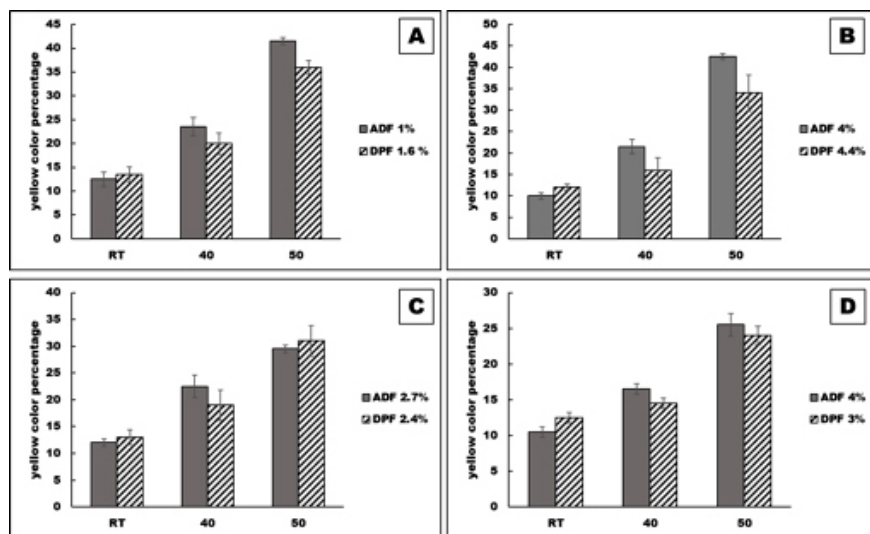


Figure 9. Comparison of the density of tablet's yellow color at different storage conditions; room temperature (RT), 40°C and 50°C, for both MS and DS. A) MS tablets: 1.0% ADF vs 1.6% DPF, B) MS tablets: 4.0% ADF vs 4.4% DPF, C) DS tablets: 2.7% ADF vs 2.4% DPF, D) DS tablets: 4% ADF vs 3.0% DPF. The error bar represents the standard deviation of the mean.

Dissolution: Dissolution of different tablet batches stored at various storage conditions were conducted in pH profile media (acidic pH 1-2 for 2 hrs then basic pH 6.8 up to 22 hrs) and compared with the results at zero time. A total of 88 graphs were plotted. A representative example are shown in Fig 10.

The drug release kinetics was studied by fitting the data of cumulative amount drug dissolved vs time to two kinetic equations: zero order and first order models⁵¹. Due to the fact that a large quantity of data were obtained, a representative results of 1 batch were shown in Table 6 (other data are shown in Table 2 in supplement file). From these data it is clear that zero order model is the one of best fit.

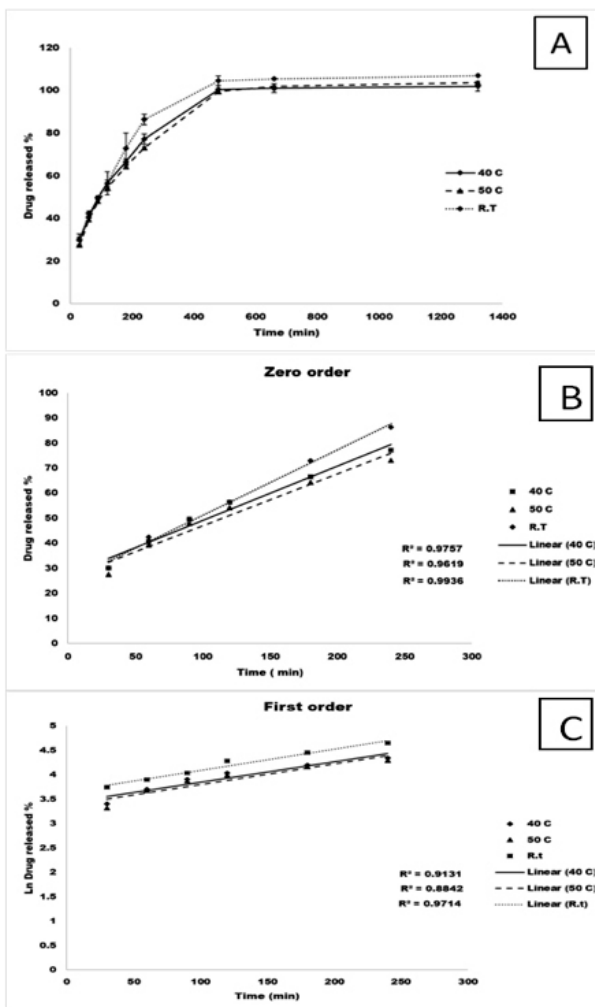


Figure 10. A model for the kinetics of drug release, the example is MS tablets coated with ERL-DPF 1.6 % CCR after 3 months of storage at different temperature. A) cumulative drug release data. B) the data fitted into zero order kinetics. C) the data transformed into natural logarithm and then fitted in to first order kinetics. Each experiment was conducted in triplicate, the error bar in graph (A) represents \pm SD. The linear regression (R^2) is shown on the graph for each storage temperature.

Table 6. An example of kinetics data. MS tablets coated with ERL-DPF 1.6 % CCR different storage time in different storage temperatures. a = slope of the linear equation, b = is the intercept with the y axis, $\text{EXP}(b)$ = inverse natural logarithm (b), R^2 = the coefficient of determination

Storage time (months)	Temperature (C)	Zero order			First order		
		R^2	a	b	R^2	A	$\text{EXP}(b)$
0		0.986	0.3125	24.12	0.9555	0.0052	30.35618
1	R.T	0.9272	0.2182	26.423	0.8128	0.0044	34.62237
	40	0.9764	0.2076	26.706	0.9253	0.0035	32.23974
	50	0.9706	0.2091	27.701	0.9072	0.0036	30.93536
2	R.T	0.9634	0.2035	29.557	0.9118	0.0035	40.97655
	40	0.9751	0.2114	26.841	0.9164	0.0039	29.89825
	50	0.9699	0.2079	26.527	0.9047	0.004	29.27693
3	R.T	0.9936	0.2612	24.97	0.9712	0.0049	37.12535
	40	0.9757	0.2168	27.429	0.9131	0.0042	30.90444
	50	0.9619	0.2075	26.176	0.8842	0.0042	29.22721

To compare the effect of two coating processes (aqueous vs dry powder), data of zero order kinetic model of 2 batches of each drug (see Table 1 in supplement file) were considered. Dissolution rate constants (a) from this table (Table 1 in supplement file) were taken as a comparison parameter and included in Table 7.

As the kinetics are more fitted into zero order, the drug release is independent on the initial concentration, and totally depends on the rate constant (a), which can mathematically be driven from the slope of linear equation. According to Table 7, the rate of release is smaller in aqueous coating than in dry coating. However, (a) values in aqueous coating were doubled with storage time while no significant changes in (a) were observed in dry coating method. One-way ANOVA were conducted to test if the change in slope (a) is statistically different between the two methods. The percentage ratios of (a) values at storage temperatures to its value at zero time were used. According to the results in Table 8, the F-value is greater than the F-critical value for the alpha level ($p < 0.001$). Therefore, the change in dissolution rates are significantly different between dry and aqueous coating and, hence, dry powder coating can improve stability of drug product with respect to dissolution rate in comparison with aqueous coating.

Table 7. Zero order dissolution rate constants (a) for the different batches from table 7.

	Storage time/Temp	RT	40C	50C
DS tablets coated ERL-ADF 2.7%				
	0	0.0243		
	1	0.0571	0.0461	0.0539
	2	0.0506	0.0415	0.0655
	3	0.0374	0.035	0.0294
DS tablets coated ERL-DPF 3.0%				
	0	0.3072		
	1	0.2916	0.2194	0.332
	2	0.3101	0.3081	0.3405
	3	0.2896	0.2872	0.2033
MS tablets coated ERL-ADF 4.0%				
	0	0.1271		
	1	0.2218	0.2244	0.2293
	2	0.2338	0.2344	0.2424
	3	0.2167	0.251	0.2301
MS tablets coated ERL-DPF 4.4%				
	0	0.2258		
	1	0.2228	0.232	0.2264
	2	0.2368	0.2567	0.2589
	3	0.2407	0.1997	0.2242

Table 8. One-way ANOVA test of the percentage ratios of (a) values at storage temperatures to its value at zero time

Drug	Source of Variation	Square sum	Medium square	F ^a
MS	Dry and aqueous coating	2.883333	2.883333	605.0239
DS	Dry and aqueous coating	4.239504	4.239504	33.76046

F critical= 4.493998

^a Significant for P < 0.001.

Drug interaction with coating materials was studied under solvent-dependent (aqueous) coating process in comparison with solventless (dry powder) coating technique. Studies on free films of ERL alone or containing drugs (MS or DS) showed a significant decrease in interaction extent in dry powder coating relative to aqueous coating. These results were confirmed using FTIR, NMR and DSC characterization methods. Tablets of either MS or DS were prepared and coated successfully in a modified Wurster fluid bed using ERL micronized

powder (solventless) as a film former and TEC as wetting agent and plasticizer. These tablets in different %CCR were tested initially for physical properties and dissolution behavior and compared to those coated with ERL aqueous dispersion. A stability study was conducted for dry coated as well as aqueous coated tablets at different storage conditions (RT, 40°C and 50°C) for up to 3 months. Dissolution testing for the stability batches showed that release rate constant calculated from zero order kinetics possessed greater change extent in aqueous than dry powder coating as indicated by ANOVA test. The results of color change study supported the above results of free films and stability batches and showed that yellowing (due to Millard reaction) in aqueous coated tablets was significantly higher than in dry coated ones. However, the need for validation process of dry powder coating method is considered a major limitation of this study, which is hopefully, a future work.

ACKNOWLEDGEMENT

This work was fully supported by the **Deanship of the Scientific Research at Yarmouk University, Irbid, Jordan**. Grant No 32/2015.

The authors wish to thank Miss **Bushra Ababneh**, MSc. Chem., Yarmouk University, for her excellent effort in achieving most of the experimental works. Also, authors would like to thank Mrs **Samia Jarrah** for her efforts in the beginning of the project.

Authors also express their best thanks to **Hikma Pharma PLC**, Jordan, **Evonik industries Co**, Germany and **FMC Co**, USA for kind donation of many materials used in this research.

Conflict of Interest

No conflict of interest

REFERENCES

1. Porter, S. C. Coating of Pharmaceutical Dosage Forms, in Gennaro, A.R. (edr), *Remington: The Science and Practice of Pharmacy*, Mack Pub. Co. **1995**, 1650-1659.
2. Omari, D. Study of Interactions of Film coating Materials with Drug Formulation Components in Solid Dosage Forms, PhD Thesis, Cairo University, Egypt, **2003**.
3. Hogan, J. Film Coating Materials and Their Properties, in Cole, G, *Pharmaceutical Coating Technology*, Tayler & Francis. **1995**, 6-52.
4. Haris, M.; Ghebre-Sellassie, I. Aqueous polymeric coating for Modified Release Oral Dosage forms in McGinity, W and Felton, L. *Aqueous Polymeric Coating of Pharmaceutical Dosage Forms*, 3rdEdn., Informa healthcare. **2008**, 47-66.
5. Aulton, M.; Twichell, A. Film coat Quality, in Cole, G. *Pharmaceutical Coating Technology*, Tayler& Francis. **1995**, 363-408.
6. Jones, D. Pharmaceutics-Dosage Form and Design, Pharmaceutical Press. **2008**, 244-251.
7. Bose, S.; Bogner, R. H. Solventless Pharmaceutical Coating Processes: A Review. *Pharm Dev Technol.* **2007**, *12*, 115-131.
8. Luo, Y.; Zhu, J.; Ma, Y.; Zhang, H. Dry coating, a novel coating technology for solid pharmaceutical dosage forms. *Int J Pharm.* **2008**, *358*, 16-22.
9. Obara, S.; Maruyama, N.; Nishiyama, Y.; Kokubo, H. Dry coating: An innovative enteric coating method using a cellulose derivative. *Eur. J. Pharm. Biopharm.* **1999**, *47*, 51-9.
10. Pearnchob, N.; Bodmeier, R. Dry Powder Coating of Pellets with Micronized Eudragit® RS for Extended Drug Release. *Pharm. Res.* **2003**, *20*, 1970-1976.
11. Diane Bruce, L.; McGinity, J. Polymer Interactions with Drugs and Excipients, in McGinity, W and Felton, L. *Aqueous Polymeric Coating of Pharmaceutical Dosage Forms*, 3rdEdn., Informa healthcare, **2008**, 369-407.
12. Jenquin, M. R.; Liebowitz, S. M.; Sarabia, R. E.; McGinity, J.W. Physical and chemical factors influencing the release of drugs from acrylic resin films. *J. Pharm. Sci.* **1990**, *79*, 811-816.
13. Crowley, M. M.; Fredersdorf, A.; Schroeder, B.; Kucera, S.; Prodduturi, S.; Repka, M. A.; McGinity, J. W. The influence of guaifenesin and ketoprofen on the properties of hot-melt extruded polyethylene oxide films. *Eur. J. Pharm. Sci.* **2004**, *22*, 409-418.
14. Wu, C.; McGinity, J. W. Influence of ibuprofen as a solid-state plasticizer in Eudragit® RS 30 D on the physicochemical properties of coated beads. *AAPS PharmSciTech.* **2001**, *2*, 35-43.
15. Wu, C.; McGinity, J. W. Non-traditional plasticization of polymeric films. *Int. J. Pharm.* **1999**, *177*, 15-27.
16. Siepmann, F.; Le Brun, V.; Siepmann, J. Drugs acting as plasticizers in polymeric systems: A quantitative treatment. *J. Control. Release.* **2006**, *115*, 298-306.
17. Glaessl, B.; Siepmann, F.; Tucker, I.; Rades, T.; Siepmann, J. Deeper insight into the drug release mechanisms in Eudragit RL-based delivery systems. *Int. J. Pharm.* **2010**, *389*, 139-46.
18. Bharate, S. S.; Bharate, S. B.; Bajaj, A. N. Interactions and incompatibilities of pharmaceu-

tical excipients with active pharmaceutical ingredients: a comprehensive review. *J. Excipients Food Chem.* **2010**, *81*, 117-122.

19. Das, A.; Sathyamoorthy, N.; Garikapati, D. Development of enteric coated pantoprazole tablets with an aqueous based polymer. *Int. J. ChemTech Res.* **2013**, *5*, 2394-2404.

20. Omari, D. M. Formulation and In vitro/In vivo evaluation of esomeprazole enteric coated minitabets. *J. Drug Deliv. Sci. Technol.* **2017**, *39*, 156-165.

21. the United States Pharmacopoeia (USP) and the National Formulary (NF). USP 24- NF19. Rockville, Md. **1999**, 2000- 2209.

22. Rohm Pharm Info Sheets, GMBH, Darmstadt. **2002**, Info: O/E 2-4, 7.7E 1-4. 7.9/E 1-4.

23. R.C. Rowe, P.J. Sheskey, M.E. Fenton. Handbook of Pharmaceutical Excipients: Pharmaceutical Excipients. **2012**, 544-557.

24. Omari, D. M. The use of Drug-Excipient Interactions in The Design of Controlled Release Dosage Forms. MSc. Thesis, Jordan Univ. Sci. Tech. Amman. **1995**, 137-140.

25. Mehta, A. M. Processing and Equipment Consideration for Aqueous Coatings, in McGinity, W and Felton, L. *Aqueous Polymeric Coating of Pharmaceutical Dosage Forms*, 3rdEdn. Informa healthcare. **2008**, 67-103.

26. Glaessl, B.; Siepmann, F.; Tucker, I.; Siepmann, J.; Rades, T. Characterization of quaternary polymethacrylate films containing tartaric acid, metoprolol free base or metoprolol tartrate. *Eur. J. Pharm. Biopharm.* **2009**, *73*, 366-72.

27. Adeyeye, M. C.; Mwangi, E.; Katondo, B.; Jain, A.; Ichikawa, H.; Fukumori, Y. Dissolution stability studies of suspensions of prolonged-release diclofenac microcapsules prepared by the Wurster process: I. Eudragit-based formulation and possible drug-excipient interaction. *J. Microencapsul.* **2005**, *22*, 333-342.

28. Lehman, K, in McGinity, J.W. *Aqueous polymeric coating for pharmaceutical dosage forms*, 2nd ed. Marcel Dekker, New York. **1997**, 101-176.

29. Omari, D. M.; Sallam, A.; Abd-Elbary, A.; El-Samaligy, M. Lactic acid-induced modifications in films of Eudragit RL and RS aqueous dispersions. *Int. J. Pharm.* **2004**, *274*, 85-96.

30. Lehman, K. Practical course in film coating of pharmaceutical dosage forms with Eudragit. Darmstadt: Pharma polymer. **2001**, 144-147.

31. Diane Bruce, L.; McGinity, J. W. Polymer Interactions with Drugs and Excipients, in McGinity, W and Felton, L. *Aqueous Polymeric Coating of Pharmaceutical Dosage Forms*, 3rdEdn., Informa healthcare. **2008**, 369.

32. Allen, D. J.; Demarco, J. D.; Kwana, K. C. Free films I: Apparatus and preliminary evaluation. *J. Pharm. Sci.* **1972**, *61*, 106-110.

33. Parikh, N. H.; Porter, S. C.; Rohera, B. D. Tensile Properties of Free Films Cast from Aqueous Ethylcellulose Dispersions. *Pharm. Res.* **1993**, *10*, 810-815.

34. MatWeb: Material Property Data; www.matweb.com/search/datasheet.aspx

35. Kumar, M.; Sachan, N. An Overview on Polymethacrylate Polymers in Gastroretentive Dosage Forms Pravin Gupta1. *Open Pharm. Sci. J.* **2015**, *2*, 31-42

36. Mishra, A.; Pathak, A. K. Plasticizers: A Vital Excipient in Novel Pharmaceutical Formula-

- tions. *Current Res. Pharm. Sci.* **2017**, *7*, 1-10.
37. Ludwig, W.; Szafran, R. G.; Kmiec, A.; Dziak, J. Dry powder coating in a modified wurster apparatus. *Procedia Eng.* **2012**, *42*, 437-446.
38. Kablitz, C. D.; Harder, K.; Urbanetz, N. A. Dry coating in a rotary fluid bed. *Eur. J. Pharm. Sci.* **2006**, *27*, 212-219.
39. Zheng, W.; Cerea, M.; Sauer, D.; McGinity, J. W. Properties of theophylline tablets powder-coated with methacrylate ester copolymers. *J. Drug Deliv. Sci. Technol.* **2004**, *14*, 319-325.
40. Sauer, D.; McGinity, J. Properties of theophylline tablets dry powder coated with Eudragit® e PO and Eudragit® L 100-55. *Pharm. Dev. Technol.* **2009**, *14*, 632-641.
41. Sauer, D. An Investigation of Formulation Factors and Processing Parameters for the Powder-Coating of Tablets, PhD Dissertation, The University of Texas at Austin, **2008**.
42. Cao, Z.; Zhang, X.; Liu, L.; Zhao, L.; Li, H.; Wang, J. Effect of pH on the aggregation of α -syn12 dimer in explicit water by replica-exchange molecular dynamics simulation. *Int. J. Mol. Sci.* **2015**, *16*, 14291-304.
43. ICH Expert Working Group, ICH Guideline Q1A(R2) Stability Testing of New Drug Substances and Products, International Conference of Harmonization, **2006**, 873.
44. Li, Y.; Polozova, A.; Gruia, F.; Feng, J. Characterization of the Degradation Products of a Color-Changed Monoclonal Antibody: Tryptophan-Derived Chromophores, *Anal. Chem.* **2014**, *86*, 6850-6857
45. Mochizuki, K.; Takayama, K. Prediction of color changes in acetaminophen solution using the time-temperature superposition principle. *Drug Dev Ind Pharm.* **2016**, *42*, 1050-1057.
46. Katsura, S.; Yamada, N.; Nakashima, A.; Shiraishi, S.; Gunji, M.; Furuishi, T.; Endo, T.; Ueda, H.; Yonemochi, E. Investigation of Discoloration of Furosemide Tablets in a Light-Shielded Environment. *Chem. Pharm. Bull.* **2017**, *65*, 373-380,
47. George, R. C.; Barbuch, R. J.; Huber, E. W.; Regg, B.T. Investigation into the yellowing on aging of sabril® tablet cores. *Drug Dev. Ind. Pharm.* **1994**, *20*, 3023-3032.
48. Reddy, R. B.; More, K. R.; Gupta, L.; Jha, M. S.; Magar, L. Identification, synthesis, isolation and characterization of new impurity in metoprolol tartrate tablets. *J. Pharm. Biomed. Anal.* **2016**, *117*, 104-108.
49. Fathima, N.; Mamatha, T.; Qureshi, H. K.; Anitha, N.; Venkateswara Rao, J. Drug-excipient interaction and its importance in dosage form development, *J. Appl. Pharm. Sci.* **2011**, *1*, 66-71.
50. Labuza, T. P.; Reineccius, G. A.; Monnier, V. M.; O'Brien, J.; Baynes, J. W. Maillard Reactions in chemistry, food and health. Woodhead. **1998**, 175-198.
51. Siepmann, J.; Siepmann, F. Mathematical Models of Drug Dissolution: A Review. *Int J Pharm.* **2013**, *453*, 12-24.

SUPPLEMENT DATA

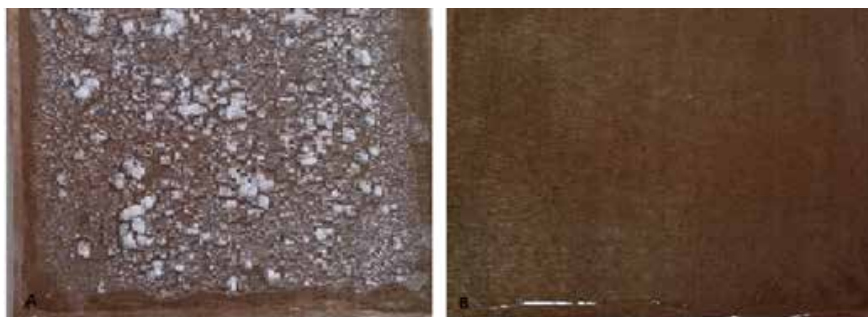


Figure 1. Interaction of model drugs with ERL aqueous dispersion without TEC a) 1 g DS unable to form a film. b) 1g MS formed a clear transparent film.

Table 1. Zero order kinetic model data of representative batches (2 of MS and 2 of DS) to compare aqueous coating with dry coating.

Drug	Coating	NCCR	months	St Temp	RZ	a	b	Drug	Coating	NCCR	months	St Temp	RZ	a	b		
diclofenac	aqueous	2.70%	0	RT	1	0.9859	0.0243	-0.301	dry	3.00%	0	RT	1	0.9977	0.3072	-0.7787	
					40	0.9885	0.0571	-1.368					40	0.9748	0.2916	9.2764	
					50	0.999	0.0481	0.1604					40	0.9954	0.2194	4.6484	
					50	0.9367	0.0989	-2.0673					50	0.9914	0.332	8.0901	
					RT	0.9822	0.0936	-1.0695					50	0.9976	0.3101	-0.149	
					40	0.9987	0.0413	-1.8966					40	0.9990	0.3081	4.8497	
	metoprolol	aqueous	3.60%	0	RT	1	0.9796	0.0274	0.2378	dry	4.40%	0	RT	1	0.9999	0.2896	3.6849
						40	0.9581	0.035	-1.8315					40	0.9627	0.2872	13.013
						50	0.9391	0.0294	0.6408					40	0.9919	0.2065	1.9912
						RT	0.9897	0.1271	8.7967					50	0.9515	0.2258	18.487
						40	0.9190	0.2238	23.611					50	0.9808	0.2218	31.596
						50	0.9411	0.2344	20.62					40	0.9834	0.232	25.795
diclofenac	aqueous	2.70%	0	RT	1	0.9353	0.3293	16.976	dry	3.00%	0	RT	1	0.9515	0.2258	18.487	
					40	0.9517	0.2388	18.343					40	0.9735	0.2368	34.595	
					50	0.9459	0.2344	13.464					40	0.9788	0.2567	19.317	
					50	0.9435	0.2424	14.288					50	0.9565	0.2589	18.711	
					RT	0.9517	0.2388	18.343					50	0.9735	0.2368	34.595	
					40	0.9459	0.2344	13.464					40	0.9788	0.2567	19.317	
	metoprolol	aqueous	3.60%	0	RT	1	0.9661	0.2187	20.951	dry	4.40%	0	RT	1	0.9657	0.2407	14.505
						40	0.9809	0.251	14.283					40	0.9737	0.1997	18.4
						50	0.9543	0.2301	17.9					50	0.9848	0.2242	22.014
						RT	0.9517	0.2388	18.343					50	0.9735	0.2368	34.595
						40	0.9459	0.2344	13.464					40	0.9788	0.2567	19.317
						50	0.9435	0.2424	14.288					50	0.9565	0.2589	18.711

FTIR Data

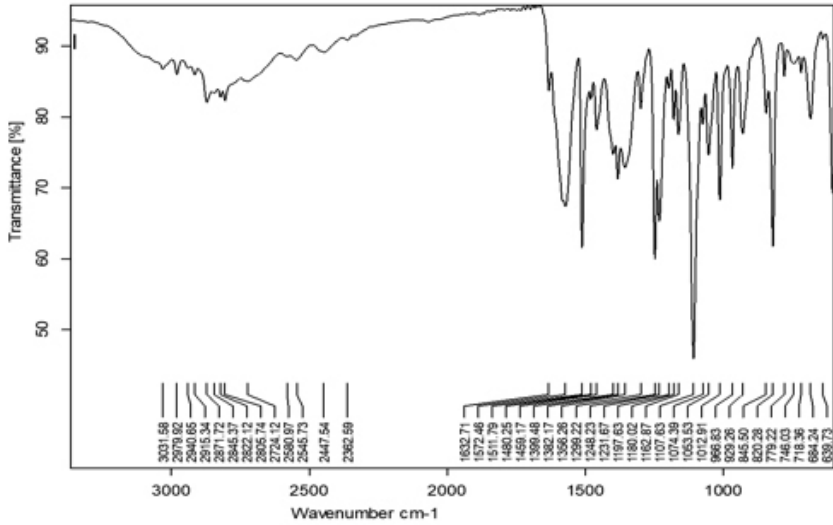


Figure 2. FTIR of metoprolol succinate

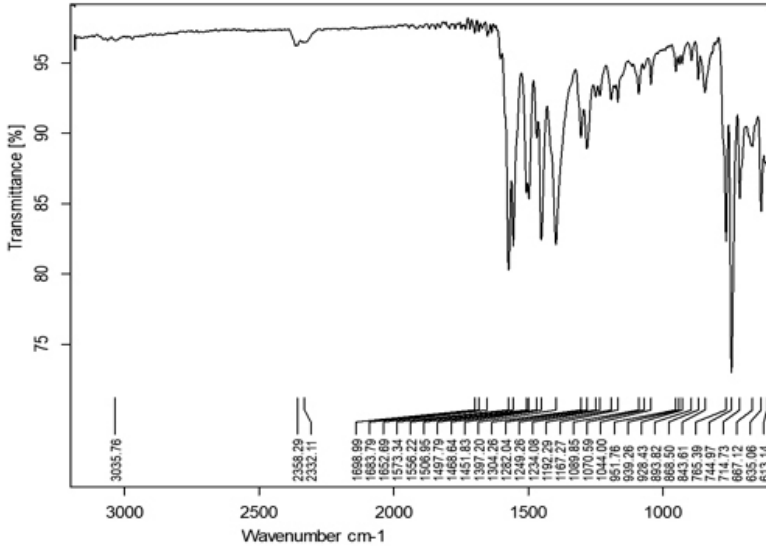


Figure 3. FTIR of Diclofenac sodium

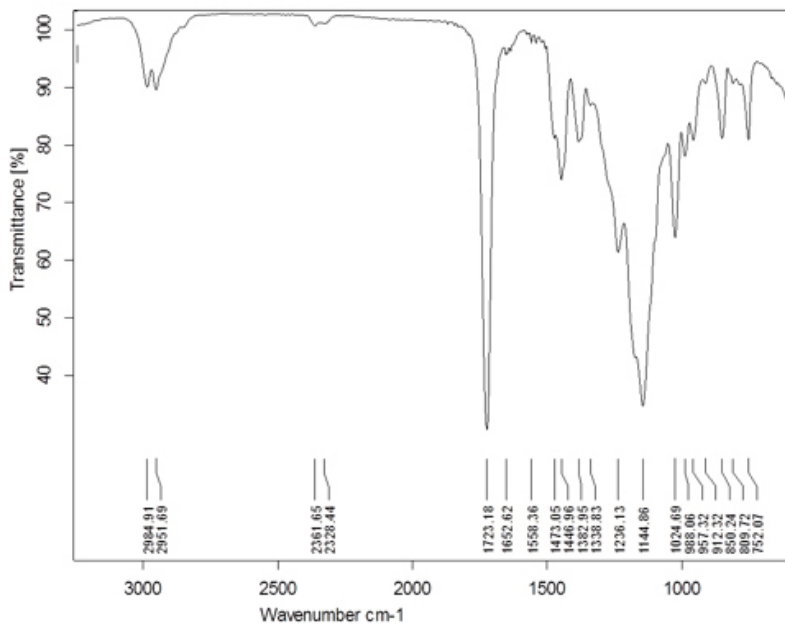


Figure 4. FTIR of ERL-100

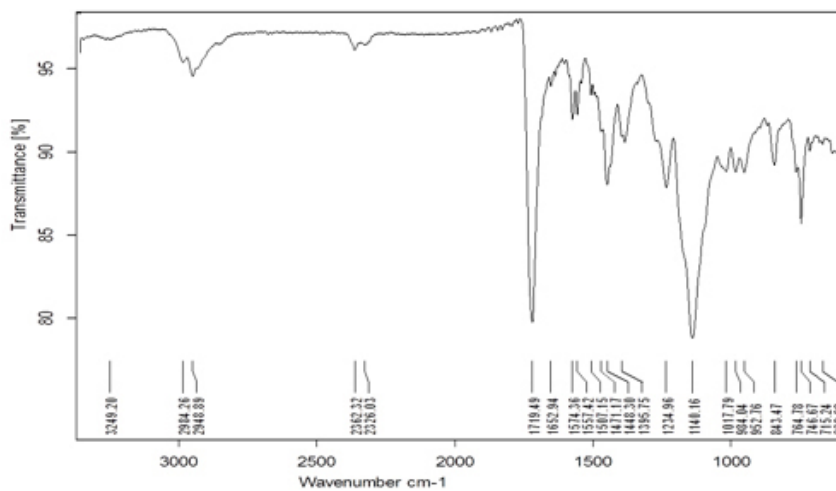


Figure 5. FTIR of ERL-DS ADF

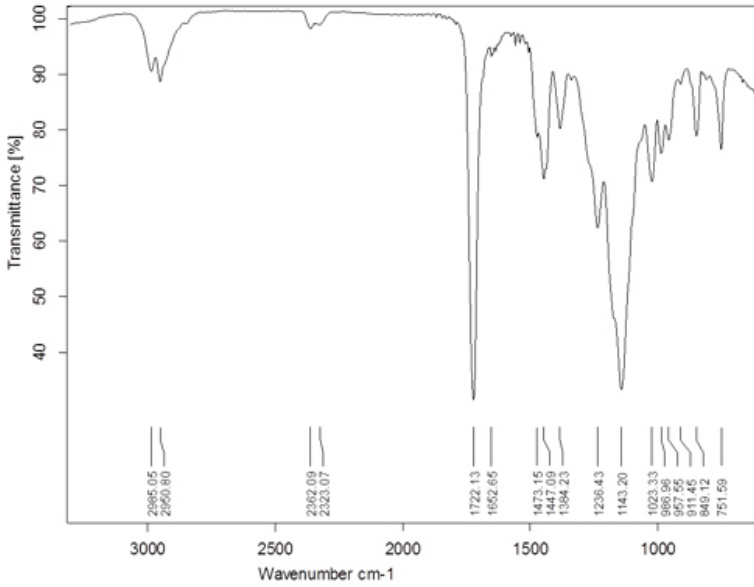


Figure 6. FTIR of ERL-DS DPF

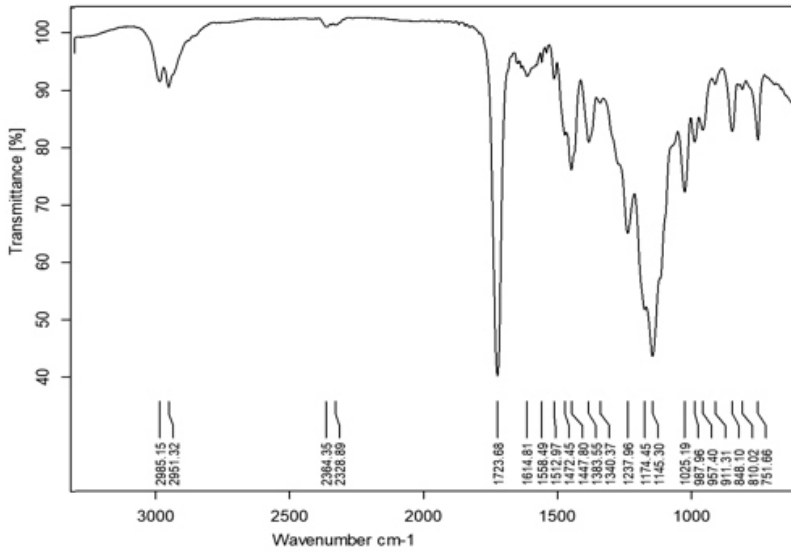


Figure 7. FTIR of ERL-MS ADF

Table 2. Kinetic data of different tablet batches in this work. For more details see Table 6 in the article, where Met: metoprolol, Dic: diclofenac sodium, Type: type of coating, To: storage temperature in Celsius, Stg: storage duration in months, Per% : percentage of coating, R.T: room temperature.

drug	Type	Per %	Stg	T°	Zero order			first order						
					R ²	a	b	R2	a	EXP (b)	b			
Met	dry	1.60	0		0.986	0.212	24.12	0.955	0.005	30.35	3.413			
				R.T	0.927	0.218	26.42	0.812	0.004	34.62	3.5445			
				40	0.976	0.207	26.70	0.925	0.003	32.23	3.4732			
				50	0.970	0.209	27.70	0.907	0.003	30.93	3.4319			
			1	R.T	0.963	0.203	29.55	0.911	0.003	40.976	3.713			
				40	0.975	0.211	26.84	0.916	0.003	29.898	3.3978			
				50	0.969	0.207	26.52	0.904	0.004	29.276	3.3768			
			2	R.T	0.993	0.261	24.97	0.971	0.004	37.125	3.6143			
				40	0.975	0.216	27.42	0.913	0.004	30.904	3.4309			
				50	0.961	0.207	26.17	0.884	0.004	29.227	3.3751			
			Met	dry	4.40	0		0.951	0.225	28.46	0.871	0.003	31.000	3.434
							R.T	0.986	0.222	31.59	0.941	0.003	41.268	3.7201
40	0.983	0.232					25.79	0.921	0.004	29.341	3.379			
50	0.985	0.226					21.70	0.922	0.004	25.459	3.2371			
1	R.T	0.9735				0.2368	24.595	0.9664	0.0045	36.64584	3.6013			
	40	0.9788				0.2567	19.337	0.8881	0.0054	24.24475	3.1882			
	50	0.9665				0.2589	18.711	0.8523	0.0056	23.24291	3.146			
2	R.T	0.9657				0.2407	24.305	0.8558	0.0044	28.76905	3.3593			
	40	0.9737				0.1997	28.4	0.8933	0.0036	31.98925	3.4654			
	50	0.9848				0.2242	22.014	0.9095	0.0043	26.94237	3.2937			
Met	aqueous	1.00				0		0.9408	0.2378	20.792	0.8357	0.0053	24.29814	3.1904
							R.T	0.9555	0.2034	20.66	0.8386	0.0045	23.91008	3.1743
			40	0.9077	0.2134		21.673	0.7827	0.0047	23.97712	3.1771			
			50	0.9075	0.1918		23.018	0.7705	0.0043	24.7667	3.2095			
			1	R.T	0.9417	0.2064	24.592	0.8225	0.0042	27.36323	3.3092			
				40	0.9298	0.2044	23.28	0.7966	0.0044	25.66941	3.2453			
				50	0.9813	0.2155	17.573	0.885	0.0047	22.22683	3.1013			
			2	R.T	0.9417	0.2064	24.592	0.8225	0.0042	27.36323	3.3092			
				40	0.9298	0.2044	23.28	0.7966	0.0044	25.66941	3.2453			
				50	0.9813	0.2155	17.573	0.885	0.0047	22.22683	3.1013			

3	R.T	0.9675	0.2078	23.448	0.8723	0.0041	27.27853	3.3061
	40	0.9562	0.2064	18.559	0.8251	0.0047	22.1536	3.098
	50	0.9744	0.2167	17.693	0.8579	0.0048	22.19795	3.1

Met	aqueous	4.00	0		0.9397	0.1271	8.7767	0.8158	0.0061	10.41555	2.3433
1	R.T	0.9193	0.2218	23.611	0.7836	0.0046	25.98709	3.2576			
	40	0.9412	0.2244	20.62	0.7977	0.0048	23.63432	3.1627			
	50	0.9333	0.2293	16.976	0.7627	0.0055	19.66224	2.9787			

2	R.T	0.9517	0.2338	18.343	0.8107	0.0051	21.99687	3.0909
	40	0.9439	0.2344	15.464	0.8567	0.0052	20.54875	3.0228
	50	0.9435	0.2424	14.088	0.8488	0.0055	19.21133	2.9555

3	R.T	0.9661	0.2167	20.951	0.8756	0.0044	25.21654	3.2275
	40	0.9809	0.251	14.282	0.8688	0.0054	20.39317	3.0152
	50	0.9543	0.2301	17.9	0.8297	0.005	22.11818	3.0964

Dic	dry	2.40	0		0.9816	0.3892	-9.2499	0.858	0.0085	9.625348	2.2644
1	R.T	0.9817	0.3273	-7.3125	0.9258	0.0096	6.920583	1.9345			
	40	0.9817	0.3489	-0.7333	0.8773	0.0084	11.13619	2.4102			
	50	0.9747	0.361	-5.8693	0.9012	0.0094	9.189854	2.2181			

2	R.T	0.9865	0.405	-9.3294	0.9245	0.012	6.579113	1.8839
	40	0.9952	0.2749	-3.66	0.9443	0.0102	6.732187	1.9069
	50	0.9795	0.382	-6.902	0.9486	0.0108	7.96375	2.0749

3	R.T	0.9846	0.3496	-9.4822	0.9292	0.0101	6.456582	1.8651
	40	0.9888	0.3168	-4.8514	0.9247	0.0089	8.19808	2.1039
	50	0.9837	0.339	-7.0188	0.9287	0.0094	7.597354	2.0278

Dic	dry	3	0		0.9977	0.3072	-0.7767	0.9391	0.0095	8.369549	2.1246
1	R.T	0.9748	0.2916	9.2784	0.8491	0.0075	15.65828	2.751			
	40	0.9956	0.2194	4.6484	0.9182	0.0076	10.73919	2.3739			
	50	0.9914	0.332	8.0902	0.978	0.0069	18.45989	2.9156			

2	R.T	0.9976	0.3101	-0.149	0.9382	0.009	10.33463	2.3355
	40	0.9992	0.3081	4.8497	0.9482	0.0077	14.26773	2.658
	50	0.9951	0.3405	11.259	0.9368	0.0068	20.35649	3.0134

3	R.T	0.9993	0.2896	3.6549	0.9246	0.0069	13.7646	2.6221
	40	0.9627	0.2872	13.013	0.8924	0.0057	20.64762	3.0276
	50	0.9919	0.2033	1.9912	0.8866	0.0074	8.641706	2.1566

Dic	aqueous	2.7	0		0.9859	0.0243	-0.301	0.959	0.0098	0.630274	-0.4616
1	R.T	0.9865	0.0571	-1.363	0.9484	0.0093	1.291753	0.256			
	40	0.995	0.0461	0.1604	0.9554	0.0072	1.960697	0.6733			
	50	0.9167	0.0539	-2.0673	0.9817	0.0099	0.924964	-0.078			

2	R.T	0.9822	0.0506	-1.0695	0.919	0.0091	1.209371	0.1901
	40	0.9697	0.0415	-1.8966	0.787	0.0157	0.186766	-1.6779
	50	0.9787	0.0655	0.0655	0.9348	0.0071	1.637548	0.4932

3	R.T	0.9798	0.0374	0.2378	0.9851	0.0065	1.851692	0.6161
	40	0.9681	0.035	-1.6313	0.9462	0.012	0.271702	-1.30305
	50	0.9391	0.0294	0.6438	0.9911	0.0077	0.935195	-0.067

Dic	aqueous	4.00	0		0.9994	0.0245	-0.6078	0.829	0.0139	0.285932	-1.252
1	R.T	0.9012	0.0299	0.1988	0.912	0.0075	1.097133	0.0927			
	40	0.994	0.0484	0.4963	0.9171	0.0071	2.169724	0.7746			
	50	0.9439	0.0134	0.0881	0.961	0.0063	0.6827	-0.3817			

2	R.T	0.9818	0.0336	-0.5651	0.9657	0.0082	1.014504	0.0144
	40	0.9474	0.0373	-0.643	0.9951	0.0076	1.266428	0.2362
	50	0.9276	0.007	0.6418	0.982	0.0038	0.891544	-0.1148

3	R.T	0.965	0.0331	-0.4349	0.8834	0.0087	0.902578	-0.1025
	40	0.9584	0.0203	-0.8317	0.8985	0.0109	0.267536	-1.3185
	50	0.8857	0.0189	-0.7867	0.9968	0.0091	0.370834	-0.992

Enterovirus Inhibiting Activities of Two Lupane Triterpenoids and Anthraquinones from *Senna Siamea* Stem Bark Against Three Serotypes of Echovirus

Omonike O. Ogbole^{1*}, Toluwanimi E. Akinleye¹, Temitope O. C. Faleye^{2,3},
Adekunle J. Adeniji³

1 University of Ibadan, Department of Pharmacognosy, Ibadan, Nigeria

2 University of Ibadan, Department of Virology, College of Medicine, Ibadan, Nigeria

3 Ekiti State University, Department of Microbiology, Ado Ekiti, Nigeria

ABSTRACT

Echovirus 7, 13 and 19 are part of the diseases-causing enteroviruses identified in Nigeria. Presently, no treatment modality is clinically available against these enteric viruses. Herein, we investigated the ability of two anthraquinones (physcion and chrysophanol) and two lupane triterpenoids (betulinic acid and lupeol), isolated from the stem bark of *Senna siamea*, to reduce the viral-induced cytopathic effect on rhabdomyosarcoma cells using MTT (3-[4,5-dimethylthiazol-2-yl]-2,5-diphenyltetrazolium bromide) colorimetric method. Viral-induced CPE by E7 and E19 was inhibited in the presence of all tested compounds, E13 was resistant to all the compounds except betulinic acid. Physcion was the most active with IC₅₀ of 0.42 and 0.33 µg/mL on E7 and E19, respectively. We concluded that these compounds from *Senna siamea* possess anti-enteroviral activities and betulinic acid may represent a potential therapeutic agent to control E7, E13, and E19 infections, especially due its ability to inhibit CPE caused by the impervious E13.

Keywords: Enteroviruses, cytopathic effect, *Cassia siamea*, anthraquinones, triterpenoids.

*Corresponding Author: Omonike Ogbole, e-mail: nikeoa@yahoo.com

Omonike O. Ogbole ORCID Number: 0000-0002-6487-9494

Toluwanimi E. Akinleye ORCID Number: 0000-0002-7202-8112

Temitope O. C. Faleye ORCID Number: 0000-0001-7706-9493

Adekunle J. Adeniji ORCID Number: 0000-0002-0406-6707

(Received 18 April 2019, accepted 20 May 2019)

INTRODUCTION

Echoviruses are members of Species B within the genus Enterovirus, family Picornaviridae, order Picornavirales. Within the genus are 15 Species (Enterovirus [EV] A - L and Rhinovirus A - C). The Polioviruses (PVs) are the best studied members of the genus and belong to EV-C. Enteroviruses are naked viruses with icosahedral symmetry and a diameter of 28-30nm. Within the virion is an approximately 7.5kb, positive-sense, single-stranded RNA genome. The genome encodes one large (>2,000 amino acid [Aa]) open reading frame (ORF) and sometimes, a recently described¹ small ORF (67Aa) that overlaps the large ORF and is involved in facilitating gut infection. The large ORF is translated into a polyprotein that is auto-catalytically cleaved into 11 proteins (four structural and seven non-structural proteins). The structural and non-structural proteins are encoded in the 5' and 3'-ends of the ORF (and consequently, the genome), respectively.

Enteroviruses are associated with over a dozen clinical manifestations², one of which is Acute flaccid Paralysis (AFP), the clinical presentation of poliomyelitis³. In Nigeria alone, over 10,000 suspected AFP cases are recorded annually⁴. This gives a sense of the clinical significance of EV infections globally. Many members of the genus have more than one clinical presentation². Though vaccines exist for the PVs and EV-A71, neither vaccines nor chemotherapeutic agents exist for the control of other non-polio enteroviruses (NPEV) despite their association with different clinical presentations⁵⁻⁸. This therefore highlights the significance of antiviral drug development for EVs⁹.

Natural products, either in form of pure compounds or standardized plant extracts, continue to provide rich and boundless source for the discovery and development of novel drug leads. The protective role of plant derived natural compounds against viral infection has been suggested by several studies¹⁰⁻¹³. Anthraquinones which are a class of naturally occurring and functionally diverse aromatic organic compounds, and are structurally related to or derived from anthracene have displayed well-known biological effects¹⁴. The antiviral activities of some anthraquinones such as physcion **(a)**, chrysophanol **(b)** (**figure 1**), emodin, rhein, aloe-emodin, and chrysophanic acid against a range of viruses are well documented¹⁵⁻¹⁸. They inactivated enveloped virus or inhibit replication of un-enveloped virus such as EV-A71 *in vitro*^{14, 19}.

Lupane triterpenoids such as Betulinic acid **(c)** and Lupeol **(d)** (**figure 1**) have in the last two decades become of pharmacological interest when the anti-HIV and antineoplastic activities of betulinic acid was revealed²⁰. The ability of betulinic acid to inhibit the replication of HIV and herpes simplex virus 1 (HSV-1)

has been documented^{21, 22}. The anti-HIV protease activity and significant inhibition of HSV by lupeol has also been reported²³.

Our previous work²⁴ detailed the anti-poliovirus activities of two anthraquinones (physcion and chrysophanol) (IC_{50} values of 1.568 and 0.4571 $\mu\text{g}/\text{mL}$ respectively), and two triterpenoids (lupeol and betulinic acid) ($IC_{50} = 0.14 \mu\text{g}/\text{mL}$). In continual pursuit of lead compounds that possess significant antiviral activity against EVs, this work therefore attempts to explore the anti-EV activities of two anthraquinones (physcion and chrysophanol) and two triterpenoids (lupeol and betulinic acid) isolated from *Senna siamea* against three (E7, E13, and E19) Echovirus types using cell-based antiviral assay.

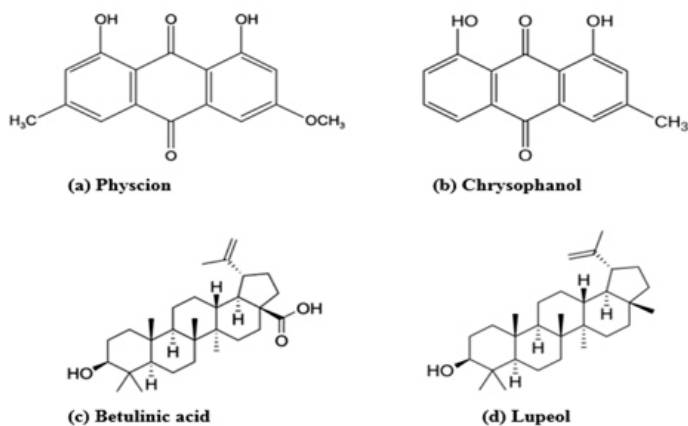


Figure 1. Structure of selected anthraquinones (a and b) and Lupane triterpenoids (c and d).

METHODOLOGY

Compounds isolation

The details of isolation of the anthraquinones (physcion and chrysophanol) and the triterpenoids (lupeol and betulinic acid) from the stem bark of *Senna siamea*, and the spectroscopic methods employed for their structural elucidation have been previously described²⁴.

Viruses and Cells

The three serotypes of Echovirus (E7, E13, and E19) used in this study were obtained from faeces of children with acute flaccid paralysis (AFP) in Nigeria⁴. The isolates were provided by the Enterovirus Study Group (ESG), Department of Virology, University of Ibadan, Nigeria. Until use, all viruses were stored at -80°C .

The antiviral and cytotoxic properties were measured in human rhabdomyosarcoma (RD) cells. The cell line was provided by the WHO National Polio Laboratory, University of Ibadan, Nigeria. The cells were grown in Eagle's minimum essential medium (MEM; Sigma-Aldrich) supplemented with 10% fetal bovine serum (FBS), 100 units/mL of penicillin, 100 µg/mL of streptomycin, 2 mM L-glutamine, 0.07% NaHCO₃, 1% non-essential amino acids and vitamin solution. The cells were incubated at 37 °C throughout the study period. The test medium used for cytotoxic assays and antiviral assays contained only 2% of fetal bovine serum (maintenance medium).

Tissue culture infective dose (TCID)

Virus-induced cytopathic effect (CPE) in RD cell culture was used in determining virus titres, which were expressed as 50% tissue culture infective dose (TCID₅₀) per mL using Spearman-Kärber's method. Microtitre plates were used for this assay and the assay was done in Triplicates. Precisely, 100 µL RD cell suspension (1×10^6 cells/mL) was seeded into 96-well microtitre plates and incubated for 24 h to form monolayer. Ten-fold serial dilutions of the virus stock was made and 100 µL of each dilution was inoculated into the wells. The cell control wells contained 100 µL RD cell suspension alongside 100 µL of medium without any virus. The microtitre plate was sealed and incubated at 37 °C. Daily CPE scoring was done till the cells in the control wells started dying. The TCID₅₀ values was determined using Spearman-Kärber's method.

Cytotoxicity assay

The maximum non-toxic concentration (MNTC) and the 50% cytotoxic concentration (CC₅₀) for each compound was obtained using MTT cytotoxicity assay. Each compound was pre-solubilized in DMSO to give 1 mg/mL stock solution. Ten-fold serial dilutions (1000 to 0.01 µg/mL) of the compounds were made using the maintenance medium. Confluent monolayers of RD cells in each well of a 96-well microplate was treated with the different concentrations of each compound. Plates were incubated at 37 °C for 72 h. Subsequently, plates were observed under the inverted microscope for cytopathic effect (CPE). The old medium was then removed and 25 µL of MTT solution (2 mg/mL) was added to each well and incubated for 2 h at 37 °C. Thereafter, the MTT solution was removed from the wells and DMSO (75 µL) was added. Spectrophotometric (Multiscan 347, MTX lab) measurement of the plates was made at 490 nm to obtain optical density values, and the 50% cytotoxic concentration (CC₅₀) was calculated. The experiment was conducted in triplicate.

Antiviral activity assay

The antiviral effect of the compounds against E7, E13, and E19 was determined pre-infection (prophylactic) using a cell culture-based assay that measures viral cytopathic effect inhibition. The method as previously described²⁵ was modified and used in this assay. Briefly, RD cells were seeded in a 96-well microplate and incubated for 24 h to grow to confluence. After the incubation period, two-fold serial dilutions, obtained from the MNTC of each compound were added in triplicate into all the wells with the exception of the negative control wells that contained only RD cells and the virus control that contained virus without any compound. After about an hour, 50 μL of 100 TCID₅₀ virus suspension were added to all the wells except the negative control wells. The plates were incubated at 37 °C in the incubator for 72 h after which the cell viability was measured using the MTT assay as earlier described. The 50% inhibitory concentration (IC₅₀) was estimated from the obtained optical density. No drug control was used in this study, since there are no antiviral drugs approved for the treatment of EV infections.

Data analysis

The CC₅₀ (50% cytotoxic concentration) and the IC₅₀ (50% inhibitory concentration) for the compounds were calculated from concentration-effect-curves after linear regression analysis using GraphPad Prism5 and Microsoft Excel. The selectivity index (SI), defined as CC₅₀ over IC₅₀, for each active compound were also determined.

RESULTS AND DISCUSSION

MNTC and CC₅₀ of compounds

Lupeol exacted the most cytotoxic effect on the RD cells in culture by having the lowest maximum non-toxic concentration (MNTC) of 0.1 $\mu\text{g}/\text{mL}$ and CC₅₀ value of 0.51 $\mu\text{g}/\text{mL}$. Other lupane triterpenoid (Betulinic acid) and anthraquinones (Physcion and Chrysophanol) all had moderate cytotoxic effect on the RD cells with equal MNTC of 10 $\mu\text{g}/\text{mL}$ and CC₅₀ values of 49.50, 39.12, and 14.91 $\mu\text{g}/\text{mL}$, respectively. Results are presented in Table 1.

Antiviral activities of compounds

E13 was resistant to the CPE inhibitory effect of all the compounds tested except Betulinic acid. Physcion had the highest antiviral activity on the E7 and E19 serotypes with IC₅₀ values of 0.42 and 0.33 $\mu\text{g}/\text{mL}$, respectively. Physcion also displayed good selectivity, with sufficiently high selective indices of 93.14 and 118.55, respectively on E7 and E19. Triterpenoid, Lupeol displayed low an-

tiviral activity against the three serotypes, and particularly no selectivity with SI values less than 1 for the three serotypes. However, Betulinic acid which is also a triterpenoid had the highest antiviral activity on E19 ($IC_{50} = 0.31 \mu\text{g/mL}$) and moderate antiviral activity on E7 and E13 ($IC_{50} = 4.46$ and $4.43 \mu\text{g/mL}$, respectively). It also displayed good selectivity (>10) for the three serotypes. The results are presented in Table 1.

Nigerian ethnobotany has reported *Senna siamea* Lam (Fabaceae) as a component of remedies used against viral infections in the country²⁶. Furthermore, the antiviral activities of various compounds (such as chromones, triterpenoids, and anthraquinones) isolated from the stem of this plant against HIV-1, poliovirus-1 (PV-1) and tobacco mosaic virus (TMV) has been reported^{24, 27}. In this study, we confirm these findings and further expand the breadth of EV types against which these compounds have documented antiviral activity.

Physcion which was isolated as yellow crystals from the hexane soluble fraction of *Senna siamea* stem bark displayed the highest inhibition and good selective indices against E7 and E19 (Table 1). However, a similar anthraquinone (chrysophanol, Figure 1), which had been previously documented^{24, 28} to have anti-poliovirus activity, only had moderate inhibitory effect with low selective index on these Echovirus types.

Betulinic acid was the next in the antiviral activity against the three Echovirus types investigated in this study (Table 1). It is important to note that E19 was significantly more inhibited by betulinic acid in tissue culture than E7 and 13. The pronounced inhibitory effect of betulinic acid on another serotype of echovirus (E6) has been reported²⁰. Therefore, the findings of this study appear to support that of Tolstikova and others (2006).

While betulinic acid showed significant anti-Echovirus activity in this study, it showed weak anti-poliovirus activity in our previous study²⁴. As with the anthraquinones, a similar triterpenoid (Lupeol, Figure 1), which had been previously documented^{24, 28} to strongly inhibit poliovirus-induced CPE, herein exhibited the least antiviral activity with poor selectivity ($SI = <1$) against E7 and E19 and none against E13 (Table 1).

Considering, the Echoviruses investigated in this study (Table 1) and the PVs investigated in our previous study^{24, 28} belong to Species EV-B and EV-C, respectively, the contrasting antiviral activity of the two anthraquinones and triterpenoids appear to be in consonance with the different EV species. This suggests that peculiar biological properties of EVs that follow species demarcations might be responsible for their sensitivity to selected anthraquinones and triterpenoids.

It did not escape our notice that within the Echoviruses (which are all EV-B members) described in this study, differences also exist in their sensitivity to the anthraquinones and triterpenoids. It should be noted that only two of the Echoviruses analysed in this study were sensitive to the anti-Echovirus activity of the anthraquinone Physcion. On the other hand, all three viruses were sensitive to the anti-Echovirus activity of the triterpenoid, Betulinic acid. Furthermore, though the actual values as measured in the assays differ (Table 1), the degree of anti-Echovirus activity of Physcion seems to be similar for E7 and E19 while that for Betulinic acid seems similar for E7 and E13. Put together, these patterns suggest that the mechanism of action of anti-Echovirus activity of Physcion and Betulinic acid might differ.

Table 1. Anti-Echovirus activity of compounds

Compound	MNTC (µg/mL)	CC ₅₀ (µg/mL)	IC ₅₀ (µg/mL)			SI		
			E7	E13	E19	E7	E13	E19
Physcion	10	39.12	0.42	NA	0.33	93.14	NA	118.55
Chrysophanol	10	14.91	5.42	NA	5.75	2.75	NA	2.59
Betulinic Acid	10	49.50	4.46	4.43	0.31	11.10	11.17	159.68
Lupeol	0.1	0.51	7.10	NA	6.43	<1	NA	<1

NA- Not active; SI- selective index; IC₅₀ - 50% inhibitory concentration; CC₅₀ - 50% cytotoxic concentration

Considering the design of the assay for antiviral activity, only prophylactic and not therapeutic activity was assayed. Hence, it is either the compounds prevented attachment or entry of the virus into the permissive and susceptible cell line used for this assay, or they induced an antiviral state by targeting a replication stage that is downstream of entry. The fact that E7, E13 and E19 have been documented to all use the same cell surface receptor (Decay-Accelerating Factor [DAF]) for entry into susceptible cells^{2, 29, 30}, the differing assay results for the three EVs suggest inhibition might not have occurred at entry. However, if their footprints³¹ on the receptor differ or if alternate cell surface receptors^{32, 33} exist for one or more of the Echoviruses analysed in this study, then it is possible that the observed phenotype might be due to attachment or entry inhibition.

Physcion has been documented to interact with pathways involved in post -attachment or -entry stages of EV replication like the autophagy pathway^{34, 35}. Therefore, considering the reasons mentioned above we are of the opinion that the inhibition of Echovirus (7, 13 and 19) replication observed in this study occurred at a post -attachment or -entry stage. Hence, effort is ongoing to further dissect the molecular basis of these activities in an effort to understand the biological basis of observed variations both within and among EV Species.

In summary, we have reported the antiviral activity of two anthraquinones (physcion and chrysophanol) and two triterpenoids (betulinic acid and lupeol) isolated from the stem bark of *Senna siamea* against three serotypes of Echovirus (E7, E13, and E19), with physcion exhibiting the most potent antiviral activity.

National Research Council recommended that an ideal poliovirus drug must be one that is also active on other enteroviruses³⁶. Therefore, the anthraquinones (physcion and chrysophanol) which were previously reported active on poliovirus could be considered for development into poliovirus therapeutic agents. However, particularly fascinating is the fact that we have found it difficult to find compounds that inhibit E13 replication³⁷, Hence the observation that E13 is susceptible to inhibition by Betulinic acid is remarkable and therefore also deserves further investigation.

REFERENCES

1. Lulla, V.; Dinan, A. M.; Hosmillo, M.; Chaudhry, Y.; Sherry, L.; Irigoyen, N.; Nayak, K. M.; Stonehouse, N. J.; Zilbauer, M.; Goodfellow, I. An Upstream Protein-Coding Region in Enteroviruses Modulates Virus Infection in Gut Epithelial Cells. *Nature microbiology* **2019**, *4*, 280.
2. Royston, L.; Tapparel, C. Rhinoviruses and Respiratory Enteroviruses: Not as Simple as Abc. *Viruses* **2016**, *8*, 16.
3. WHO, *Polio Laboratory Manual*. 4th Edition ed. 2004, Geneva, Switzerland: World Health Organisation.
4. Faleye, T.; Adewumi, M.; Japhet, M.; David, O.; Oluyeye, A.; Adeniji, J.; Famurewa, O. Non-Polio Enteroviruses in Faeces of Children Diagnosed with Acute Flaccid Paralysis in Nigeria. *Virol. J.* **2017**, *14*, 175.
5. Park, K. S.; Choi, Y. J.; Park, J. S. Enterovirus Infection in Korean Children and Anti-Enteroviral Potential Candidate Agents. *Korean J. Pediatr.* **2012**, *55*, 359-366.
6. Kang, H.; Kim, C.; Kim, D. E.; Song, J. H.; Choi, M.; Choi, K.; Kang, M.; Lee, K.; Kim, H. S.; Shin, J. S.; Kim, J.; Han, S. B.; Lee, M. Y.; Lee, S. U.; Lee, C. K.; Kim, M.; Ko, H. J.; van Kuppeveld, F. J.; Cho, S. Synergistic Antiviral Activity of Gemcitabine and Ribavirin against Enteroviruses. *Antiviral. Res.* **2015**, *124*, 1-10.
7. Zuo, J.; Kye, S.; Quinn, K. K.; Cooper, P.; Damoiseaux, R.; Krogstad, P. Discovery of Structurally Diverse Small-Molecule Compounds with Broad Antiviral Activity against Enteroviruses. *Antimicrob. Agents Chemother.* **2015**, *60*, 1615-26.
8. Nikonov, O. S.; Chernykh, E. S.; Garber, M. B.; Nikonova, E. Y. Enteroviruses: Classification, Diseases They Cause, and Approaches to Development of Antiviral Drugs. *Biochem. (Mosc)* **2017**, *82*, 1615-1631.
9. Abzug, M. J. The Enteroviruses: Problems in Need of Treatments. *J. Infect.* **2014**, *68*, S108-S114.
10. Zarubaev, V. V.; Anfimov, P. M.; Shtro, A. A.; Garshinina, A. V.; Meleshkina, I. A.; Karpinskaya, L. A.; Kozeletskaya, K. N. Kiselev, O. I. [Development of Novel Drugs against Influenza Virus Based on Synthetic and Natural Compounds]. *Vopr. Virusol.* **2012**, *57*, 30-6.
11. Numakawa, T. Possible Protective Action of Neurotrophic Factors and Natural Compounds against Common Neurodegenerative Diseases. *Neural. Regen. Res.* **2014**, *9*, 1506-8.
12. Mohd Sairazi, N. S.; Sirajudeen, K. N.; Asari, M. A.; Muzaimi, M.; Mummedy, S. Sulaiman, S. A. Kainic Acid-Induced Excitotoxicity Experimental Model: Protective Merits of Natural Products and Plant Extracts. *Evid. Based Complement. Alternat. Med.* **2015**, *2015*, 1-15.
13. Jardim, A. C. G.; Shimizu, J. F.; Rahal, P.; Harris, M. Plant-Derived Antivirals against Hepatitis C Virus Infection. *Virol. J.* **2018**, *15*, 34.
14. Dave, H.; Ledwani, L. A Review on Anthraquinones Isolated from Cassia Species and Their Applications. *Indian J. Nat. Prod. Resour.* **2012**, *3*, 291-319.
15. Abd-Alla, H. I.; Abu-Gabal, N. S.; Hassan, A. Z.; El-Safty, M. M.; Shalaby, N. M. Antiviral Activity of Aloe Hijazensis against Some Haemagglutinating Viruses Infection and Its Phytoconstituents. *Arch. Pharm. Res.* **2012**, *35*, 1347-1354.
16. Al-Mohizea, A. M.; Al-Omar, M. A.; Abdalla, M. M.; Amr, A. G. 5 α -Reductase Inhibitors, Antiviral and Anti-Tumor Activities of Some Steroidal Cyanopyridinone Derivatives. *Int. J. Biol. Macromol.* **2012**, *50*, 171-9.

17. Alam, Z.; Al-Mahdi, Z.; Zhu, Y.; McKee, Z.; Parris, D. S.; Parikh, H. I.; Kellogg, G. E.; Kuchta, A.; McVoy, M. A. Anti-Cytomegalovirus Activity of the Anthraquinone Atanyl Blue Prl. *Antiviral Res.* **2015**, *114*, 86-95.
18. Fouillaud, M.; Venkatachalam, M.; Girard-Valenciennes, E.; Caro, Y.; Dufosse, L. Anthraquinones and Derivatives from Marine-Derived Fungi: Structural Diversity and Selected Biological Activities. *Mar. Drugs*, **2016**, *14*, 64.
19. Li, S. W.; Yang, T. C.; Lai, C. C.; Huang, S. H.; Liao, J. M.; Wan, L.; Lin, Y. J.; Lin, C. W. Antiviral Activity of Aloe-Emodin against Influenza A Virus Via Galectin-3 up-Regulation. *Eur. J. Pharm.* **2014**, *738*, 125-132.
20. Tolstikova, T.; Sorokina, I.; Tolstikov, G.; Tolstikov, A.; Flekhter, O. Biological Activity and Pharmacological Prospects of Lupane Terpenoids: I. Natural Lupane Derivatives. *Russ. J. Bioorgan. Chem.* **2006**, *32*, 37-49.
21. Ryu, S. Y.; Lee, C. K.; Lee, C. O.; Kim, H. S.; Zee, O. P. Antiviral Triterpenes From *Prunella Vulgaris*. *Arch. Pharmacol Res.* **1992**, *15*, 242-245.
22. Moghaddam, M. G.; Ahmad, F. B. H. and Samzadeh-Kermani, A. Biological Activity of Betulinic Acid: A Review. *Pharmacol. Pharm.* **2012**, *3*, 119.
23. Wei, Y.; Ma, C. M.; Chen, D. Y.; Hattori, M. Anti-Hiv-1 Protease Triterpenoids from *Stauntonia Obovatifoliola* Hayata Subsp. *Intermedia. Phytochem.* **2008**, *69*, 1875-1879.
24. Ogbole, O.; Adeniji, J.; Ajaiyeoba, E.; Kamdem, R.; Choudhary, M. Anthraquinones and Triterpenoids from *Senna Siamea* (Fabaceae) Lam Inhibit Poliovirus Activity. *Afr. J. Microbiol. Res.* **2014**, *8*, 2955-2963.
25. Lin, Y. J.; Chang, Y. C.; Hsiao, N. W.; Hsieh, J. L.; Wang, C. Y.; Kung, S. H.; Tsai, F. J.; Lan, Y. C.; Lin, C. W. Fisetin and Rutin as 3c Protease Inhibitors of Enterovirus A71. *J. Virol. Methods* **2012**, *182*, 93-98.
26. Ajaiyeoba, E.; Ogbole, O.; Ogundipe, O. Ethnobotanical Survey of Plants Used in the Traditional Management of Viral Infections in Ogun State of Nigeria. *Eur. J. Sci. Res.* **2006**, *13*, 64-73.
27. Hu, Q. F.; Zhou, B.; Gao, X. M.; Yang, L. Y.; Shu, L. D.; Shen, Y.; Li, G. P.; Che, C. T.; Yang, G. Y. Antiviral Chromones from the Stem of *Cassia Siamea*. *J. Nat. Prod.* **2012**, *75*, 1909-1914.
28. Semple, S. J.; Pyke, S. M.; Reynolds, G. D.; Flower, R. L. In Vitro Antiviral Activity of the Anthraquinone Chrysophanic Acid against Poliovirus. *Antiviral Res.* **2001**, *49*, 169-178.
29. Powell, R. M.; Ward, T.; Goodfellow, I.; Almond, J. W.; Evans, D. J. Mapping the Binding Domains on Decay Accelerating Factor (Daf) for Haemagglutinating Enteroviruses: Implications for the Evolution of a Daf-Binding Phenotype. *J. Gen. Virol.* **1999**, *80*, 3145-3152.
30. Baggen, J.; Thibaut, H.; Strating, J. R.; van Kuppeveld, F. J. The Life Cycle of Non-Polio Enteroviruses and How to Target It. *Nat. Rev. Microbiol.* **2018**, *16*, 368-381.
31. Yoder, J. D.; Cifuentes, J. O.; Pan, J.; Bergelson, J. M.; Hafenstein, S. The Crystal Structure of a Cocksackievirus B3-Rd Variant and a Refined 9-Angstrom Cryo-Electron Microscopy Reconstruction of the Virus Complexed with Decay-Accelerating Factor (Daf) Provide a New Footprint of Daf on the Virus Surface. *J. Virol.* **2012**, *86*, 12571-12581.
32. Pinkert, S.; Röger, C.; Kurreck, J.; Bergelson, J. M.; Fechner, H. The Cocksackievirus and Adenovirus Receptor: Glycosylation and the Extracellular D2 Domain Are Not Required for Cocksackievirus B3 Infection. *J. Virol.* **2016**, *90*, 5601-5610.
33. Novoselov, A. V.; Rezaikin, A. V.; Sergeev, A. G.; Fadeyev, F. A.; Grigoryeva, J. V.; Sokolo-

- va, Z. I. A Single Amino Acid Substitution Controls Daf-Dependent Phenotype of Echovirus 11 in Rhabdomyosarcoma Cells. *Vir. Res.* **2012**, *166*, 87-96.
34. Pang, M. J.; Yang, Z.; Zhang, X. L.; Liu, Z. F.; Fan, J.; Zhang, H. Y. Phycion, a Naturally Occurring Anthraquinone Derivative, Induces Apoptosis and Autophagy in Human Nasopharyngeal Carcinoma. *Acta Pharm. Sin.* **2016**, *37*, 1623.
35. Mohamud, Y.; Luo, H. The Intertwined Life Cycles of Enterovirus and Autophagy. *Virul.* **2018**, [Epub ahead of print], 1-11.
36. National Research Council. 2006. *Exploring the Role of Antiviral Drugs in the Eradication of Polio: Workshop Report*. Washington, DC: The National Academies Press.
37. Ogbole, O. O.; Akinleye, T. E.; Segun, P. A.; Faleye, T. C.; Adeniji, A. J. In Vitro Antiviral Activity of Twenty-Seven Medicinal Plant Extracts from Southwest Nigeria against Three Serotypes of Echoviruses. *Virol. J.* **2018**, *15*, 110.

Two New Spectrophotometric Methods for the Determination of Isoniazid in Bulk form and Tablet Dosage Form

Olajire Adegoke^{1*}, Olusegun Thomas¹, Deborah Babatunde¹, Oyindamola Oyelami¹, Adeyinka Adediran¹, Abayomi Omotosho²

¹ University of Ibadan, Pharmaceutical Chemistry, Ibadan, Nigeria

² University of Port Harcourt, Pharmaceutical and Medicinal Chemistry, Port Harcourt, Nigeria

ABSTRACT

To develop two new spectrophotometric methods for the analysis of isoniazid in bulk form and tablets. The methods involved condensation of isoniazid with salicylaldehyde and diazo coupling with diazotized *p*-nitroaniline. Critical factors were optimised; evidence for new product formation, selection of analytical wavelengths, temperature and time and solvent for dilution. Validation was carried out according to ICH guidelines. The new methods were used for isoniazid tablets. Isoniazid formed an imine and azo adduct readily with the two reagents at 30 °C after 5 and 20 mins, and determined at 405 and 420 nm, respectively. Low LODs were obtained for the two methods and recoveries were generally above 98%. The methods were successfully adopted for the assay of isoniazid in tablets and there were no significant differences in the contents when compared with the official titrimetric method of analysis. The methods could find application as in-process method in pharmaceutical industries.

Keywords: Isoniazid, spectrophotometric, hydrazone, *para*-nitroaniline, salicylaldehyde.

INTRODUCTION

Tuberculosis is a communicable infectious disease characterised by weight loss, fatigue, productive cough and night sweats following alveolar implantation of

*Corresponding author: Olajire Adegoke, e-mail: ao.adegoke@mail.ui.edu.ng

Olajire Adegoke ORCID Number: 0000-0002-8623-3635

Olusegun Thomas ORCID Number: 0000-0001-8519-2125

Deborah Babatunde ORCID Number: 0000-0002-0911-4851

Oyindamola Oyelami ORCID Number: 0000-0002-6891-4277

Adeyinka Adediran ORCID Number: 0000-0003-1136-7089

Abayomi Omotosho ORCID Number: 0000-0002-4633-5338

(Received 11 May 2019, accepted 7 June 2019)

the causative organism, *Mycobacterium tuberculosis*^{1,2}. With 1.6 million deaths in 2017 alone, tuberculosis (TB) is not only one of the top causes of death worldwide but the emergence of over half a million new cases of multidrug-resistant TB in the same year makes it a health-security threat¹. Although there is only a 5-15% lifetime risk of developing the disease following infection, compromised immunity such as in people living with HIV increases the risk and fatality of TB. Nearly half of all HIV-negative and all of HIV-positive individuals with active TB will die without proper drug treatment which often consists of a combination of first line drugs including isoniazid². Isoniazid, chemically pyridine-4-carbohydrazide, is converted to the active form which is bacteriostatic for latent bacteria and bactericidal for actively dividing microbes^{3,4}.

Several methods have been reported for the quantitative estimation of isoniazid in bulk form, single- and multi-component dosage forms. These methods include HPLC analysis for both dosage and biological sample matrices using UV detection^{5,6} or less frequently mass spectrometry^{7,8}, flow-injection chemiluminescence⁹⁻¹¹, fluorimetry¹², electrochemical methods¹³ and titrimetry^{14,15}. Apart from the use of derivative spectroscopy and partial least squares^{16,17}, the majority of spectrophotometric methods for the quantification of isoniazid takes advantage of the varied functionality and moderate reactivity of the drug which also serve to improve sensitivity and selectivity of the resulting methods. Thus, isoniazid because of its activated amino pyridine skeleton, has been used as coupling agents with diazotized reagents such as dapsone and 1-amino anthraquinone zinc chloride^{18,19}; in Schiff base formation with *cis*-cinnamaldehyde²⁰, 4-dimethylaminocinnamaldehyde²¹ and as substrate for nucleophilic substitution reactions with epichlorohydrine and 4-hydroxyphenylchloride²². The donor capability of the drug has also been employed in charge-transfer complexation with various acceptors including chloranil, bromanil²³ etc. and condensation reactions with 6,7-dichloroquinoline-5,8-dione, sodium 1,2-naphthoquinone-4-sulphonate^{24,25} etc. Colorimetric methods for the quantitative estimation of the analyte have also been reported based on the photodecomposition of Cu (II)-neocuproine complex and chlorpromazine free radical solutions following their reduction by isoniazid^{14,26}.

These methods have their merits but suffer one or two drawbacks which include the use of expensive instrumentation and/or reagents that are not readily available in resource-limited countries, drastic reaction conditions such as elevated reaction times, long reaction times and strict control of pH.

The objective of this study was therefore to develop two simple, accurate and reliable colorimetric assay procedures for isoniazid following azo coupling with diazotized *p*-nitroaniline and Schiff base formation with salicylaldehyde.

METHODOLOGY

Chemicals and Reagents

Salicylaldehyde, Isoniazid tablets, 1 M H₂SO₄, 96% ethanol, methanol, *n*-hexane, ethyl acetate, propan-1-ol, propan-2-ol, 1 M HCl, *para*-nitroaniline, sodium nitrite, potassium bromate powder, methyl red powder, potassium bromide powder, concentrated HCl (all analytical reagent grade from BDH, Poole, UK), isoniazid reference standard.

Equipment

Analytical balance (Mettler H80), magnetic stirrer, pre-coated aluminium TLC plate, ultraviolet lamp 254/364 mm (PW Allen and Co., London), thermostated water bath, thermometer and Lambda 25 UV/VIS spectrophotometer (Perkin Elmer, UK).

Methods

Preparation of isoniazid stock solution

For the first method involving condensation with salicylaldehyde, a 0.0245 M solution of isoniazid (INH) was made by dissolving 0.0336 g of INH in sufficient quantity of ethanol and made up to 10 mL with ethanol. For method B involving diazo coupling reaction with *p*-nitroaniline, a 4.53×10^{-2} M solution was prepared by weighing 0.0621 g quantity of INH and adding sufficient quantity of ethanol to make up to the 10 mL mark.

Preparation of reagents

Preparation of sulphuric acid

Sulphuric acid (1 M) was prepared by diluting 13.5 mL of concentrated sulphuric acid with sufficient distilled water and making up to volume in a 250 mL volumetric flask.

Preparation of 1 M HCl

About 100 mL of distilled water was measured into a 250 mL volumetric flask; 44 mL of concentrated hydrochloric acid was also measured in the fume cupboard and added to the distilled water present in the volumetric flask. Distilled water was then added to make up to the 250 mL volume and the solution was shaken properly at intervals.

Preparation of salicylaldehyde solution (Method A)

A 0.0245 M solution of salicylaldehyde in 1M sulphuric acid was prepared by

dissolving 0.13 mL of salicylaldehyde solution which is equivalent to 0.15 g of salicylaldehyde in 50 mL of sulphuric acid in a volumetric flask with vigorous shaking. The solution was then filtered to obtain a clear solution.

Preparation of diazotized para-nitroaniline (DPNA) - Method B

A 100 mg quantity of *para*-nitroaniline was weighed into a beaker and 15 mL 1 M HCl was added. This was placed on a hot water bath till it completely dissolved and then cooled to about 15 °C and a 10%w/v solution of NaNO₂ (prepared by weighing 1 g of NaNO₂ into a 10 mL volumetric flask, distilled water was added to 10 mL) was added and stirred until one drop of the mixture turned starch iodide paper blue-black.

Preparation of methyl red solution

Methyl red (25 mg) was dissolved in a mixture of 0.93 mL of 0.1 M NaOH and 25 mL of ethanol (96%) in a 50 mL volumetric flask, sufficient distilled water was added to make up to 50 mL.

Preparation of 0.0167 M Potassium bromate

Potassium bromate (0.696 g) was weighed and transferred into a 250 mL volumetric flask, 100 mL of distilled water was added to dissolve the powder and distilled water was added to make 250 mL.

Condensation of isoniazid with salicylaldehyde (Method A)

Evidence of condensation

Simple colour test (Spot test)

A 0.5 mL aliquot of the stock solution of isoniazid was reacted with 0.5 mL of the stock solution of salicylaldehyde in a test tube. The change that occurred was observed immediately as well as after 20 minutes. The reaction was then repeated in another test tube. The test tube was thereafter immersed in a water bath at 60 °C and the colour change was observed after 5 and 20 minutes.

Thin layer chromatography

Thin layer chromatographic analysis was carried out using pre-coated aluminium TLC plates. Samples of isoniazid, salicylaldehyde and adduct produced were spotted and the plates developed using three solvent systems; Ethyl acetate and Methanol (9:1); Ethyl acetate and Methanol (7:3) and Ethyl acetate and Hexane (5:5). The chromatographs were dried and visualized under visible light and UV lamp at wavelengths of 254 nm and 365 nm.

Optimization studies

Selection of analytical wavelength

An aliquot of isoniazid stock solution (0.5 mL) was reacted with 0.5 mL of the stock solution of salicylaldehyde. This was then made up to 5 mL with methanol in a sample bottle. 0.5 mL of the stock solution of isoniazid and 0.5 mL of the stock solution of salicylaldehyde were also made up to 5 mL with methanol in separate sample bottles. Using methanol as the blank for all three, the absorption spectra of isoniazid, salicylaldehyde and the reaction adduct were recorded using wavelength range of 190-800 nm. The spectra of the three solutions were then overlaid and the wavelength at which the reaction mixture showed absorbance without significant interference from the other two spectra was selected as the analytical wavelength.

Optimization of solvent

For this optimization step, the effect of completing the reaction with solvents such as methanol, ethanol, propan-1-ol and propan-2-ol was studied using reaction mixtures as previously described. The adduct in four separate test tubes were each made up to 5 mL with methanol, ethanol, propan-1-ol and propan-2-ol, respectively. Using each solvent as blank for the corresponding tubes, the absorbance of the condensation adduct in the different test tubes were determined at the selected analytical wavelength. The solvent which gave the highest absorbance reading was then selected as the best diluting solvent.

Optimization of temperature

A 0.1 mL quantity of the stock solution of INH was reacted with 0.1 mL of the stock solution of salicylaldehyde. The mixture was then incubated at 30 °C for 5 minutes and 20 minutes. This was repeated at 50 °C, 60 °C and 70 °C. In each case 4 mL of methanol was added to quench the reaction after cooling the tubes in an ice bath. This was done in duplicates. The absorbance of the sample mixture at each temperature was then measured to obtain optimal temperature.

Optimization of time

This reaction step was carried out by adding 0.1 mL of the drug solution to 0.1 mL of the salicylaldehyde solution in test tubes and incubated at the optimal temperature for 0, 2, 5, 10, 15, 20, 25 and 30 mins. The absorbance was measured at the selected analytical wavelength after terminating the reaction by cooling in an ice bath and thereafter adding 4 mL of methanol.

Optimization of acid concentration

Different stock solutions of salicylaldehyde were prepared using different concentrations of sulphuric acid; 0.03125 M, 0.0625 M, 0.125 M, 0.25 M, 0.5 M, 1 M and 2 M solutions. 0.1 mL of the drug solution was then added to 0.1 mL of the different salicylaldehyde solution. The reaction was incubated at 30 °C for 5 min and was terminated by cooling in ice-cold water and adding 4 mL of methanol. The absorbance of each mixture was then measured at 405 nm to determine the optimum acid concentration. This procedure was carried out twice.

Stoichiometric ratio determination

Equimolar (0.0245 M) solutions of INH and salicylaldehyde were prepared in their respective solvents. 0, 0.05, 0.066, 0.1, 0.134, 0.15, 0.2 mL of salicylaldehyde solution were measured into different test tubes and each was made up to 2 mL with the drug solution. The reaction mixtures were incubated at 30 °C for 5 min. The reaction was terminated by cooling the reaction tubes in ice-cold water and making up to 5 mL with methanol. This was carried out in duplicate. The absorbance of each mixture was then measured at the selected wavelength.

Calibration curve

Calibration curve was prepared for the new condensation product within the concentration range 13.436 - 53.744 µg/mL of isoniazid (the linear part of the curve obtained from the determination of linearity of response) from the drug stock solution. To different test tubes containing 0.1 mL of salicylaldehyde solution each of 20, 30, 40, 50, 60, 70 and 80 µL of drug solution was added. The reaction was allowed to proceed at 30 °C for 5 min. The reaction was quenched by cooling in ice-cold water and making the reaction mixture up to 5 mL with methanol. Triplicate preparations of each concentration were made and the absorbance determined at 405 nm against a reagent blank. The calibration curve was repeated on three consecutive days and the average values were used to generate a 3-day pooled calibration curve. The regression line equation and correlation coefficient were obtained from the calibration curve using linear regression analysis. The limits of detection and of quantification were obtained according to the ICH ²⁷ guidelines using equations (1) and (2).

$$\text{LOD} = \frac{3.3\sigma}{s} \quad \text{----- (1)}$$

$$\text{LOQ} = \frac{10\sigma}{s} \quad \text{----- (2)}$$

Where σ is the standard deviation of the blank signals and s is the slope of the calibration line.

Validation studies

Accuracy and Repeatability

The new condensation reaction method was validated according to the International Conference on Harmonization (ICH) guidelines for validation of analytical procedures (ICH, 2005²⁷). Accuracy was evaluated at three concentrations (20.154, 33.59, 47.026 $\mu\text{g}/\text{mL}$) levels of the drug solution. To three test tubes containing 0.1 mL of salicylaldehyde solution, each of 30, 50, 70 μL of drug solution was added. The reaction mixtures were incubated at 30 °C for 5 min and the reaction quenched by cooling in ice and making up to 5 mL with methanol. The absorbance of the reaction mixture was determined at 405 nm. The precision of the method was assessed with quadruple samples at each concentration and then estimated with percentage relative standard deviation (% coefficient of variation) while the accuracy was estimated with the recovery and percentage relative error.

Interference studies/ method selectivity

The effect of common tablet excipients on the absorbance of reaction mixture was evaluated by weighing 5 mg of each of starch, talc, lactose, gelatin, magnesium stearate and a mixture of all 5 excipients into different test tubes. To each of the test tubes, 0.1 mL of salicylaldehyde solution was added. 0.05 mL of the isoniazid solution was added to each of the test tubes, the reaction mixtures were incubated at 30 °C for 5 min and the reaction quenched by cooling in ice-cold water and making up to 5 mL with methanol. Quadruple sample preparations of each excipient mixture were made and the absorbance of each determined at 405 nm.

Analytical signal stability

Volumes of salicylaldehyde and isoniazid solution corresponding to the mid-range concentration of the calibration curve (33.59 $\mu\text{g}/\text{mL}$) were measured into a test tube and the reaction mixture was incubated at 30 °C for 5 min. The reaction was quenched by cooling the reaction mixture in ice cold water and making up to 5 mL with methanol. The absorbance of the reaction mixture was then determined at 0 min, 30 min, 1 hr, 1 hr 30 min, 2 hrs, 2 hrs 30 min, 3 hrs, 3hrs 30 min, 4 hrs and 24 hrs.

Dosage form analysis

Tablets of isoniazid were weighed and crushed and an amount of each brand equivalent to 0.03359 g of isoniazid was weighed and allowed to disperse in 10 mL of ethanol. The mixture was then filtered and 50 μ L (33.59 μ g/mL) of the solution was measured into a test tube containing 100 μ L of the salicylaldehyde stock solution. The reaction mixture was incubated at 30 °C for 5 min and the reaction was stopped by cooling in ice cold water and making up to 5 mL with methanol. The absorbance of the reaction solution was then determined at 405 nm. Five replicates were determined. This procedure was repeated for tablet brand B using an equivalent weight of 0.062 g.

Diazo coupling reaction of isoniazid with DPNA (Method B)

Evidence of coupling reaction

A 0.5 mL aliquot of diazotized *para*-nitroaniline (DPNA) was added to a test tube containing 0.5 mL of INH stock solution. The immediate colour change and the colour change after 20 minutes were observed. The colour formed was noted. The test tube was immersed in a water bath at 70 °C for 5 minutes and 20 minutes and the colour change observed was noted. With significant colour change observed, TLC was carried out. On the TLC plate, the isoniazid (INH) stock, *para*-nitroaniline (PNA), DPNA and the azo adduct were spotted. The TLC plate was developed in mobile phase combinations as utilized for Method A.

Selection of analytical wavelength

A 0.5 mL aliquot of DPNA was added to a test tube containing 0.5 mL of INH stock solution. The analytical wavelength was determined by recording the UV-VIS spectra from 190 to 800 nm using a scanning UV Spectrophotometer.

Optimization of coupling reaction temperature and time

This reaction for the optimization of temperature was carried out as previously described for Method A using 0.1 mL aliquot of DPNA and 0.1 mL of INH stock solution. The reaction was terminated by placing the test tubes in an ice-bath. 10 mL of ethyl acetate was added to each reaction mixture and extracted. The absorbance value of the extract at 420 nm (λ_{max}) was recorded. All determinations were done in duplicates. For the optimization of reaction time, the procedure was repeated at 30 °C for 0, 2, 5, 10, 15, 20, 25, 30, 35 and 40 minutes. The resulting reaction products were extracted into ethyl acetate and absorbance readings taken at 420 nm. All determinations were done in duplicates.

Stoichiometric ratio of reagent-drug adduct formation

Aliquots of INH stock solution: 0, 50, 66, 100, 134, 150 and 200 μL were transferred respectively into 7 test tubes. Into each test tube, 200, 150, 134, 100, 66, 50 and 0 μL of DPNA was added respectively. This was followed by incubation at 30 $^{\circ}\text{C}$ for 20 minutes and 10 mL of ethyl acetate was added to each reaction mixture. The absorbance was measured at 420 nm and all determinations were done in duplicates.

Validation Studies

Calibration line

Calibration lines using standard solutions of 6.212, 12.424, 18.636, 24.848, 31.06 and 37.272 $\mu\text{g}/\text{mL}$ of INH and 0.1 mL of DPNA were generated on three successive days using the optimal analytical conditions as described above. Linear regression analysis was used to calculate the slope, intercept and the correlation coefficient (r) of the calibration line.

Accuracy and Repeatability

Three different concentrations; 12.424, 24.848 and 37.272 $\mu\text{g}/\text{mL}$ of INH stock solution representing the lower, middle and upper range of the calibration line respectively were selected and each in turn was coupled with 0.1 mL of DPNA. This was done in quadruplicates and taken through the optimal analytical conditions already described. The absorbance values were determined at 420 nm. This determination was repeated for three days. Using the calibration line, the concentrations corresponding to these absorbance values obtained were determined and were used to calculate the errors, relative errors, standard deviations, relative standard deviations and recoveries of isoniazid from the quality control samples.

Interference studies

A 0.57156 $\mu\text{g}/\text{mL}$ solution of INH was coupled with 0.1 mL of DPNA in 4 test-tubes each with 5 mg quantities of the excipients described for Method A. Five different excipients were used (talc, starch, gelatin, magnesium stearate and lactose). Also another set of 4 test-tubes contained a mixture of all the excipients. The coupled adduct was taken through the optimal analytical conditions and absorbance value was determined at 420 nm.

Analytical Signal Stability Test

A 0.57156 $\mu\text{g}/\text{mL}$ solution of INH was coupled with 0.1 mL of DPNA, this was taken through optimal analytical conditions and the absorbance value was taken at 30 minutes interval for a period of 4 hours, as well as after 24 hours.

Dosage form analysis

For dosage form analysis using the newly developed method, a 0.57156 µg/mL solution was taken from the stock solution prepared and coupled with 0.1 mL of DPNA. This was taken through optimal analytical conditions and the absorbance value for six replicates was determined at 420 nm.

For the official method (British Pharmacopoeia ⁴), the quantity of isoniazid powder (crushed tablets) equivalent to 0.250 g was dissolved in distilled water in a 100 mL volumetric flask and diluted to the 100 mL mark with distilled water. 100 mL of distilled water was added to 20 mL of the solution and 20 mL of concentrated HCl was added as well. 0.2 g of potassium bromide was weighed and added and 0.1 mL of methyl red solution was added as indicator. This was titrated drop-wise with 0.0167 M of potassium bromate until the red colour disappeared.

RESULTS AND DISCUSSION

The two new procedures described in this research involved the spectrophotometric determination of isoniazid following condensation reaction with salicylaldehyde to form hydrazone as well as diazo coupling reaction of INH with diazotized *para*-nitroaniline. The two procedures provided accurate and simple approaches for the determination of this important anti-tubercular drug. Isoniazid still remains an important drug in the drug management of tuberculosis in the tropics. The need to provide readily adaptable methodologies for the determination of INH formed the primary motivation for this research design.

Evidence of reaction between INH and reagents

In both methods A and B, evidences for condensation and diazo coupling reactions were established by spot tests and analytical thin layer chromatographic analyses. In method A, both the INH and salicylaldehyde solutions hitherto colourless produced a yellow colour following contact with each other. The intense yellow colour became pronounced with time and at elevated temperatures. Likewise for method B, diazo-coupling reaction between INH and DPNA gave a yellow colour indicating the formation of an azo dye. Similarly, for the DPNA method, the colour produced became intense at elevated temperatures.

Thin layer chromatographic analyses revealed the formation of new products that are distinct from the starting materials. The results obtained for the thin layer chromatographic analyses are presented in Table 1. In method A, thin layer chromatography also showed that a new product was formed with R_f value that is distinct from those of isoniazid and salicylaldehyde. From the struc-

ture of salicylaldehyde (Fig. 1), the presence of the carbonyl group which is capable of hydrogen bond acceptance, coupled with the O-H bond, which allows for hydrogen bond donation, makes it polar but if compared to isoniazid, the latter has 2 sites for accepting hydrogen and a hydrazine moiety (NHNH₂) that can give out hydrogen which is less polar. Moreover, intramolecular hydrogen bond can be formed between the carbonyl group and the O-H bond which will make the system look like a two-ring system (Fig. 1). This also reduces the polarity of salicylaldehyde. It follows that its R_f value should be the highest. For isoniazid, the presence of the pyridine ring in its structure contributes more to its polarity than benzene ring contributes to the polarity of salicylaldehyde. The hydrazine moiety (NHNH₂) is capable of hydrogen bond donation which is stronger compared to the O-H bond in salicylaldehyde (already involved in intramolecular hydrogen bonding). The resultant effect is that isoniazid behaves in a more polar fashion than salicylaldehyde. The condensation reaction between the amino functional group of isoniazid and the carbonyl of salicylaldehyde to give the imine group reduces the hydrogen bond donation capability of the hydrazine group in isoniazid, making it less polar than isoniazid. That loss is however compensated by the additional phenolic OH in its structure. Furthermore; the extra aromatic ring character in the condensation product makes the condensation product less polar than isoniazid but more polar than salicylaldehyde. Hence, the R_f value obtained showed that the condensation product is of intermediate polarity between the slightly polar isoniazid and the non-polar salicylaldehyde. The non-polar nature of salicylaldehyde became clearly evident as it was the only component that migrated in the highly non-polar solvent combinations of ethyl acetate: hexane. Neither the drug nor the reagent moved from the origin in this particular mobile phase system. For method B, the R_f values obtained also confirmed the presence of completely different compounds relative to the starting materials of INH and DPNA. Unlike the scenario observed for Method A, the azo adduct was the least polar of the three components. The non-polar nature became apparent while using the third mobile phase system (EtOAc: *n*-Hexane) where it was the only spot that migrated from the origin. The presence of two ring systems bridged by the azo linkage and the presence of the residual nitro group of DPNA must be responsible for this relatively non-polar behaviour.

Table 1. Thin Layer Chromatographic analyses for the two methods

Solvent System	INH	Method A		Method B	
		Salicylaldehyde	Condensation product	DPNA	Azo adduct
EtOAc: MeOH (7:3)	0.47	0.73	0.59	0.51	0.70
EtOAc: MeOH (9:1)	0.22	0.6	0.43	0.51	0.77
EtOAc: n-Hex (5:5)	0	0.61	0	0	0.49

EtOAc = Ethyl acetate; MeOH = Methanol; *n*-Hex = *n*-Hexane; DPNA = Diazotized *para*-nitroaniline

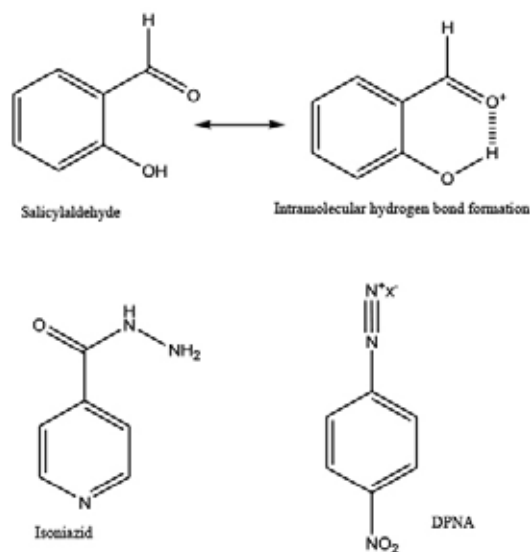


Figure 1. Structures of salicylaldehyde, pseudo ring structure of salicylaldehyde, Isoniazid and Diazotized *para* nitroaniline (DPNA).

Selection of Analytical Wavelengths

The results obtained for the selection of analytical wavelengths for methods A and B are presented in Figures 2 and 3 respectively. The UV-Vis spectra for the condensation reaction between INH and salicylaldehyde (method A) as presented in Figure 2 shows that absorbance for INH and salicylaldehyde are almost non-existent beyond 380 nm. The condensation reaction produced a new spectral pattern for the reaction with INH which an evidence of condensation reaction is. The spectrum of the condensation adduct however resulted in a hyperchromic effect in the spectra; that is, an increase in the intensity of absorption. This new absorption maximum is also accompanied by slight bathochromic shift ($+\Delta\lambda = 2\text{-}5\text{ nm}$). Optimal difference in absorptivity between

salicylaldehyde and the condensation product was found at 405 nm which was selected as the analytical wavelength for subsequent analytical work. In figure 3, it can be observed that absorbances for INH and DPNA were almost non-existent beyond 350 nm wavelength. However, both adduct and PNA had significant absorbance beyond 400 nm, that is, there was a bathochromic shift. Also, for the new adduct, a hyperchromic effect was observed. At around 420 nm, there was an observed difference in absorbance of PNA and adduct hence 420 nm was selected as the analytical wavelength. The observed difference between absorbance of PNA and adduct was further confirmed by taking the absorbance of both solutions at selected wavelengths around visible region and this was used to determine the final choice of analytical wavelength at 420 nm.

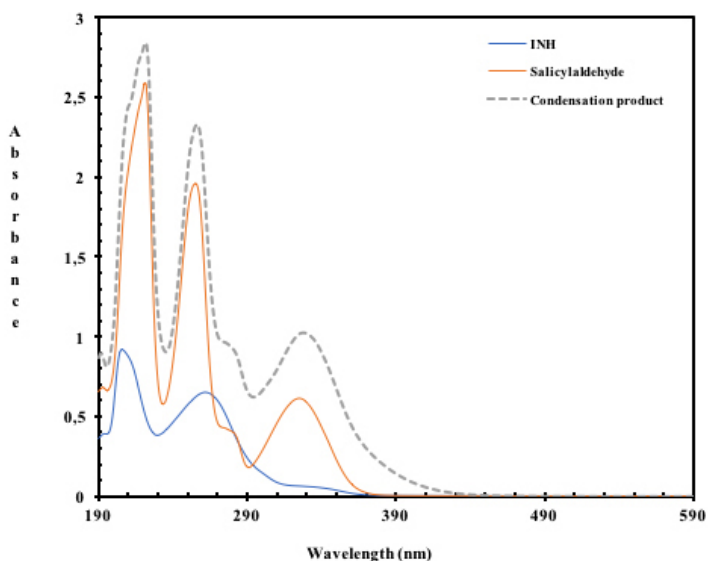


Figure 2. Overlaid absorption spectra for the condensation reaction between INH and Salicylaldehyde.

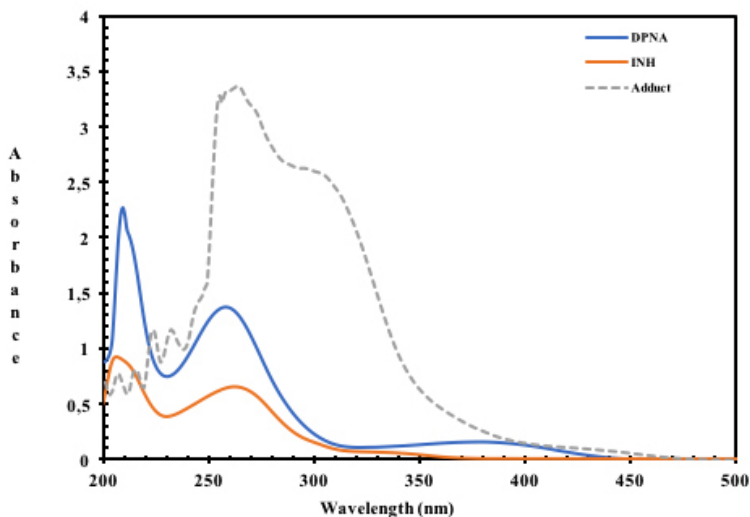


Figure 3. Absorption spectra for the azo dye formation between INH and DPNA.

Optimisation studies

Several factors that can affect the formation of coloured products between INH and the two derivatisation reagents were identified and optimised in a series of steps in order to improve the accuracy of the new methods.

Optimisation of solvent for dilution

For method A, the condensation reaction will involve expulsion of water as INH reacts with salicylaldehyde. Thus, the formation of the Schiff base will be promoted by a solvent that will remove the water molecule so that it will not catalyze the decomposition of the product formed. In this assessment the alcohols, methanol, ethanol, propan-1-ol and propan-2-ol were utilized. Methanol gave the optimum absorbance value among the alcohols and was therefore selected as the optimal solvent. Methanol is more effective than the other solvents listed above in extracting water thereby stabilizing the product as the equilibrium is moved more towards the right, favoring formation of the Schiff base (adduct) rather than its hydrolysis back to the aldehyde. The suitability of methanol may be explained by its 50:50 ratio of hydrophobic to hydrophilic component. For method B, extraction of the azo adduct formed into ethyl acetate was found to give the optimal result.

Optimisation of temperature and time of reaction

The results obtained for the optimisation of temperature are presented in Figure 4 for both methods A and B. For method A using salicylaldehyde and meth-

od B using diazotised *p*-nitroaniline, the optimisation of temperature which was done at 5 different temperatures showed that 30 °C was the optimum temperature. The absorbance was the highest both at 5 and 20 minutes, the absorbance values thereafter declined at higher temperatures. This decrease in absorbance at increased temperature could be due to thermal decomposition of the reaction products formed. However, for method B, the temperature pattern was not readily deciphered for the 5 min profile. This might be due to the insufficient energy available to drive the reaction at such low duration of exposure. In the assessment for method B, 50 °C was required before optimal absorptivity could be attained and thereafter attained a plateau at 60 °C. Since a higher advantage will be derived from determining INH at a lower temperature of 30 °C (a gain of over 45% in absorptivity between the two temperature levels) at 20 mins, the effect of varying reaction condition at this temperature was further investigated.

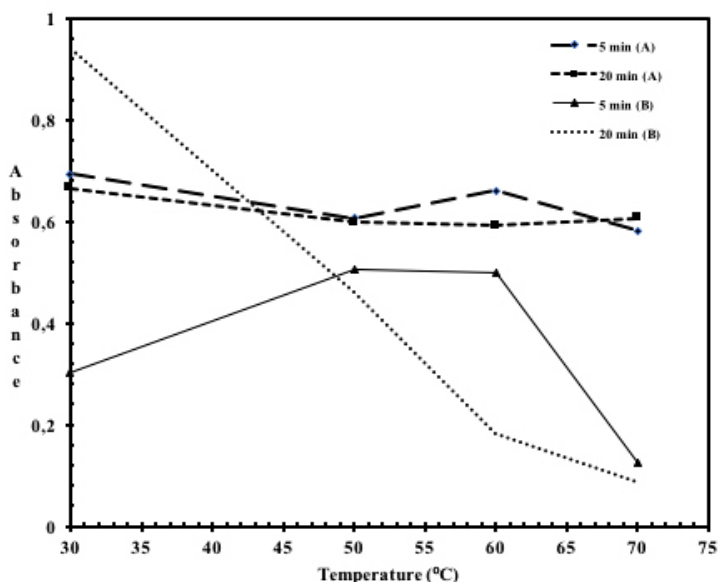


Figure 4. Optimization of temperature for the two new methods.

At the optimum temperature of 30 °C, the time required for maximum absorbance was investigated for the two methods. The results are presented in figure 5. Salicylaldehyde was established to react with isoniazid at 30 °C for 5 minutes. The optimum time was determined at the following reaction times; 0, 2, 5, 10, 15, 20, 25 and 30 min. The absorbance was highest at 5 minutes. Hence, 5 minutes was selected as the optimum time for reaction. For the DPNA method, optimum time was found to be 20 minutes. This is in consonance with the result obtained for the temperature optimisation.

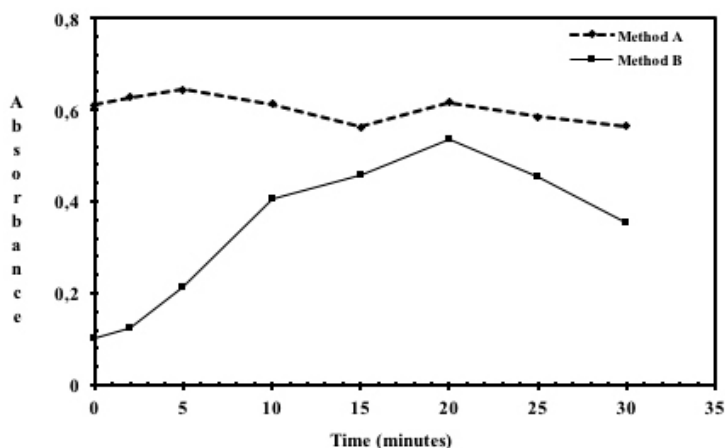


Figure 5. Effect of time allowed for reaction at optimal temperatures for methods A and B.

Effect of acid concentration (method A)

The effect of varying the concentration of H_2SO_4 used to prepare salicylaldehyde solution was studied at different concentrations from 0.03125 to 2 mol/L. The absorbance peaked at 1mol/L acid concentration, after which it declined. If the reaction medium is too acidic, the amine in the isoniazid structure becomes protonated such that it lacks the unshared electrons and is no longer nucleophilic. This inhibits the first step in the nucleophilic addition of the amine to the carbonyl function in salicylaldehyde. However, the reaction medium must be sufficiently acidic to promote the carbonyl oxygen of salicylaldehyde as this makes coupling easier since the carbonyl carbon then becomes more electrophilic (as seen in fig. 6). The optimum acid concentration selected was 1 mol/L.

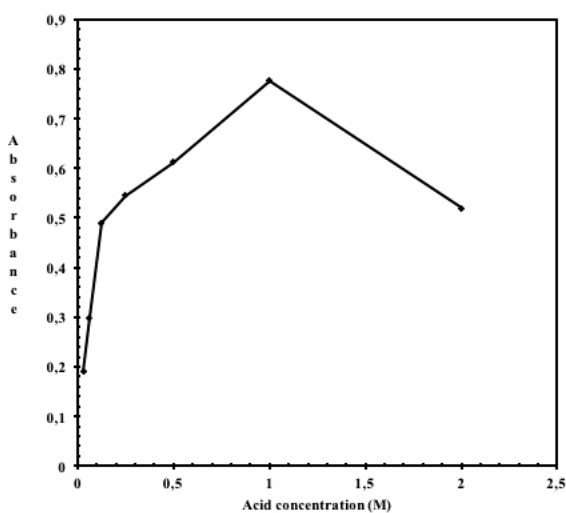


Figure 6. Effect of acid concentration on the condensation reaction (Method A).

Stoichiometric ratio determination

Optimal absorbance was observed at the drug-adduct ratio 1:1 for both methods A and B as presented in fig. 7. Hence, subsequent analytical work was carried out with this drug-adduct ratio. In the reaction of INH with salicylaldehyde, the result obtained implies that the nucleophilic addition involved the primary amine in isoniazid rather than its secondary amine. For the nucleophilic addition to occur with the secondary amine, a dehydrating agent will be required to expunge water resulting in the corresponding enamine product. However, in this case, the primary amine can be said to undergo nucleophilic addition in the absence of a dehydrating agent to give the imine containing compound, a hydrazine. The reaction between INH and DPNA (method B) giving a 1:1 mole ratio also implies that only one site is available on the INH molecule for the electrophilic attack as evidenced also by a single spot on TLC analysis.

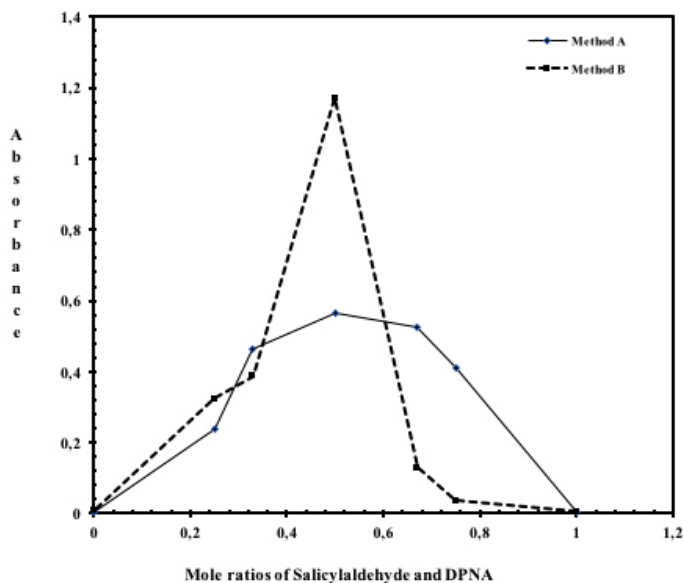


Figure 7. Stoichiometric ratio determination for INH using methods A and B.

Validation studies

The results obtained for the analytical and validation parameters for the assessment of INH by the two new spectrophotometric methods are presented in Table 2. For the utilisation of salicylaldehyde (method A), calibration curves were prepared under the established conditions, by plotting absorbance as a function of the corresponding concentrations for the average of the results obtained on each of 3 consecutive days. A linear relationship was observed

between absorbance at 405 nm and concentrations of isoniazid in the range of 13.436 - 53.744 µg/mL. Linear regression was obtained for the reaction between salicylaldehyde and isoniazid with a correlation coefficient of 0.9967 and a coefficient of determination of 0.9935. Molar absorptivity was calculated from the calibration curve. For method B, a pooled calibration data for three days over the concentrations range of 6.212 – 37.272 µg/mL gave an excellent curve with a correlation coefficient (r) of 0.9965 and coefficient of determination (r²) of 0.993. In both methodologies adopted for the analysis of INH, low values were obtained for the LOD and LOQ. These results point to the sensitivity and suitability of the methods for the determination of INH.

Table 2. Analytical and Validation parameters for the two spectrophotometric methods

Parameter	Method A	Method B
Analytical wavelength (nm)	405	420
Beer's law limit (µg/mL)	13.436 - 53.744	6.212 – 37.272
Correlation coefficient (r)	0.9967	0.9965
Coefficient of determination (r ²)	0.9935	0.9930
Slope ±95% Confidence interval	0.0096 ± 0.0008	0.0358 ± 0.000058
Intercept ± 95% Confidence interval	0.0552 ± 0.0176	0.2068 ± 0.0007
Molar absorptivity (L mol ⁻¹ cm ⁻¹)	1.597x 10 ³	4.04 x 10 ³
LOD (µg/mL)	0.230	0.101
LOQ (µg/mL)	0.695	0.306

Assessments of Accuracy and Repeatability

Using the optimised conditions for both methods A and B, the accuracy and repeatability assessments were carried out using a 3-day period. The results for the intra-day and inter-day accuracy and precision are presented in Tables 3 and 4 respectively.

Table 3. Intra-day accuracy and repeatability determination

Method A						
Concentration taken (µg/mL)	Concentration found (µg/mL)	Recovery (%)*	S.D.	RSD (%)	Error	Relative error (%)
20.154	20.55	101.98	0.37	1.78	0.39	1.94
33.59	33.03	98.32	0.47	1.42	0.56	1.71
47.026	49.02	104.23	2.01	4.09	1.99	4.06
Method B						
12.424	12.180	98.04	0.05	0.39	0.24	1.96
24.848	25.162	101.26	0.09	0.36	0.31	1.26
37.272	37.257	99.96	0.02	0.06	0.02	0.04

**n* = 4 for each concentration level; SD = standard deviation; RSD = Relative standard deviation

Table 4. Assessments of Inter-day accuracy and repeatability

Method A						
Concentration taken (µg/mL)	Concentration found (µg/mL)	Recovery (%)*	S.D.	RSD (%)	Error	Relative error (%)
20.154	20.33	100.86	0.45	2.20	0.17	0.85
33.59	33.75	100.47	0.78	2.31	0.16	0.46
47.026	48.45	103.03	2.22	4.58	1.43	2.94
Method B						
12.424	12.199	98.19	0.06	0.45	0.23	1.81
24.848	25.169	101.29	0.07	0.27	0.32	1.29
37.272	37.259	99.97	0.03	0.08	0.01	0.03

**n* = 12 for each concentration level; SD = standard deviation; RSD = Relative standard deviation

For method A, the percentage relative error for intra-day accuracy was less than 5%, with recovery of 98.32–105.06%, indicating good accuracy. The percentage relative standard deviation for the intra-day precision did not exceed 5%, indicating good repeatability. For inter-day accuracy, the percentage relative error was less than 5%, with recovery of 100.47–103.03%. The percentage relative standard deviation was 2.20 – 4.58%, indicating good reproducibility. Recovery studies also measure the effectiveness of sample preparation. The results showed that 33.59 µg/mL was the optimal analyte size recommended for routine use of this assay procedure. For method B, the recoveries for the intra-day assessment ranged between 98.04 and 99.96% while the RSD and relative errors were generally less than 0.5% and 2.0% respectively. For the inter-day analysis of the recovery studies, 98.19 – 101.29 range was obtained with RSD and % relative error less than 0.5% and 2.0% respectively. The high recoveries obtained coupled with low errors and low relative standard deviations attest to the suitability of the two methods for the analysis of INH in bulk drug.

Interference liabilities

A study of possible interference by common excipients used in formulation (starch, lactose, talc, magnesium stearate and gelatin) of pharmaceuticals showed no interference from any of the excipients. The results are presented in Table 5. The percentage recoveries obtained for method A were between 95.37-103.44% which shows good accuracy with relative errors generally less than 4%. Similarly, for method B, there was no interference from the matrix of the tablet excipients as recoveries of 99.22 – 101.41% were obtained. In addition, the relative error and relative standard deviation were less than 0.5 and 1.5% respectively. These results once again establish the ability of the two methods to selectively determine INH in the presence of tablet excipients and thus conferring great measure of accuracy.

Table 5. Interference liabilities with common tablet excipients

Excipients	Method A			Method B		
	Concentration taken ($\mu\text{g/mL}$)	Concentration found ($\mu\text{g/mL}$)	Recovery \pm S.D. (%)	Concentration taken ($\mu\text{g/mL}$)	Concentration found ($\mu\text{g/mL}$)	Recovery \pm S.D. (%)
Talc	33.59	32.40	96.46 \pm 0.23	21.742	21.663	99.63 \pm 0.08
Starch	33.59	32.04	95.37 \pm 0.53	21.742	21.718	99.89 \pm 0.03
Lactose	33.59	33.86	100.80 \pm 0.89	21.742	21.607	99.38 \pm 0.09
Gelatin	33.59	34.74	103.44 \pm 0.71	21.742	21.573	99.22 \pm 0.05
Magnesium stearate	33.59	34.59	102.97 \pm 0.77	21.742	21.814	100.33 \pm 0.08
Mixture of excipients	33.59	34.69	103.28 \pm 1.12	21.742	22.048	101.41 \pm 0.05

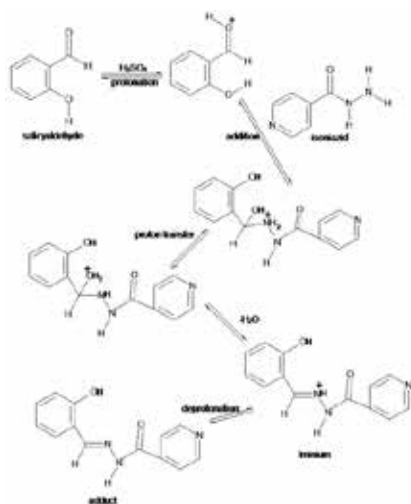
* $n = 4$ for each concentration level; SD = standard deviation

Analytical signal stability

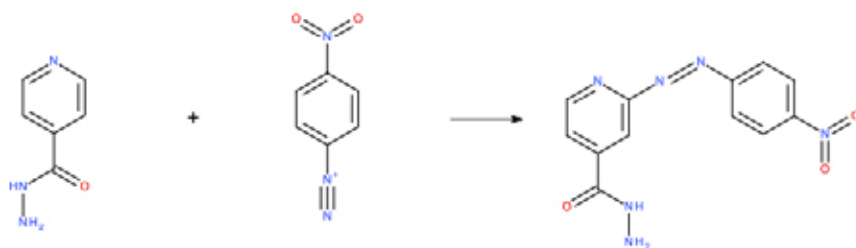
For method A, good analytical signal stability was obtained for the entire period. However, for method B, it was observed that the wrapped adduct was more stable than the unwrapped. Over a period of 30 minutes, absorbance values of both wrapped and unwrapped samples attained constant stability but the variation in stability for the wrapped was relatively higher when compared to the unwrapped for the entire study period.

Reaction Mechanisms of the two new spectrophotometric methods

The proposed reaction pathways for the two methods for the determination of INH are presented in Schemes 1 and 2 for the salicylaldehyde and DPNA respectively. For the condensation reaction (Scheme 1), a nucleophilic reaction between INH and salicylaldehyde occurs *via* the formation of an iminium and eventually a mole of water was expunged to create a stable molecule, (*E*)-*N*'-(2-hydroxybenzylidene)isonicotinohydrazide. For the diazo coupling reaction of INH with diazotized *para*-nitroaniline (method B, Scheme 2), an aromatic ring undergoing attack by a diazonium must generally contain a powerful nucleophile (an electron donating group) such as $-\text{OH}$, $-\text{NH}_2$ etc. Possibly due to the size of the attacking species, coupling takes place almost always at the *para* position to the activating group except if the *para* position is occupied, in which case, coupling occurs at the *ortho* position to the activating group (Adegoke, 2012)²⁸. Since the *para* position to the activating group in INH is occupied by a hydrazide moiety, which is actually a *meta*-directing group, this leaves the *ortho* position to the activating group as the available coupling site. This *ortho* position is also at the *meta* position relative to the hydrazide hence there is further reinforcement of the position for coupling to occur to give the molecule (*Z*)-2-(2-(4-nitrophenyl)diazenyl)pyridine-4-carbohydrazide as the azo adduct.



Scheme 1. Proposed condensation reaction between INH and salicylaldehyde in methanol.



Scheme 2. Coupling pattern between INH and DPNA in ethyl acetate medium.

Dosage forms Analysis

The proposed methods were adopted for the determination of INH in two commercial brands of isoniazid tablets containing 300 mg isoniazid active ingredient. The samples passed the weight uniformity test and the quantitative determination using the new methods. The recoveries obtained were $98.75\% \pm 0.69$ and $99.67\% \pm 1.58$ for brands A and B respectively using the condensation method. For the second method, recoveries obtained for tablet brands A and B are $99.13\% \pm 1.73$ and $99.13\% \pm 1.47$ respectively. On calculating the recoveries of isoniazid from the tablet brands relative to the official titrimetric assay, values close to 100 % were obtained by both methods. This implies that the two new methods can accurately determine the contents of isoniazid in tablets. The *F* test was used to estimate the difference in variance between the new method and the official method, while Student's *t* test was used to compare the mean recovery, with 95% confidence interval. The results obtained are presented in Table 6. The two tests showed lack of statistical significant differences in the precision and accuracy of the two new methods compared to the official method and thus implies that the methods are equivalent.

Table 6. Comparative tablet analysis using methods A, B and official titrimetric method

Tablet Formulation	Method A				Statistics ^b		Method B				Statistics ^b		Official method	
	Found (%)	RSD (%)	Recovery (%) ^a	Error (%)	t-test	F-test	Found (%)	RSD (%)	Recovery (%) ^a	Error (%)	t-test	F-test	Found (%)	RSD (%)
A	98.75	0.69	99.86	0.142	0.78	0.67	99.13	1.75	100.24	0.242	0.78	0.05	98.89	0.58
B	99.67	1.58	99.81	0.191	0.86	0.32	99.13	0.14	99.27	0.736	0.18	0.06	99.86	0.84

^aMean value calculated from the recoveries of new methods and official assay (n=6) ^bp-values

Many spectrophotometric methods reported in the literature either lack sensitivity or specificity. However, the specificity of this method has been proven by the determination of the drug in the presence of commonly used excipients and no interference was recorded. The azo adduct and the condensation products obtained also showed good stability over 4hrs and 24hrs.

The 3D optimized structures of the resultant products from the two reaction mechanisms are presented in Figure 8. The predicted Log P values for the respective adducts using condensation and azo adduct formation are 1.64 and 1.08. This explains the results obtained from the TLC analyses where significant migrations were observed for the new products under the normal phase mode. A cursory look at the 3D structures for the products revealed the staggered natures of the products and hence accounting for the stabilities observed on the bench. The staggered natures of the bonds allowed for optimal stability with minimal steric hindrance. The heat of formation of the condensation product was predicted as -214.17kJ/mol justifying the spontaneity of the formation of the condensation product in the presence of a mineral acid.

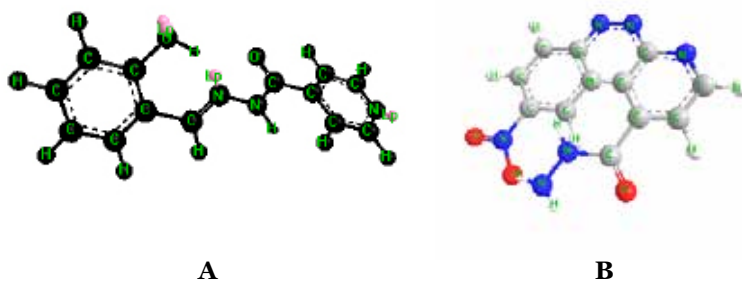


Figure 8. 3D optimized structures for the reaction products of isoniazid with salicylaldehyde and diazotized p-nitroaniline.

Advantages of the methods over previously reported methods

The new methods as proposed in this report are simple and easy to carry out compared to the HPLC method described in the United States Pharmacopoeia ³⁰. The methods also have lower limits of detection when compared with previously reported methods. The methods are also simpler than the method developed by Jennings *et al.* (1974) ³⁰ which involves the conversion of the analyte

from one oxidation state to another before its determination.

The proposed methods do not require the use of sophisticated equipment when compared with the method developed by Lapa *et al.* (2000)¹² which involves fluorimetric analysis. The reagents used for the proposed methods are readily available and environmentally friendly when compared with the reagents required for the method developed by El-Brashy *et al.* (1992)¹⁴ which requires the use of reagents such as neocuproine and epichlorohydrine which may not be readily available to the analyst.

Two new spectrophotometric methods involving relatively available reagents were successfully developed for the assay of isoniazid in bulk and tablet dosage forms. The methods are simple and could find applications in the in-process quality control for the manufacture of isoniazid tablet and as rapid analytical methods for the assay of the drug.

REFERENCES

1. WHO 2019. *Tuberculosis*. Retrieved May 10, 2019 from <http://www.who.int/news-room/fact-sheets/detail/tuberculosis>.
2. World Health Organisation. *Guidelines for treatment of tuberculosis. 4th ed., Document number WHO/HTM/TB/2009.420*. WHO: Geneva, **2010**.
3. *Martindale The Complete Drug Reference 36th ed.* Pharmaceutical Press: London, **2009**.
4. The British Pharmacopoeia Commission, *British Pharmacopoeia*. The Stationery Office: London, **2009**.
5. Hakkimane, S. S.; Guru, B.R. Nano formulation analysis: analytical method development of isoniazid and simultaneous estimation of anti-tubercular drugs isoniazid and rifampicin by RP-HPLC. *Asian J. Pharm. Clin. Res.* **2017**, *10*, 330-335.
6. Kuhuawar, M.; Rind, F.; Rajper, A. High-performance liquid chromatographic determination of isoniazid, pyrazinamide, and indomethacin in pharmaceutical preparations. *Acta Chromatogr.* **2005**, *15*, 269.
7. Cao, X.; Rui, J.; Wang, Y.; Li, J.; Ma, B.; Yang, Z.; Liu, Y. Simultaneous determination of isoniazid and acetylisoniazid in human plasma by hydrophilic interaction liquid chromatography tandem mass spectrometry and its application to a pharmacokinetics related to N-Acetyltransferase 2 genetic polymorphism. *Anal. Lett.* **2012**, *45*, 2125-2135.
8. Hee, K. H.; Seo, J. J.; Lee, L. S. Development and validation of liquid chromatography tandem mass spectrometry method for simultaneous quantification of first line tuberculosis drugs and metabolites in human plasma and its application in clinical study. *J. Pharm. Biomed. Anal.* **2015**, *102*, 253-260.
9. Haghighi, B.; Bozorgzadeh, S. Flow injection chemiluminescence determination of isoniazid using luminol and silver nanoparticles. *Microchem. J.* **2010**, *95*, 192-197.
10. Xi, J.; Shi, B.; Ai, X.; He, Z. Chemiluminescence detection of isoniazid using Ru(phen)₃(2+)-isoniazid-Ce(IV) system. *J. Pharm. Biomed. Anal.* **2004**, *36*, 237-41.
11. Huang, Y.; Zhang, Z. Flow injection chemiluminescent analysis of isoniazid by direct hexacyanoferrate(III) oxidation. *Anal. Lett.* **2001**, *34*, 1703-1710.
12. Lapa, R.A.; Lima, J. L.; Santos, J. L. Fluorimetric determination of isoniazid by oxidation with cerium (IV) in a multicommutated flow system. *Anal. Chim. Acta.* **2000**, *419*, 17-23.
13. Yun Xia, H.; Ya Hu, X. Determination of isoniazid using a gold electrode by differential pulse voltammetry. *Anal. Lett.* **2005**, *38*, 1405-1414.
14. El-Brashy, A. M.; El-Ashry, S. M. Colorimetric and titrimetric assay of isoniazid. *J. Pharm. Biomed. Anal.* **1992**, *10*, 421-426.
15. Blake, M. I.; Bode, D.; Rhodes, H. J. Comparison of analysis of isoniazid and its dosage forms by several methods. *J. Pharm. Sci.* **1974**, *63*, 1303-1306.
16. Benetton, S.; Kedor-Hackmann, E.; Santoro, M.; Borges, V. Visible spectrophotometric and first-derivative UV spectrophotometric determination of rifampicin and isoniazid in pharmaceutical preparations. *Talanta.* **1998**, *47*, 639-643.
17. Espinosa-Mansilla, A.; Acedo Valenzuela, M.I.; Muñoz de la Peña, A.; Salinas, F.; Cañada, F.C. Comparative study of partial least squares and a modification of hybrid linear analysis calibration in the simultaneous spectrophotometric determination of rifampicin, pyrazinamide and isoniazid. *Anal. Chim. Acta.* **2001**, *427*, 129-136.

18. Nagaraja, P.; Sunitha, K.; Vasantha, R.; Yathirajan, H. Novel method for the spectrophotometric determination of isoniazid and ritodrine hydrochloride. *Turk. J. Chem.* **2002**, *26*, 743-750.
19. Mahfouz, N. M.; Emara, K. M. Colorimetric determination of isoniazid and its pharmaceutical formulations. *Talanta.* **1993**, *40*, 1023-1029.
20. Almani, K.; Laghari, M.; Memon, A.; Rind, F.; Mughal, U.; Maheshwari, M.; Khuhawer, M. Spectrophotometric Determination of Isoniazid from Pharmaceutical Preparations Using Natural Aldehyde. *Asian J. Chem.* **2013**, *25*, 2522-2526.
21. El-Brashy, A. M.; El-Hussein, L. A. Colorimetric Determination of Some Important Hydrazine Derivatives. *Anal. Lett.* **1997**, *30*, 609-622.
22. Shetty, D. N.; Narayana, B.; Samshuddin, S. Novel Reagents for the Spectrophotometric Determination of Isoniazid. *ISRN Spectroscopy.* **2012**, *2012*, 1-5.
23. Hassan, H. Y.; Mohamed, A. M. I.; Mohamed, F. A. Utility of Certain π -Acceptors for the spectrophotometric determination of isoniazid. *Anal. Lett.* **1990**, *23*, 617-625.
24. El-Kommos, M.E.; Yanni, A.S. Spectrophotometric determination of isoniazid using 6, 7-dichloroquinoline-5, 8-dione. *Analyst.* **1988**, *113*, 1091-1095.
25. Nagaraja, P.; Murthy, K.; Yathirajan, H. Spectrophotometric determination of isoniazid with sodium 1, 2-naphthoquinone-4-sulphonate and cetyltrimethyl ammonium bromide. *Talanta.* **1996**, *43*, 1075-1080.
26. Safavi, A.; Karimi, M. A.; Nezhad, H.; Kamali, R.; Saghir, N. Sensitive indirect spectrophotometric determination of isoniazid. *Spectrochim. Acta A.* **2004**, *60*, 765-769.
27. ICH Topic Q2 (R1), Validation of Analytical Procedures: Text and Methodology (CPMP/ICH/281/95); accessed December 22, 2018
28. Adegoke, O. A. Chemical derivatization methodologies for uv-visible spectrophotometric determination of pharmaceuticals. *Int. J. Pharm. Sci. Rev. Res.* **2012**, *14*, 6-24.
29. United States Pharmacopoeia, 2007, 30th revision. **2007**, 1912. US Pharmacopoeial Convention.
30. Jennings, V. J.; Dodson, A.; Harrison, A. Coulometric microtitration of arsenic (III) and isoniazid using a vitreous carbon generating electrode. *Analyst.* **1974**, *99*, 145-148.

ACTA
PHARMACEUTICA
SCIENCIA

International Journal in Pharmaceutical Sciences, Published Quarterly

57 [3]